DEPARTMENT OF BIOMEDICAL ENGINEERING

University of Strathclyde Engineering

Biomechanical Biomarkers of Cancer

Megan Barbara Clark
201370134

Supervised by Dr Phil Riches

Thesis submitted towards the partial fulfilment of
MSc Biomedical Engineering
Academic Year 2013/2014

Declaration

This thesis is the result of the author's original research. It has been composed by the author and has not been previously submitted for examination which has led to the award of a degree.

The copyright of this thesis belongs to the author under the terms of the United Kingdom Copyright Acts as qualified by University of Strathclyde Regulation 3.50. Due acknowledgement must always be made of the use of any material contained in, or derived from, this thesis.

Signed: Date:

Acknowledgements

It is only with the help and support from several people that the completion of this project was possible.

First and foremost I would like to take this opportunity to thank my supervisor Dr Phil Riches for his invaluable support, assistance and guidance throughout my project. I am extremely grateful for the time that he provided, especially in helping me with MATLAB and assisting me in writing the correct codes. I would like to thank him for continually believing I was capable of more.

I would like to acknowledge Brian Cartlidge and thank him for the computational assistance provided during the semester; it was especially appreciated when initially setting up the work station.

I would also like to recognise the work carried out by Busby and colleagues (2013), without which I would not have any reference to base my investigation on.

Additionally, I would also like to say a huge thank you to all my close friends and family. Not only for their continuing support and encouragement throughout my Undergraduate degree, but for being just as supportive this past year during my Postgrad. A special mention must go to my mum and Craig, as they have been nothing but a pillar of support and have yet to call me mad for contemplating another year of University.

Table of Contents

List of Tables

List of Figures

Abstract

Cancer is a major health issue within the UK, with more than one third of people developing it within their lifetime. As there are so many different types of cancer, a quick, accurate and non-obtrusive diagnostic technique would be beneficial. A potential diagnosis technique under investigation is the use of a biomechanical biomarker. A biomarker is a signal of a biological state, which is specific to a particular type of disease. It helps validate diagnosis relative to disease progression and is therefore very important in malignant tumour detection. A biomechanical biomarker is a combination of model parameters that best identify tumours and tumour growth.

This project investigated the possibility of obtaining a biomechanical biomarker of cancer using the newly develop finite element programme *FEBio*. A previous study by Busby *et al*. suggested that confined compression, along with biphasic theory, was a suitable technique for determining the mechanical properties of collagen hydrogels. Therefore, *FEBio* was used to create both force and displacement control confined compression tests of tissues modelled by collagen hydrogels. The tissue models contained a 'tumour' layer and the effects of varying the stiffness parameters of this 'tumour' layer were investigated. Any change in mechanical response of the tissue at platen level was regarded as a possible biomechanical biomarker.

It was concluded that the possibility of a biomechanical biomarker was conceivable, but further research into the area is required. A potential biomarker established was the output equilibrium stress recorded from a displacement control test. It was found that the Young's modulus and permeability stiffness parameters, as well as the distance of the 'tumour' layer from the surface, had significant effect on the stiffness of the 'tumour' layer and consequently the output response recorded.

1. Introduction

Cancer Research UK[1] has revealed statistics that more than one third of people develop cancer in their lifetime, with cancer causing more than a quarter of all deaths in the UK. There are more than 200 types of cancer[1], each with different causes and symptoms, and therefore accurate and prompt diagnosis is desirable. Additionally, accurate pre-operative staging of cancer has become essential for optimal patient care[2].

The most popular method of cancer staging is done by examining a tissue sample, obtained via a biopsy. However, as a biopsy is very time consuming and with someone in the UK being diagnosed with cancer every 2 minutes[1], a faster diagnosis technique is required. The method proposed is to determine a biomechanical biomarker as a non-obtrusive method of cancer tumour detection.

Biomarkers are parameters that work as signals of a biological state[3]. They are specific to a particular disease, and are used to validate diagnosis relative to disease progression or treatment. Biomarkers are used to enable early diagnosis of a disease[3], therefore they are very important in malignant tumour detection. There are numerous genetic biomarkers of cancer; however, the possibility of biomechanical properties as independent biomarkers is largely unexplored.

The correlation between cell composition and the cell's mechanical properties has been under investigation for many decades. However, to date, the mechanical behaviour of cancerous tissues is still largely understood, as there is difficulty in *in vivo* experimentation. A recent study (Busby *et al.*, 2013[4]) suggests that confined compression, together with biphasic theory, is a suitable technique for assessing the mechanical properties of collagen hydrogels. Therefore there is a possibility that the biomechanical properties of soft tissues, modelled by a collagen hydrogels, can be used as a biomarker.

This theoretical study aims to use a finite element (FE) analysis programme *FEBio*[5] to determine the mechanical properties of a collagen hydrogel model in an attempt to define a biomechanical biomarker, which would lead to new approaches in cancer diagnosis and prognosis. A biphasic FE model will be created, with a 'tumour' layer of varying stiffness. The stiffness parameters under investigation are Young's modulus (E) and permeability (k). The 'tumour' layer will also vary in position in order to establish if tumour depth has an influence on the biomarker found. The mechanical behaviour of

the model tissue will be analysed in order to see the biomechanical effect on the surface of the corresponding stress caused by the 'tumour' layer. The 'tumour' layer represents the surface at which experimental measures are made. Models will be compared in order to determine the effect of tumour stiffness and depth on the biomechanical biomarker. Ideally, the biomarker should be specific, sensitive and proportional to tumour grade. If it can be shown that these models predict an appropriate sensitivity to parameter variation, finite theoretical and experimental work could be done to ascertain the biomechanical biomarker of cancer.

The remainder of this project report is organised as follows: Chapter 2 provides a review of the existing literature. This chapter is split into different sections which include: an explanation of cancer and collagen gels; methods of cancer diagnosis and prognosis; a definition of biomarkers and a review of current cancer biomarkers; a description of biphasic theory; an explanation of current mathematical modelling techniques, and the FE analysis programme *FEBio* that will be used; concluding with a review of the thesis aims. Following this chapter, chapter 3 presents a description of the methodology for each section of the thesis and chapter 4 provides the results found. An analysis and explanation of the results, as well as a summary of the project, is written in chapter 5; with chapter 6 providing a pertinent conclusion and chapter 7 giving a discussion of the limitations encountered and possible future work.

2. Literature Review

2.1 Cancer

Cancer is a condition where a group of cells in a specific part of the body grow and reproduce uncontrollably[6]. It is a general term for more than 100 diseases characterised by the uncontrolled, abnormal growth of cells[7]. The main characteristic of cancer cells is that the growth rate is much greater than the death rate, as the death rate is essentially non-existent unless the cancer is being treated. Due to theie uncontrollably growth, the cancerous cells within the body can invade and destroy normal tissue and organs[6], resulting in the formation of an abnormal tissue growth called a tumour. Therefore it is important to diagnose cancer quickly and effectively.

There are more than 200 different types of cancer, each with different causes, symptoms and methods of diagnosis and treatment[1]. This means that the correct diagnosis of type and stage of cancer is crucial in order to successfully treat the patient. Conventionally, accurate cancer diagnosis can take weeks or months[6]. The NHS[6] states that this does not usually impact the effectiveness of treatment as cancer generally develops slowly over several years, so waiting a few weeks does not change the diagnosis. However, in the last decade cancer management has become more and more complex[2] with more than one third of people in the UK developing some form of cancer in their lifetime[1]. As a result it is imperative to investigate faster and easier methods of diagnosis.

2.1.1 Cancer Diagnosis

Cancer is easier to treat and, hopefully, cure if it is diagnosed early. Therefore a lot of research is being carried out on different ways to detect early signs of the disease. Currently, diagnosis of cancer is done by endoscopy, blood and tissue samples, and imagining[1] – namely X-rays, Computed Tomography (CT), Magnetic Resonance Imaging (MRI), Positron Emission Tomography (PET) and Ultrasound. The most accurate diagnosis is through taking tissue samples via a biopsy. This is because certain imaging techniques are unable to clearly show an area of cancerous tumour tissue. For example[8] in a mammogram, used for breast cancer, cancerous tumour tissue appears white. However, dense normal tissue also appears white, meaning that it is difficult to differentiate the tumour from the normal tissue and successfully diagnose the patient.

Cancer Research UK[1] defines a biopsy as an examination of the tissue removed from a patient to discover the presence, extent and cause of disease. A biopsy involves taking a small sample of a patient's tissue and examining it under a microscope, in order to help diagnose, or rule out, a number of different health conditions[9]. Biopsies are used to identify abnormal cells, such as cancer cells, and help identify a specific condition. If the condition is already known, the biopsy can be used to measure how severe the condition is or what stage it is at[9]. Knowing the stage of cancer is essential for optimal patient care[2].

In most cases a biopsy is the only way to reach a definitive diagnosis of the staging of cancer[7]. However, a biopsy is generally only able to be performed in the later stages of the disease after a noticeable collection of cells has occurred[10]. Additionally, most biopsies require some form of anaesthesia, and the results can take several days to get back to the patient. Therefore, it would be beneficial to have an alternative, non-invasive diagnostic test that still recognised the same characteristics of a biopsy – in order to define a correct stage for the tumour.

2.1.2 Staging of Cancer

Clinical staging of cancer is a way to describe the extent of the cancer in a patient, using characteristics as the size of the tumour (T), lymph node involvement (N) and where the cancer has spread (M) - this is known as TNM (Tumour, Node, Metastasis) staging[1,7]. For most cancers there are four stages, with stage one being the smallest, primary cancer and stage four is where the cancer has spread to other parts of the body[1]. Therefore pre-operative staging of a malignant tumour is important in order to determine the proper treatment required[7]. Staging also helps predict the course the disease will take and its prognosis, indicating how quickly a tumour is likely to grow. With an increased accuracy of staging, this assists in providing optimal cancer treatment[2]. Different cancers are staged in different ways, with some staging techniques being subjective. Systems of staging are also being 'custom designed' for specific cancers in order to obtain precise information on characteristics of that particular cancer[7].

2.2 Collagen

Collagen is a major structural protein that appears in some shape or form in virtually every tissue of the human body[11]. It is the most abundant protein[11], providing structure, protection and support to the cells and tissues in our bodies.

Collagen is the basic structural unit for many tissues, and has a different organisation and structure in each type[8]. It is the structure of the collagen that contributes to the cell's mechanical properties. It has been identified[11] that the influence of the collagen environment on cell differentiation and proliferation has significant associations with many diseases, including cancer. Many previous investigations have established the correlation between cell stiffness and cell microstructure, including collagen content of the cells. They have noted that changes in cellular function during differentiation or due to disease are reflected in the cell microstructure. When considering breast cancer, it has been established that the stiffness of the breast tissue is significantly affected by amount of collagen content in the tissue[8]. A study of the mechanical properties of cancer has suggested that a change of stiffness of cells can indicate the presence of malignancy[13]. Compared to normal tissue, a tissue with altered density (e.g. a cancerous tumour) is said to show greater resistance to deformation[8], which in turn causes a change in the mechanical properties of the tissue. Considering a cancerous tumour, as the cancer progresses the density of the tissue would change, causing a variation in the mechanical properties. Therefore, it has been suggested that the rigidity of tumours correlates with the tumour grade, and the relationship can be seen through biomechanical analysis.

Previous studies on the association of mechanical properties and tumour stiffness have predominantly been carried out on the cellular level. As a result, there are a limited number of investigations into the mechanical effects seen at the tissue level. This project will hence be focused on the relationship between stiffness and tumour detection on the tissue level as it provides a faster and non-invasive method of diagnosis. The tissues under investigation will be modelled by a collagen hydrogel - collagen hydrogels are often used for *in-vitro* investigations of cell behaviour. A previous investigation[4] noted that experimental testing of the mechanical behaviour of collagen hydrogels is difficult due to their very high water content. For that reason this project will be conducted using computational models, as it is a cheaper, easier and a more controllable method to use.

2.3 Biomarkers

A biomarker is defined as a substance or a parameter that works as a signal of a biological state[3]. They are used in biomedicine to provide early diagnosis and improve efficiency of treatment of a disease. Biomarkers are specific to a particular disease and are used to validate diagnosis relative to disease progression, treatment or follow-up[3]. Therefore a cancer biomarker refers to a substance or process that is indicative of the presence of cancer in the body - with each cancer having a specific biomarker. A cancer biomarker may be a molecule secreted by a tumour or a specific response of the body to the presence of cancer. As a result, the future of cancer diagnostics is currently focused on finding a biomarker that detects the early stages of malignant tumour formation. The aim is to be able to determine the clinical staging of the tumour, as well as being able to individualise the course of diagnosis and treatment for the patient.

A biomarker has to be easily quantifiable and obtained without difficulty. This is to ensure the process is fast and simple for the patient, as well as cost and time effective for the medical team. The biomarker should have both pre-clinical and clinical importance, along with ensuring it is valid for animals, humans and *ex-vivo* cell models[3].

In cancer research, biomarkers are used primarily in diagnostics and prognostics: to help identify the type and stage of cancer, to forecast how aggressive the cancer is, and to determine the course of treatment. Ideally, the biomarker should also be used to predict how well a patient will respond to a treatment and in monitoring the patients' treatment response, to decide whether or not it is the correct treatment being used. Therefore an ideal biomarker will enable early diagnosis of disease, identify subgroups of patients responding to treatment, and evaluate the follow-up of therapy whilst tracking the progression/regression of the disease[3].

A biomarker can be apparent at molecular, cell or biomechanical level[3]. There are many known genetic biomarkers that indicate the presence of a specific cancer or cancer treatment; however, the possibility of biomechanical properties as independent biomarkers is largely unexplored. It is beneficial to investigate a biomechanical biomarker, as it is costly and challenging to look for biomarkers at the genetic level[3].

Recently, Pachenari *et al.*[14] proposed the use of the biomechanical properties of cancer cells as a promising biomarker, to investigate cancer progression and staging. A biomechanical biomarker of cancer is a mechanical property of a malignant tumour

that is apparent on the surface when the tissue is under certain stresses, which takes away the need for invasive surgery.

In 2012, Xu *et al.*[13] suggested that cell stiffness may be an important biomarker due to the development of fast and effective biomechanical testing procedures. They noted the correlation between cell stiffness and relative metastatic potential of ovarian cancer cells, with the potential to determine the spread of other types of cancer cells. They stated that developing a biomechanical biomarker would be an accurate and non-invasive method with the potential to be individualised. Although this investigation is supportive of the aim of this project, the measurements were done at cellular rather than tissue level, meaning that the tumour micro-environment was not taken into account. There have also been other studies at cellular level, including Guck et al.[10], who examined the relationship between function and elasticity of cells, suggesting that a cell's rigidity is able to provide information about its state and is possible cell marker for diagnosis of disease.

This study will investigate a possible biomechanical biomarker at tissue level, rather than cellular level, in an attempt to create a non-obtrusive method of cancer diagnosis and prognosis. The objective is to determine a biomarker specific to different cancers and staging, with the intention of a quick prognosis that would decide how to treat cancer patients on an individual basis. The biomarker should have a direct comparison to tumour grade/stiffness.

2.4 Biphasic Theory

Collagen gels are often used for *in vitro* studies of cell behaviour and to model biological tissues[12]; however, their mechanical behaviour is not fully understood. A recent study[4] suggests that confined compression, together with biphasic theory, is a suitable technique for assessing the mechanical properties of collagen hydrogels. This research looked at hydrogels of 0.2%, 0.3% and 0.4% collagen to determine whether or not the biphasic model can be used to determine differences in stiffness between the gels. The results demonstrated that both peak and equilibrium stress showed significant increases relative to collagen content of the hydrogel. Therefore, the peak and equilibrium stresses are considered to be the best parameters to effectively characterise the mechanical differences in hydrogel properties.

The development of finite element (FE) codes relating to multiphase systems is generally found in literature on the investigation of soil mechanics[15]. Originally, the poroelastic theory was developed to describe soil mechanics[16], then Mow *et al*.[17] developed an alternative formulation based on the theory of mixtures[18] (the biphasic theory) and applied it specifically to the analysis of articular cartilage and load-bearing soft tissues. Prendergast *et al.*[18] concluded that the poroelastic FE code developed for soil mechanics had the ability to be used to model biphasic tissues with reasonable accuracy. The results found for both the linear and non-linear case were close to those found by Spilker *et al.*[15], and therefore it was hypothesised that the FE codes of the biphasic theory had the capability to analysis the mechanical behaviour of biological tissues.

In the biphasic theory, biological tissues are assumed to co-exist in two phases: a solid phase and a fluid phase[16]. It is a localised, continuum theory whereby each point in the tissue is taken to exist simultaneously of both solid and fluid elements and transient stress and strain gradients can be predicted within the tissue[16]. Therefore, a biphasic material is modelled as a continuous distribution of both solid and fluid phases. A biphasic material is illustrated as a deformable, permeable, porous solid matrix that co-exists with an interstitial fluid[19]. Both parts are modelled to be non-dissipative and intrinsically incompressible. It is assumed that the only dissipation comes from the frictional drag of relative motion between the phases[17], and that the mixture is incompressible as the pores of the solid matrix may gain or lose fluid under general loading conditions[19].

The mechanical properties of each phase provide each tissue with its individual, interesting rheological behaviour[17]. The biphasic theory has previously been used to characterise cartilaginous tissues (including work by Mow *et al.*, 1980; Spilker *et al.,* 1988; Ateshian *et al.*, 1997; and Périé *et al.*, 2005), which are considered to be similar in composition to collagen hydrogels. The biphasic theory was determined to be the only consistent rheological model capable of describing the mechanical behaviour of articular cartilage[17], and other load-bearing soft tissues. Busby *et al.*[4] demonstrated that collagen hydrogels may be considered as biphasic - with a loosely connected network of collagen fibrils representing the solid phase, which is filled with a large excess of interstitial fluid demonstrating the fluid phase. The fluid phase of collagen hydrogels is typically $\geq 99.5\%$[4].

The soft tissues of the body, including skin and cartilage, are composed of large amounts of fluid in a solid matrix of collagen and proteins[18]. Therefore, the fluid component of the soft tissues is important, and thus those of which are undergoing deformations can be modelled using the biphasic theory[17].

2.4.1 Constitutive Equations

The linear biphasic theory developed by Mow *et al*. in 1980[17] allows the structural basis of the biological tissues to be considered. The mathematical representations of the behaviours of the material are known as the constitutive relations, or equations, of the material – these equations are validated against experimental results. In the biphasic theory[17], there is no description of pores or microstructure of the solid matrix, though a major part of the derivation concerns the flow of fluid through the solid phase[16] - this connects the two phases together.

Fluid motion through a porous solid can be described using Darcy's Law:

$$w = -k\frac{\partial P}{\partial x} \qquad \ldots(1)$$

Where w is the discharge per unit area, also known as the flux or the flow rate (units: m/s); k is the hydraulic permeability (units: $m^2/Pa.s \equiv m^4/Ns$); and $\frac{\partial P}{\partial x}$ is the rate of change of pressure P over a distance x, also known as the pressure gradient (units: $Pa/m \equiv N/m^3$). Darcy's Law illustrates that fluid flows down a pressure gradient, from a high pressure to a low pressure area. The flow of the fluid is governed by k, which describes the ability of the fluid to flow through the porous medium[16].

For the linear biphasic model, or KLM model[17], in confined compression the stress can be described as a linear function of strain, specifically:

$$\frac{\partial u}{\partial t} = kH_A\frac{\partial^2 u}{\partial x^2} \qquad \ldots(2)$$

Where k is as defined above; the aggregate modulus, H_A (units: $Pa = N/m^2$), is the stiffness modulus in confined compression; and $u = u(x,t)$ is the displacement of the solid phase in the direction of x at time t. Equation 2 describes confined compression, where the tissue is prevented from lateral expansion or contraction under load[16].

When Poisson's ratio (ν) is zero, the aggregate modulus can be considered to be equal to the Young's modulus (E). However, it is more likely that ν is not zero. Therefore,

experimentally the tissue must be confined and prevented from lateral expansion under load. Then the aggregate modulus and Young's modulus values can be associated via Equation 3:

$$H_A = \frac{E(1-\nu)}{[(1+\nu)(1-2\nu)]} \quad \ldots(3)$$

These equations are written into the biphasic code of mathematical models, in order to investigate the mechanical behaviour of biological materials.

2.4.2 Confined Compression

In a uniaxial confined compression test, the tissue under investigation is confined laterally and on the lower surface. The top surface is then compressed using a porous platen. This ensures that no displacement or flow is permitted in a normal direction to the surface of the specimen[15]. True confined compression is difficult to achieve experimentally, as it is impossible to cut a cylindrical specimen with smooth sidewalls and an accurate diameter[17].For that reason, computational models are becoming increasingly popular in order to represent the ideal situation of confined compression.

2.4.3 Biphasic parameters

In this thesis, the aim is to develop a relationship between the change in biphasic parameters (E and k) and the corresponding change in the mechanical behaviour of the surrounding tissue. Busby *et al.*[4] noted that the main biphasic parameters of confined compression, H_A and k, varied with collagen content. This clearly illustrates that H_A and k characterise the physical properties of stiffness and permeability. Increasing the collagen content of a hydrogel results in a greater fibril density[4]. Therefore the permeability should decrease, as a larger collagen content would increase the viscous drag on the fluid flow. Consequently, measurement of H_A is important to measure scaffold stiffness, as it can affect the mechanical behaviour. However, the majority of investigations into the mechanical behaviour of soft tissues involve Young's modulus (E) rather than aggregate modulus (H_A) – this is so that tissue characteristics can be compared even is different testing methodologies were used[4]. Pachenari *et al.*[14] concluded that a larger instantaneous E value is found in higher grade tumour cells, meaning that the higher the Young's modulus value, the more 'solid-like' the material. Additionally, they determined that the more aggressive and higher grade the tumour cells were, the less viscosity they have. This means that the higher the tumour grade, the easier the fluid flow, and accordingly the higher the permeability. However, Busby

et al.[4] established that a lower permeability illustrates a higher collagen content, suggesting a more 'solid-like' material behavior. As there are conflicting arguments, and little study on the permeability of soft and hard tissues, values both higher and lower than the norm permeability should be considered.

2.5 Mathematical Modelling

2.5.1 Finite Element Method (FEM)

Computational models are especially advantageous in biomedical engineering for analysing locations where it is difficult or impossible to obtain experimental measurements. Therefore, due to the difficulty in experimentally (*in-situ* or *in-vivo*) determining the mechanical behaviour of tissues deep inside the body, mathematical models are used. This involves using computer programs to model the tissue and analyse it via the finite element (FE) method. The FE method is a numerical technique used to approximate a solution for an entire model by splitting the defined structure into a finite number of disjoint (non-overlapping) components of a simple geometry – called finite elements or elements. These elements are connected to one another by nodes. The response of each element is expressed at a set of nodal points, thus creating a system of differential equations for the structure. Each element is solved in relation to another, therefore an approximate solution for the full model can be found. The FE method is ideal for the intricate geometries found in biomechanical systems as it is a consistent way to address material inhomogeneities. This is because it provides a systematic approach to approximate the response of a complex system from the individual contributions of each element[22].

2.5.2 History of FEM

The FE method is the most common solution technique used in computational biomechanics and has been used in biomechanical problems since the early 1970s[23,24]. The early work by Matthews and West[23] demonstrated the usefulness of FE modelling in predicting stiffness and stresses, by creating a finite number of discrete portions (elements), calculating their individual stiffness/stress, and re-assembling them to give the complete structure and providing a solution for the whole system. This solution can then be directly related to the structure's mechanical properties. Belytschko *et al.*[24] noted that with the advancements of computational methods, and the use of FE methods, the development of realistic models became possible. This meant that the difficulty in determining *in vivo* mechanical properties was solved. The results of both

studies (Matthews and West, 1972; Belytschko *et al.*, 1974) were compared to available experimental results at the time. They both concluded that the results found from the FE method agreed very well with the experimental results. The results of these studies illustrate the usefulness of the FE model in estimating the material properties and predicting the mechanical behaviour of a structure. Since the 1970's there has been great advancements in computer methods, and consequently the FE models constructed have become more accurate and realistic. Currently, the programs most commonly used include *ABAQUS* (*www.simulia.com*) and *COSMOL Multiphysics* (*www.uk.comsol.com*). However, these programs are not specific to the needs of computational biomechanics, and have thus limited the progression in the field of biomechanical engineering. Recently, in 2012, an open-source FE program *FEBio* was developed by Gerard Ateshian *et al.*[22] (Downloadable from the University of Utah for non-commercial use: *http://mrl.sci.utah.edu/software/febio*).

2.5.3 FEBio

FEBio is an implicit FE solver that was specifically designed for three-dimensional (3*D*) problems in computational solid biomechanics[22,25]. It differs from many of the existing software currently used for research as it is a non-linear solver, meaning that the permeability of the material is a function of the deformation. As *FEBio* (an acronym for *'Finite Elements for Biomechanics'*) is specifically designed for biomechanical problems it offers modelling scenarios, constitutive models and boundary conditions specifically relevant to the research areas in biomechanics[22].The mathematical model in *FEBio* is based on the governing equations of continuum mechanics, the associated boundary conditions, initial conditions and constitutive equations[22].

Two software packages, *PreView* and *PostView,* which have been designed specifically for use with the *FEBio* software, are also available. Together these programs provide a tailored solution for research and development in computational biomechanics[22]. *PreView* is a FE pre-processor that facilitates the process of defining the FE models, and creating the input files for *FEBio*. *PreView* is a user-friendly environment that allows the creation of simple geometry and the specification of the boundary conditions and material properties[22]. *FEBio* does not have mesh generating capabilities, and therefore requires pre-processor software *PreView* which has several mesh editing tools available that can be used to customise the geometry. After the problem has been defined in *PreView* it is exported for use in *FEBio.* After being ran through *FEBio*, the finite element model can then be visualised and analysed in the FE post-processor

PostView if required. *PostView* is a graphical interface that is designed to post-process the results from *FEBio*. It contains tools that can be used to visualise data such as displacements, velocities, strains, stresses, fluid pressure, fluid flux and many more.

Maas *et al.* [22] noted that in order to verify the numerical methods and computational implementation of the mathematical model in *FEBio*, the results have to be comparable to analytical solutions or results from a different, established FE code. They verified that the *FEBio* code[22] worked for various set-ups, including a cartilage layer being compressed by a flat, rigid, impermeable surface. As the results found were in very good agreement with previous results, this gave the researchers confidence that the *FEBio* code could provide accurate results for their other computational research questions.

Throughout the project the *FEBio* software (Version 1.8) will be used to do the finite element analysis, along with *PreView* and *PostView.* The complexity of the model will increase, as it is expected that the added complexities will produce more realistic and accurate results. The accurate and quantitative simulation of the biomechanics of tissues has the potential to assist advancements in nearly every aspect of medicine and biology[22], with the possibility of patient specific modelling[26,27] which could revolutionise diagnosis, prognosis and treatment of different diseases. With the advancement of FE models and corresponding algorithms[25,28], *FEBio* has the potential to determine the relationship between cancer properties and the biomechanical properties of cancer tissues.

Two of the important FE algorithms formulated and implemented within *FEBio*, for the contact mechanism of porous media, are described below. Other FE codes that use these formulations are not generally available to the public[25].

In 2010[25], Ateshian *et al.* formulated and implemented a contact FE algorithm for solid-fluid mixtures (biphasic materials) under large deformation and sliding. Contact problems are fundamental to the study of biological tissues[25] and in the study of soft tissues, large deformations are often encountered. They noted that porous media theories are widely applicable to the analysis of biological tissues. There are some available for different FE programs, but they are not commercially available. The theories describe the deformation of the solid matrix and the flow of the interstitial fluid. However, the theories do not address the biomechanics of the porous-permeable

contact of the soft tissues. The algorithm created uses a penalty method regularised with an augmented Lagrangian, in order to enforce the continuity of contact traction and the normal component of fluid flux across the contact interface[25].

In 2011, the same researchers went on to formulate and implement a FE algorithm to analyse the mechano-chemical events that occurred in the finite deformation of porous media[28]. Biological tissues and cells may be modelled as porous media consisting of a solid matrix and an interstitial fluid[28]. In the presence of a porous solid matrix, additional interactions occur between the solute and the matrix, giving rise to additional diffusion and convection effects. Therefore the ability to model the transport of a solute in a deformable porous medium is important in biomedical engineering. As biological soft tissues and cells may undergo both mechanical and chemical loading in their natural environment it is important to analyse the solute-solid interactions.

The accuracy of the implementation of both algorithms was verified using standard problems with exact analytical solutions available via an alternative FE code. To date, biphasic-biphasic contact has been formulated and implemented for idealised geometries, but has yet to be accessible for more general and realistic geometries that would be applicable in biological studies[29].

2.5.4 Input for FEBio

As said previously, *FEBio* is a FE solver and therefore requires *PreView* software to set-up the FE model. The following section will describe the material, geometry, constraint and meshing input utilised by the *PreView* software, obtained from the *PreView* and *FEBio* User's Manuals[19] (Version 1.12 and 1.8 respectively).

In *PreView*, many different constitutive models are available to represent biological materials and synthetic biomaterials[22].After creating the required geometry of the model, different materials can be specified. The biphasic material model is used to model a deformable porous media that shows flow-dependent viscoelastic behaviour resulting from the frictional interactions of the fluid and solid. A biphasic material represents a mixture of a porous-permeable solid matrix and an interstitial fluid. Each constituent is intrinsically incompressible, but the mixture is compressible and may change volume as interstitial fluid is exchanged with the pore space of the solid – the pores of the solid matrix may gain or lose fluid under general loading conditions.

Therefore it is necessary that the fluid permeates the solid, as for a deformable porous media a coupled solid-fluid problem is solved[22].

As established previously, this investigation will be using a biphasic material. In *PreView* a constitutive relation must be selected for both the solid matrix and the hydraulic permeability of the interstitial fluid flowing within the porous deformable solid matrix.

After creating a material and assigning it to a specific part of the model, the material parameters can then be defined. The available parameters will depend on the particular material type. For a biphasic material, along with the specification of the solid and permeability type, the solid volume fraction (φ) must be defined for $0 < \varphi < 1$ – where 0 symbolises 'no solid' and 1 signifies 'no porosity'[19].

There are several isotropic constitutive models for the solid matrix available - such as neo-Hookean, Mooney-Rivlin, Ogden, Arruda-Boyce and Veronda-Westmann - which all have a non-linear stress-strain response and are objective for large deformations. A compressible neo-Hookean material[30] has non-linear stress-strain behaviour, but reduces to the classical linear elasticity model for small strains and small rotations[19].

Unnikrishnan *et al.*[8] used a neo-Hookean material to model breast tissue when investigating the effect of collagen and tissue density. It is commonly used for biphasic materials as it uses a standard displacement-based element formulation, so reduces computational complexity. The neo-Hookean constitutive equation is derived from the following hyperelastic strain-energy function:

$$W = \frac{\mu}{2}(I_1 - 3) - \mu \ln J + \frac{\lambda}{2}(\ln J)^2 \qquad \ldots(4)$$

Where I_1 is the first invariant of the right Cauchy-Green deformation tensor; μ is the viscosity; and J is the determinant of the deformation gradient tensor.

In addition to the general specifications for a biphasic material, for a neo-Hookean solid Young's modulus (E) and Poisson's ratio (ν) parameters must be defined.

Young's modulus, or elastic modulus, is the measure of the stiffness of a material; therefore a stiffer material would have a larger Young's modulus value. There have been numerous studies (including Mow *et al.*, 1980, Prendergast *et al.*, 1996; Ateshian *et al*., 1997; Unnikrishnan *et al.*, 2012; Périé *et* al., 2005; and Busby *et al.*, 2013) which

have involved the use of, or the determination of, a tissue's Young's modulus or aggregate modulus value. In the most recent study, by Busby *et al.*[4] on the confined compression of 0.3% collagen hydrogels, the aggregate modulus (H_A) was found to be $1 \pm 0.08kPa$. This value will be taken as the most relevant as the body tissue and tumour tissue will both be modelled as a collagen gel, and there are no relative recent investigations into the Young's modulus of collagen gels. The aggregate modulus (H_A) is a measure of stiffness in confined compression[19], and can be converted to Young's modulus (E) via Equation 3 defined previously in Section 2.4.1. The value quoted for aggregate modulus of a 0.3% collagen gel is converted into a Young's modulus value (see Appendix 1) of $0.00096429\,MPa \equiv 0.001MPa$. Subsequently, as in this investigation a 0.3% collagen gel was used, the solid volume fraction value (φ) will be taken as 0.003.

Poisson's ratio is defined as the ratio of transverse to axial strain, meaning it is the fraction of expansion over compression. It is said that if a tissue is incompressible it's Poisson's ratio $\cong 0.5$. In the comparison of FE codes for biphasic problems (Prendergast *et al.*, 1996) the Poisson's ratio value was taken to be 0.1667for cartilage; and in an investigation of the true Poisson's ratio of nucleus pulposus (Farrell and Riches, 2012) it was found to be 0.125 ± 0.072. Taking the result from the most recent study to be more accurate and reliable, the Poisson's ratio value of soft tissue, modelled by a collagen gel is taken to be 0.125.

Permeability refers to the ease by which the interstitial fluid flows through the solid matrix[18]. Therefore a high permeability means the fluid flows easier and faster, and there are only small drag forces generated. Permeable materials provide a constitutive relation for the hydraulic permeability of a biphasic material. The simplest model is when the permeability is considered to be isotropic. The isotropic material model uses the biphasic theory for describing the time-dependent material behaviour of materials that consist of both a solid and fluid phase. For a constant isotropic permeability the hydraulic permeability (k) must be defined. Using the same study that the Young's modulus is taken from (Busby *et al.*, 2013) the hydraulic permeability of the collagen matrix is taken to be $0.28 \pm 0.01x10^{-10}\ m^4/Ns$.

FEBio also contains a rigid body constitutive model which can be used to represent structures whose deformation is negligible compared to that of other structures in the

overall model[22]. The manual states that the Young's modulus and Poisson ratio of the rigid body currently have no effect on the results.

A mesh is added to the FE model to create the different elements and to define nodes at the locations where changes of geometry or loading occur. Noted in previous studies, including a comparison of different FE codes by Prendergast *et al.*[18], there is no radial variation in a confined compression test. Therefore, only one mesh element is required in the *xy* plane. This means that more elements can be created in the *z*-direction, as this is where the changes will occur. This will in turn assist in reducing computational time.

Various boundary conditions and loads can be applied with *PreView*. These include fixed constraints, prescribed constraints, prescribed surface loads and tractions, body forces, etc. The fixed and prescribed constraints can be applied in each different degree of freedom (x, y or z): either to constrain the structure to prevent body motion and restrict motion in non-desirable directions; or to apply a set motion in a given direction through an associated load curve, which can be modified in the Curve Editor. Fixed constraints are generally called zero constraints, as the corresponding degree of freedom is kept zero throughout the entire analysis. This means that the nodes are restricted form moving and/or rotating. In biphasic analysis, there is a fluid pressure boundary condition which can either be a zero or a prescribed constraint. It can be set to zero on a surface to define a free-draining surface, meaning that fluid will be able to leave the model through this surface. Rigid body constraints are also available to specifically constrain the degrees of freedom of a rigid body, as they are initially unconstrained in this version of *FEBio*.

PreView can be used to set-up several types of contact conditions including rigid, sliding, rigid wall, rigid joint, tied, biphasic and biphasic-solute. These contact conditions allow the connection of non-conforming meshes to each other or the specification of non-penetrating constraints. A rigid tied-interface is used to connect a part of the deformable mesh to a non-conforming rigid body. This only means that little, or no, nodes are shared between the two objects and the nodes on the mesh of the deformable object do not compare directly to the nodes of the rigid body at the interface. The biphasic contact defines a non-penetrating constraint between two surfaces that allows fluid flow across the interface from one part of the model into the other, if both contacting surfaces are defined as a biphasic material. Fluid will flow through the contact interface in the presence of a fluid pressure gradient across the

interface[22]. A tied interface can be used to link two possibly non-conforming surfaces together. Therefore, a tied-biphasic interface can be used between two biphasic materials to ensure continuity of fluid flow across the biphasic-biphasic contact interface, independent of position of the nodes on each element.

PreView is used to create the FE model and divide it into different elements using the meshing function. The elements are connected at nodes, and it is at these nodes that the boundary conditions are applied. The output of *PreView* is then run in *FEBio*, which solves the system of equations involving the unknown quantities at the nodes, approximates a system of equations for the whole structure and calculates the desired quantities at the selected elements.

The *FEBio* software also requires some programming skills in order to add new functionality to the codes that you are unable to do in *PreView*. Such additions include having a numerical log file containing the results that can then be used in a different program to plot the output response of the model (see Appendix 2).

2.5.5 FEBio vs. ABAQUS

In 2013, Meng *et al.*[32] directly compared two FE modelling programs, *ABAQUS* (Version 6.9-EF1) and *FEBio* (Version 1.5.0). Three different practical contact problems involving cartilage were modelling using both programs, and the results were compared. It is important to compare different FE codes for verification, and also for practical problems where no analytical solution exists[32]. It is common practice in biomechanical analyses to compare the solutions of the same problem produced by different codes to ensure newly developed software is accurate. Additionally, in biomedical applications, the problems generally involve a complex geometry and/or un-realistic conditions, so it is essential to use the most accurate and precise numerical approximation technique in order to overcome these limitations. The comparison of *ABAQUS* and *FEBio* is necessary as *ABAQUS* is one of the most widely used commercial FE programs, and *FEBio* has only been developed recently, in 2012. *ABAQUS* is one of the most established FE software packages available and provides many powerful features, however, it is said that its biphasic contact implementation shows significant limitations[29].Conversely, as *FEBio* is based on biphasic theory that is derived from mixture theory of porous media[22], meaning it has a biphasic material model embedded within the code.

A wide range of comparative tests were performed to examine the performance of newly developed *FEBio* to existing program ABAQUS, for different material models, geometry and conditions. Through direct comparison, it was found that there was excellent agreement between *ABAQUS* and *FEBio* for all model types, and across the full range of material properties investigated[32].No biphasic problems were included in this comparison, but it was found under different loading conditions and for a range of material properties, the two programs produced similar results. *FEBio* has a slight advantage as it enforces contact-dependent surface fluid flow boundary conditions automatically[32].

Previously, there have been comparisons made between other software packages to analyse biphasic tissue mechanics, using the standard confined compression problem[18]. Prendergast *et al.*[18] compared their results to the results of Spilker, Suh and Mow[15] who first presented a solution to the confined compression problem for cartilage, and found a close comparison for both the linear and non-linear case. It was concluded that even though there are some theoretical differences, it is acceptable to use available soil mechanics codes for the analysis of linear and non-linear problems in biphasic tissue mechanics[18]. However, other aspects of the tissue behaviour, such as tissue reactivity and movement of charged phases, are not being considered. Therefore a purpose-written code for the analysis of biphasic tissue mechanics problems would be beneficial.

From the review of different FE programs, *FEBio* appears to be the most accurate for biphasic problems as it has been specifically designed for biomechanics problems[22,25]. Additionally, since little investigations have been carried out using it, it will be used in this research in the determination of a biomechanical biomarker of cancer.

2.5.6 Mathematical Modelling in Cancer Research

Mathematical modelling has been proposed to be advantageous and beneficial in cancer research, over *in-situ* or *in-vivo* investigations, as they are cheaper and more controllable. Computations and mathematical models also have the ability to determine tissue behaviours of tumours deep inside the human body, taking away the need for surgical procedures[8]. Computations involving mathematical models, such as FE models, provide a quantitative analysis of the local mechanical properties of the tumour itself and the tissue surrounding it. Therefore computational simulations have been said to have the potential to assist in the early detection and prognosis of tumour tissues.

Before a medical procedure, such as surgery to remove a tumour, it is important to determine the etiology of the tumour[8]. In these situations it would be beneficial to have an accurate computational model that could predict the prognosis, in order to determine the correct surgical procedure. For computational modelling, the numerical data required includes both the tumour and host tissue geometry, as well as the material behaviour representation of both the tumour and host tissues[8]. Biddiss *et al.*[33] indicated that an accurate and constitutive model of tumour tissue would increase the preciseness of the biomechanical simulations and decrease computational time. They noted that in turn this would help provide real-time diagnosis.

In 2012, Unnikrishnan *et al.*[8] conducted a computational based biomechanical study of normal breast tissue density and position and size of a breast tumour, and the direct correlation with the micro-structural constituents of the normal breast tissue. They wanted to estimate the mechanical properties of the breast tissue, as well as finding the comparison between the computational simulation, experimental observations and theoretical analysis. They performed FE simulations of the whole breast to determine the macro-scale deformation response of the breast under the influence of an underlying tissue. They developed computational simulation for a variety of sizes and positions of the tumour and different breast tissue densities to simulate routine clinical examinations – to see if tumour size/position or breast tissue density affected the results. It was concluded that an increase in collagen content had a significant effect on the stiffness of the tissue, and that the higher the density of the tissue the greater resistance it had to deformation. They determined that the stress and strain within the breast can be used as an indicator of whether the tissue is cancerous of not, going on to establish that the tumour size and tumour depth within the tissue caused differences in tumour detection, with the size of the 'tumour' being less distinctive when the tumour is positioned further from the surface[8]. Consequently, this study can be said to provide a fundamental understanding of the change in the biomechanical behaviour of a denser breast compared to normal breast.

There have been several investigations into the mechanical behaviour of cells, including one by Pachenari *et al.*[14] who developed a FE model validate actual experimental results and to predict the behavior of cells. However, this investigation will be conducted on the tissue level so that the environment surrounding the tumour can also be included in the analysis. Another investigation by Guo and Spilker[29] developed a biphasic FE formulation for the frictionless contact of soft tissues in the

commercial software *COSMOL Multiphysics*. They stated that the study of biphasic contact was fundamental in understanding the biomechanical behaviour of soft tissue. Therefore, it is important in this study to understand the biomechanical behaviour of the tumour tissue, the host tissue and the contact interface between the soft tissue layers. This will assist in better diagnostic techniques, as well as improving surgical procedures.

2.6 Thesis Aim

The NHS states[9] it is impossible to tell whether a lump or growth in your body if malignant (cancerous) or benign (non-cancerous) just by observation or external examination, and a biopsy should be used to provide this information. However, in 2012, Xu *et al.*[13] suggested that cell stiffness was a possible biomarker of the metastatic potential of ovarian cancer cells. They proposed that mechanical stiffness may be a useful biomarker in the development of an accurate and non-invasive method of evaluating the spread of cancer cells[13]. This project's aim is to develop a biomechanical examining technique to determine a biomechanical biomarker that will assess the grade and type of tumour present. This would create a quicker and equally effective diagnosis technique that has the ability to identify the same staging characteristics as a biopsy. It would be beneficial in reducing the amount of invasive surgery the patient is undergoing, reducing patient morbidity and making better use of operating theatre time[2].

As defined previously, a higher collagen content causes the tissue to appear denser and become stiffer and more 'solid-like'. Therefore with a higher collagen content the tissue will exhibit different biomechanical characteristics. The FE analysis programme *FEBio* will be used to model different biphasic confined compression experiments, based on the tests carried out by Busby *et al.*[4]. The stiffness parameters will be taken from previous research, as stated in the literature review, and the tissue will be compressed in both displacement and force loading conditions. The stiffness parameters of the biphasic material will be altered in order to illustrate a varying collagen content, and it will be determined whether or not the change in stiffness parameters has an effect on the mechanics of the tissue at the surface. Since *FEBio* is a relatively new and untested code, especially for biphasic studies including contact interfaces, a variety of preliminary assessments were made to ensure the correct operation and implementation of the biphasic contact problem.

The main aim of this project will be split into two sections, each with a small number of objectives. The first part of the aim will be model validation in *FEBio* which includes validation of *PreView* biphasic material, validation of *PreView* tied-biphasic contact interface, and validation of *FEBio* coding. The second part of the aim will be parameter sensitivity analysis which consists of stiffness parameter specification, force control testing, and displacement control testing.

3. Methodology

3.1 Model Validation

3.1.1 Validation of *PreView* Biphasic Material

In *PreView* a simple model of a one-dimensional (1D) confined compression of a homogeneous media was created. It consisted of a simple geometry cube element ($10x10x10$) illustrating the tissue, and a combination of two cubes, a platen ($10x10x5$) and a handle ($3x3x7$), to create the plunger (see Figure 1).

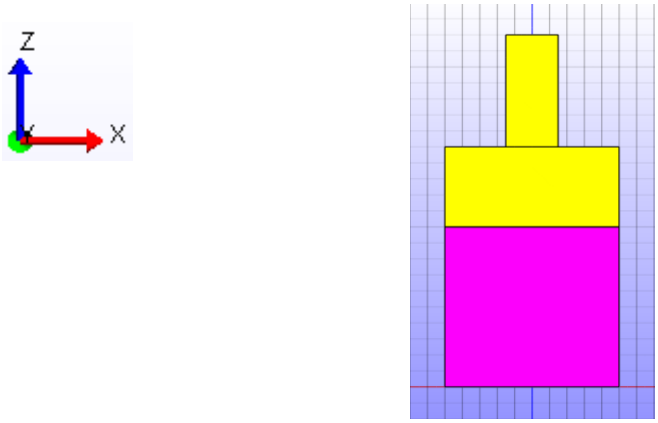

Figure 1 - *PreView* set-up of 1D Biphasic Control Model

Both the platen and handle were modelled by a rigid body material of density 1 and COM's (Centre of mass) at (0,0,12.5) and (0,0,18.5) respectively. The Young's modulus and Poisson's ratio of the rigid body materials were both set to zero, as the material of these parts has no influence on the results. A biphasic material with neo-Hookean solid and constant isotropic permeability '*perm-const-iso*' was assigned to the 'tissue', using parameters for solid volume fraction (φ), density (d), Young's modulus (E), Poisson's ratio (v) and hydraulic permeability (k) taken from examples in the *PreView* User's Manual. The parameters to be used are shown below, with E in units of MPa and k in units of mm^4/Ns:

$\boldsymbol{\varphi}$	0.2
$\boldsymbol{d}$	1
$\boldsymbol{E}$	1
$\boldsymbol{v}$	0.1
$\boldsymbol{k}$	0.001

Table 1 - *PreView* Parameters of Biphasic Material for Control Model

As there is no radial variation in the model, so the analysis will be in the vertical direction only. Consequently, a mesh with one element in the xy plane and 100 elements in the z-direction ($nx = ny = 1$; $nz = 100$) was applied to the 'tissue'. Both the platen and the handle had a one element mesh in each direction ($nx = ny = nz = 1$), as these parts of the model will not be included in the analysis (see Figure 2).

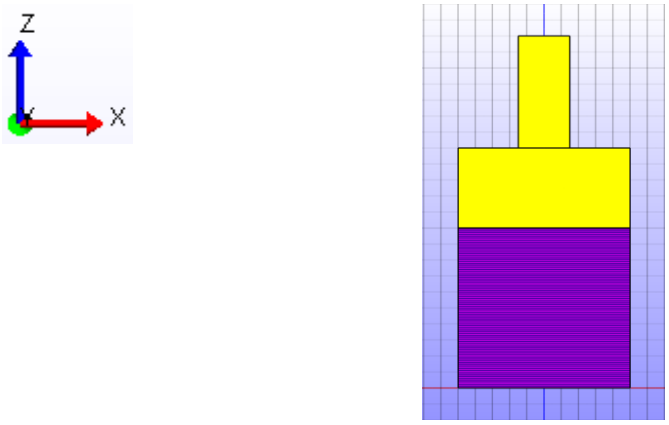

Figure 2 - *PreView* Image of 1D Biphasic Control Model with Mesh applied

A rigid interface was applied between the two rigid bodies of the plunger, at a joint position of (0,0,15), to create a solid plunger. A tied interface was placed between the bottom of the platen and the top of the 'tissue' and all outer surfaces of the 'tissue' were laterally constrained, in the x and y directions. The bottom surface was also restrained axially, in the z direction. The pore pressure on the upper surface of the 'tissue', at the tied interface, was set to zero to simulate a porous plunger, allowing the free flow of interstitial fluid out of the tissue that occurs in a confined compression experiment. A prescribed displacement of $-1mm$ was prescribed with a ramp time of $100s$, on the upper side of the plunger, illustrating a 10% compression test ($0.1\%/s$ strain rate).

The biphasic analysis consisted of one step which lasted $2000s$ and had 20,000 time steps. The file was then exported and ran in *FEBio* in order to predict whether or not the biphasic material functions correctly. If fully functioning, this model will be regarded as the control model.

3.1.2 Validation of *PreView* Tied-Biphasic Contact Interface

A similar *PreView* set-up to that described in Section 3.1.1 was used to create a 1D two-layer biphasic material model. An additional 'tissue' layer was created, so the geometry now consisted of two cube elements ($10x10x10$) below a solid plunger of the

same dimensions used in the previous section (see Figure 3). The top 'tissue' was labelled *bp-top* and the bottom one labelled *bp-bottom*.

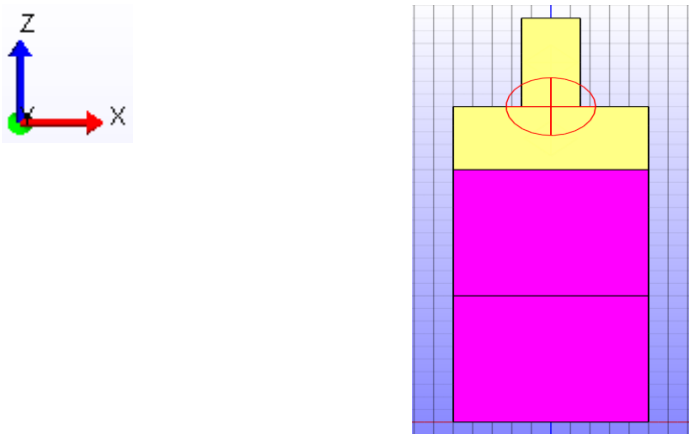

Figure 3 - *PreView* set-up of 1D Two-Layer Biphasic Model

Both the platen and handle were modelled by the same rigid body materials of density 1, and had COM's at (0,0,22.5) and (0,0,28.5) respectively. The biphasic parameters defined before (Table 1) were applied to both the biphasic layers. The same meshes were assigned to the rigid bodies; and both the biphasic layers, *bp-top* and *bp-bottom*, had a $nx = ny = 1;\ nz = 100$ mesh applied (see Figure 4).

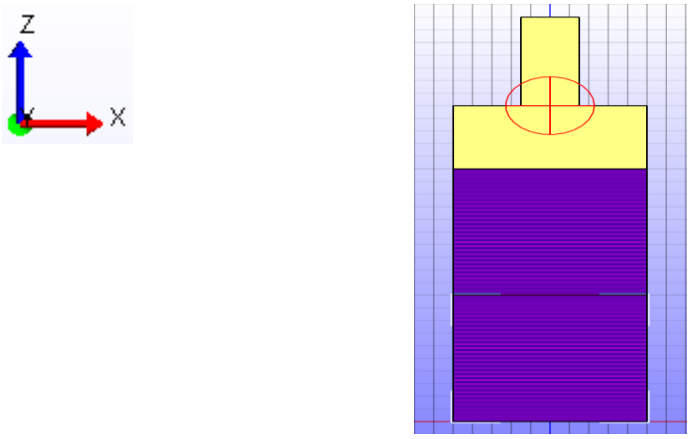

Figure 4 - *PreView* Image of 1D Two-Layer Biphasic Model with Mesh applied

A rigid interface was applied between the two rigid bodies of the plunger, at a joint position of (0,0,25), to create a solid plunger. A tied interface was placed between the bottom of the platen and the top of *bp-top,* the same as before. Additionally, a tied-biphasic interface was assigned between *bp-top* and *bp-bottom*, which allows free flow of the interstitial fluid part of the model during compression. The same boundary conditions as used for the preceding model were generated.

A prescribed displacement of $-2mm$ was prescribed with a ramp time of $100s$, on the upper side of the plunger, illustrating a 10% compression test ($0.1\%/s$ strain rate).

The biphasic analysis consisted of one step that lasted $200{,}000s$ and had 2,000,000 time-steps. The file was then exported and ran in *FEBio*, and the output was compared to the control model created in Section 3.1.1, in order to determine whether or not the tied-biphasic interface functioned properly. If the tied-biphasic interface functions correctly, it will conclude that the applied boundary conditions are satisfactory.

3.1.3 Validation of FEBio Coding

To validate the coding within the *FEBio* programme, both a force control and a displacement control model were required. As the correct force to represent a 10% compression test is unknown, the process begins with a 10% compression under displacement control. The biphasic control model created in Section 3.1.1 was modelled under a prescribed displacement of $-0.8mm$ in $100s$, illustrating a 10% compression ($0.1\%/s$ strain rate) for a geometry of $10mm \times 10mm \times 8mm$.

The output force of this model was found by running the *.feb* file through MATLAB (see Appendix 3). Under the prescribed displacement shown in Figure 5, the reaction force at the platen is shown in Figure 6.

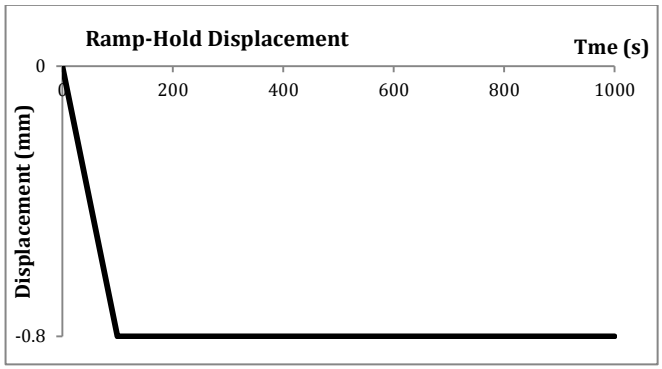

Figure 5 - 10% Ramp Compression used as Prescribed Displacement Input

The curve shown was manually adjusted by inspection, in order to smooth it and create an equivalent graph at equally spaced time steps, which is suitable for input in *PreView*. Four different methods were used in order to determine an appropriate force input curve that would provide output displacement curve of the run the same as the initial 10% ramp of the initial prescribed displacement compression (Figure 5). The *FEBio* coding is verified if there is no difference in the displacement output curve compared to the original ramp and hold input.

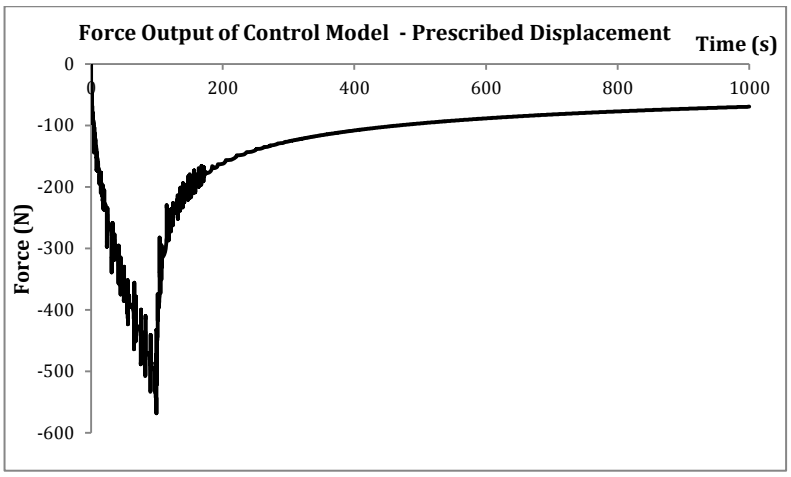

Figure 6 - Reaction Force of Control Model Under Displacement Control

The four different methods used to determine a curve that best fit the raw data were:

1) Use Original Output as Prescribed Force Input
2) Approximation of Load Curve Points
3) Averaging the Data
4) Finding the Best Approximation using the Exponential Function

The first method was attempted using the curve given in Figure 6 directly as the load curve input in *PreView*. As can be seen in Figure 6, there are a lot of discontinuities and disturbance in the force output. Therefore, the second method was used to smooth the curve in an attempt to create a better input for *PreView*.

The main force points on the curve were approximated as:

$$0N \text{ at } 0s \rightarrow (0, 0)$$
$$-550N \text{ at } 100s \rightarrow (100, -550)$$
$$-200N \text{ at } 200s \rightarrow (200, -200)$$
$$-100N \text{ at } 300s \rightarrow (300, -100)$$

Then the force is constant at approximately $-100N$ for t→equilibrium

Plotting these points (Figure 7) creates a new force graph that is now smooth enough to be used as a prescribed force input.

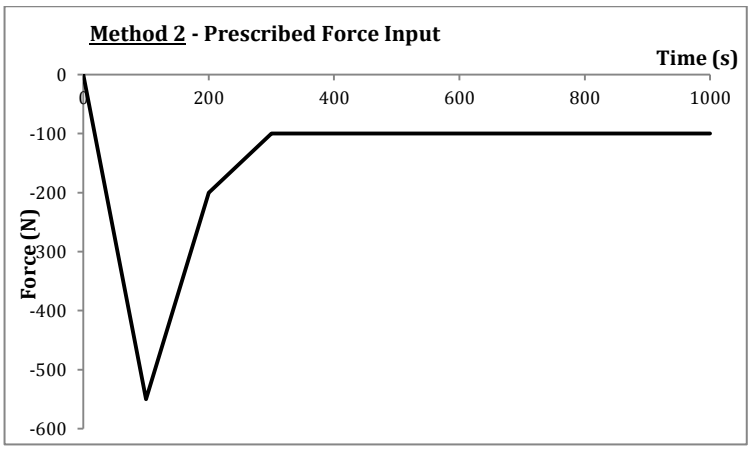

Figure 7 - Method 2 Prescribed Force Input

In order to get a better approximation of the data, and slightly more data points than in Method 2, the third method to 'smooth' the curve used the averaging function available in *Excel*. The new force graph obtained for averaging of 100 data points is shown in Figure 8 on the next page. This force curve still has a slight discontinuity after the end of the ramp phase, and is seen to not reach the correct maximum force. Therefore an additional technique was attempted in order to smooth the curve and create equally spaced time steps.

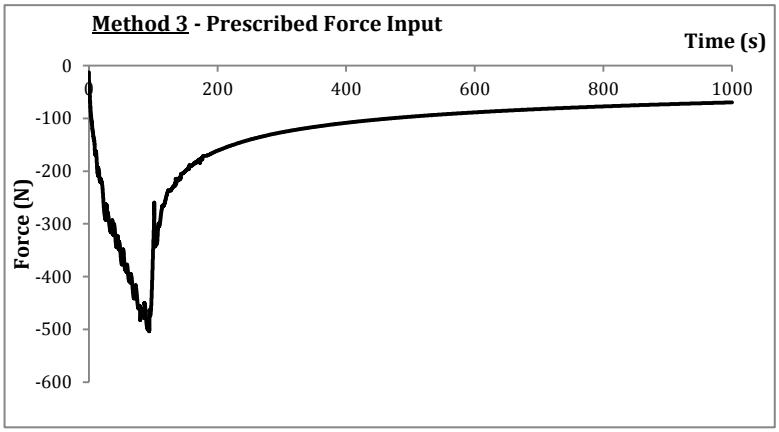

Figure 8 - Method 3 Prescribed Force Input

Method 4 used the exponential approximation function available in *Excel*.

$$Exp\ approximation = A + Bexp\left(\frac{t}{\tau_1}\right) + Cexp\left(\frac{t}{\tau_2}\right) + \cdots \quad \ldots(5)$$

When using the exponential function (Equation 5) to approximate the data, the data should be split into two parts, and the function applied to each part separately. The two sections of this data were $0s \rightarrow 100s$ (ramp section) and $100s +$ (hold section). The

curve was manually adjusted by inspected, and to ensure the boundary conditions were met the data was constrained so that the two sections met at the peak point, $t = 100s$. The equations that are found for each section, which follow the prescribed boundary conditions, were then used to compute a curve at regular intervals of t. Through curve fitting, the best approximation of the force data is presented in Figure 9 below.

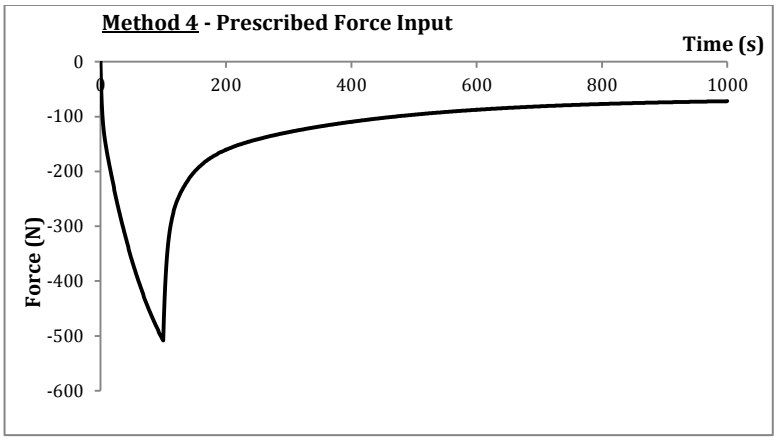

Figure 9 - Method 4 Prescribed Force Input

3.2 Parameter Sensitivity Analysis

3.2.1 Stiffness Parameter Specification

After verification that both the biphasic material and tied-biphasic interfaces function correctly in *PreView*, the set-up in Section 3.1.2 was enhanced in order to create a three-layered biphasic tissue. A commonly used testing dish (see Figure 10) was measured in order to get realistic tissue dimensions.

Figure 10 - Commonly Used Testing Dish for Biological Samples

Assuming the tissue sample is only half the depth of the testing dish, the dimensions (in mm) of an ideal experimental tissue, modelled by a cube, were found to be (see Appendix 4):

$\boldsymbol{x}$	13.3
$\boldsymbol{y}$	13.3
$\boldsymbol{z}$	8

Table 2 - Dimensions of Modelled Tissue Based on Testing Dish (units: *mm*)

Therefore, the geometry now consists of three cube elements (with a combined height of $8mm$) below a solid plunger consisting of a platen ($13.3mmx13.3mmx2mm$) and a handle ($3mmx3mmx2mm$). Both the platen and handle were modelled by the same rigid body material of density 1, with a $nx = ny = nz = 1$ mesh applied on each and had COM's at (0,0,9) and (0,0,11) respectively.

The three biphasic layers were labelled *bp-top, bp-middle* and *bp-bottom* depending on their position within the 'tissue' – *bp-middle* illustrates the 'tumour' layer of the tissue. The full dimensions of the 'tissue' are $13.3x13.3x8$. Therefore, the 'tumour' layer will be considered to be $1mm$ thick, having dimensions $13.3x13.3x1$, and will be modelled at various positions to illustrate the varying depth of a 'tumour' within the 'tissue'. The biphasic material and mesh ($nx = ny = 1;\ nz = 100$) previously defined in Section 3.1.1 were applied to all the biphasic layers.

A rigid interface was applied between the two rigid bodies of the plunger, at a joint position of (0,0,10), to create a solid plunger. A tied interface was placed between the bottom of the platen and the top of *bp-top,* as done previously. Additionally, a tied-biphasic interface was assigned between both the bottom of *bp-top* and the top of *bp-middle*, and the bottom of *bp-middle* and the top of *bp-bottom*. The same boundary conditions as Section 3.1.1 should be created.

Additionally, the geometry of the control model created in Section 3.1.1 was altered in order to have an equivalent model. The new dimensions of the homogeneous control are $13.3x13.3x8$. The control was assigned with the same biphasic material as the other models, and had a mesh $nx = ny = 1; nz = 300$ assigned in order to be comparable to the meshes on the other models. The hierarchy of models showing the seven different positions of *bp-middle*, and corresponding dimensions of *bp-top* and *bp-bottom* are presented in Figures 12-18, with the corresponding control model in Figure 11.

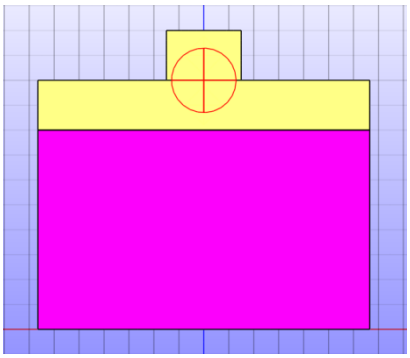

Figure 11 - Bpcontrol

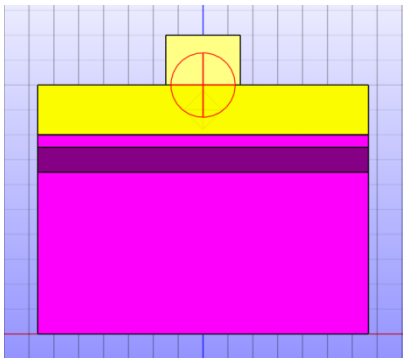

Figure 12 - Bpplaten1

bp-top = 13.3*x*13.3*x*0.5

bp-bottom = 13.3*x*13.3*x*6.5

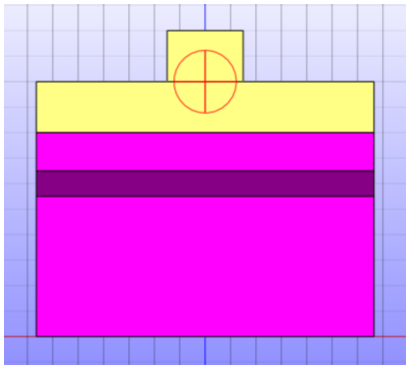

Figure 13 - Bpplaten2

bp-top = 13.3*x*13.3*x*1.5

bp-bottom = 13.3*x*13.3*x*5.5

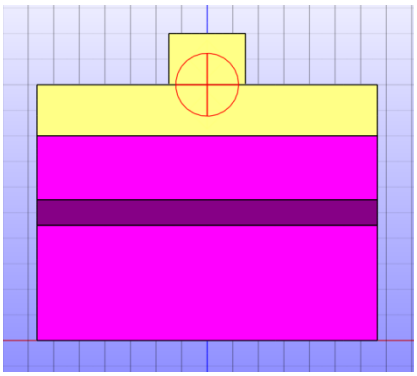

Figure 14 - Bpplaten3

bp-top = 13.3*x*13.3*x*2.5

bp-bottom = 13.3*x*13.3*x*4.5

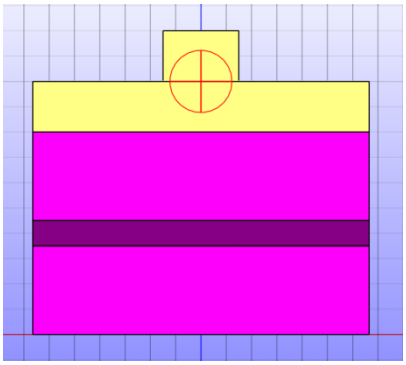

Figure 15 - Bpplaten4

bp-top = 13.3*x*13.3*x*3.5

bp-bottom = 13.3*x*13.3*x*3.5

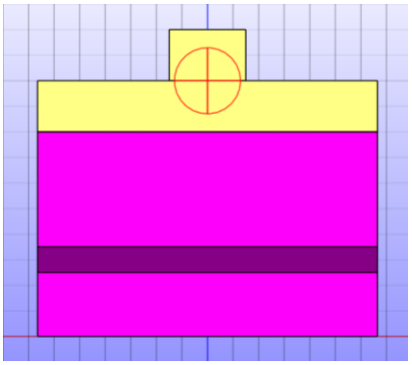

Figure 16 - Bpplaten5

bp-top = 13.3*x*13.3*x*4.5

bp-bottom = 13.3*x*13.3*x*2.5

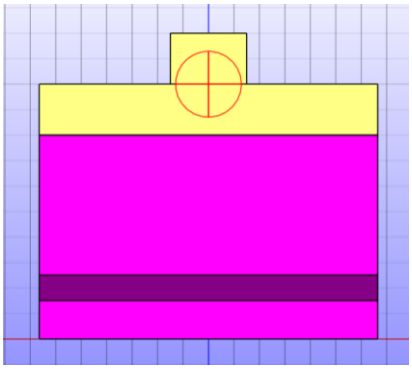

Figure 17 – Bpplaten6

bp-top = 13.3*x*13.3*x*5.5

bp-bottom = 13.3*x*13.3*x*1.5

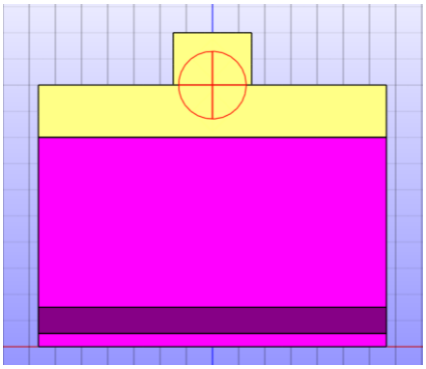

Figure 18 – Bpplaten7

bp-top = 13.3*x*13.3*x*6.5

bp-bottom = 13.3*x*13.3*x*0.5

It is expected that for the models created above, which have a 'tumour' layer in different positions within the medium, the output displacement will change from the control when the stiffness of the 'tumour' layer is altered. This change in output will provide information on whether or not the determination of a biomechanical biomarker is possible.

As stated previously, tumours are considered to be stiffer than normal body tissue, and will therefore be modelled as more 'solid-like'. To adjust the stiffness of *bp-middle* the Young's modulus (E) and permeability (k) parameters of the material were altered. As it is known that as E increases the stiffness of a material increases, the Young's modulus values should be increased in orders of magnitude to exhibit a more 'solid-like' material. The Young's modulus (E) value was increased in equal steps up to a magnitude of $x1000$ of the 'norm' value (E (0)) taken from Busby *et al.*[4]. Namely, magnitudes of $x250$, $x500$, $x750$ and $x1000$ were used (Table 3).

E (0)	0.001
E (x250)	0.241
E (x500)	0.482
E (x750)	0.723
E (x1000)	0.96429

Table 3- Increasing Values of Young's Modulus (units: mm^4/Ns)

As mentioned in the literature review, less information is known about the relationship between the permeability of a material and the material stiffness; the k values are thus changed to orders of magnitude both above and below the norm in order to model a range of stiffness's. The permeability value was changed in magnitude to values $x10$ or $x100$ larger or smaller than the 'norm' value (k (0)) taken from Busby *et al.*[4] paper as shown in Table 4 below.

k (0)	100
k (-x10)	10
k (-x100)	1
k (+x10)	1000
k (+x100)	10,000

Table 4 - Varying Values of Permeability (units: N/mm^4)

Using results from Busby *et al.*[4], the normal tissue of the models should be modelled as a 0.3% collagen gel. The parameters of the material, with symbols defined previously, are shown in Table 5 below.

φ	0.003
d	1 g/mm^3
E	0.96429 N/mm^2
k	100 mm^4/Ns

Table 5 - Material Parameters taken from Busby *et al.*[4] Investigation

These parameters are taken for a Poisson's ratio (ν) of 0.125[31] (see Section 2.5.4), and they were used for *bp-top*, *bp-bottom* and the homogeneous control material.

For each of the seven models available, 25 different stiffness circumstances were created by using five different E and k values. This gives a total of 176 runs (including the control experiment for the new parameters). The aim is to carry out parameter sensitivity analysis, by altering the height (closer to plunger) and stiffness (E and k values) of the 'tumour' layer, in order to determine changes in mechanical response and investigate when the 'tumour' layer becomes mechanically important.

3.2.2 Force Control Testing

From previous runs it was determined that prescribed displacement simulations were very time consuming, with some runs in *FEBio* taken over 4 hours. Therefore, force control testing was carried out to determine if it provided a quicker analysis. The control model created in Section 3.2.1 was initially ran through a displacement control test with the same prescribed displacement used in Section 3.1.3, Figure 5. The purpose of this was to obtain a force curve that illustrated a 10% compression, for the new parameters, that could be used as an input in *PreView* using one of the methods explained in Section 3.1.3. The reaction force found at the plunger is shown in Figure 19 below.

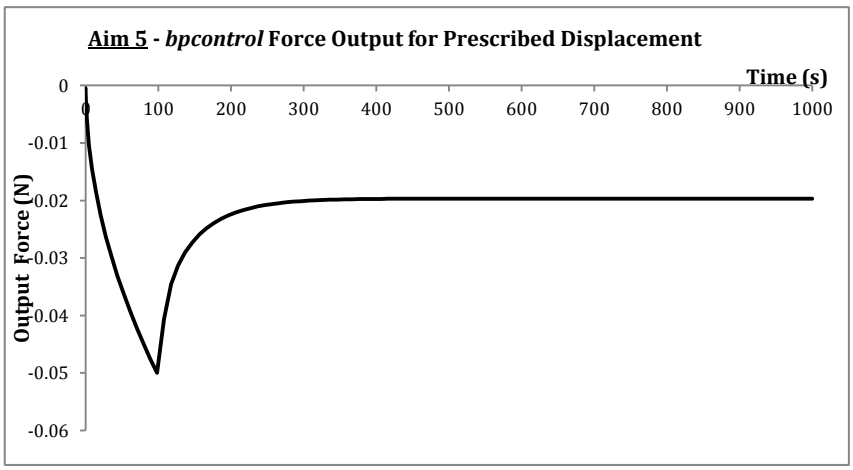

Figure 12 - Output Force for *bpcontrol* with Updated Parameters

As can clearly be seen from Figure 19, the output force is smooth, therefore no curve fitting techniques is required, and Method 1 from Section 3.1.3 can be used – the original force output is used as a prescribed force input.

The biphasic analysis consisted of one step that lasted 1000s and had 100,000 time-steps. Using the curve defined in Figure 19 and the parameters defined previously (in Tables 3, 4 and 5) the 175 different models were ran through *FEBio* under a prescribed force experiment. The control model was also run under a force control test so that it could be used as a comparison. The *.feb* files created were then ran through MATLAB (see Appendix 3 for code used), and the output graphs compared to each other and the control in order to determine the effect of position and stiffness of the 'tumour' layer under a force controlled test.

3.2.3 Displacement Control Testing

After obtaining the numerical values corresponding to the experimental data presented in the graphs of the 2013 paper by Busby *et al.*[4], it was found that the permeability was in fact $28\ mm^4/Ns$. This meant that the different k values used for varying the stiffness of the 'tumour' layer also changed. The new permeability values are noted in Table 6 below, where $k(0)$ is considered to be the control value for the permeability.

k (0)	28
k (-x10)	2.8
k (-x100)	0.28
k (+x10)	280
k(+x100)	2800

Table 6 - Permeability Values for Displacement Control Test (units: mm⁴/Ns)

Using the updated parameters, the *.feb* files from Section 3.3.2 were altered in order to create a more representative model of the samples used by Busby *et al.*[4]. The other parameters used for the models, with symbols and units as defined previously, are displayed in Tables 7 and 8.

φ	0.003
d	1
ν	0.125

Table 7 - *PreView* Parameters for Displacement Control Test

E (0)	0.001
E (x250)	0.241
E (x500)	0.482
E (x750)	0.723
E (x1000)	0.96429

Table 8 - Young's modulus Values for Displacement Control Test (units: N/mm⁴)

From Section 3.3.2, the prescribed force simulations were found to take a similar amount of time to some of the prescribed displacement tests. Therefore, as the displacement control testing procedure is easier experimentally, it means that the results can be compared directly to previous experimental studies. For that reason, each model, with the updated parameters, will be tested under a displacement control simulation. The prescribed a displacement was similar to the experimental ramp-hold displacement carried out by Busby et al.[4], who applied a compressive strain of 0.5%/s - which is equivalent to a prescribed displacement of -0.4mm with a ramp time of 10s - illustrating a 5% compression test (see Figure 20). The biphasic analysis consisted of one step that lasted 1000s and had 100,000 time-steps.

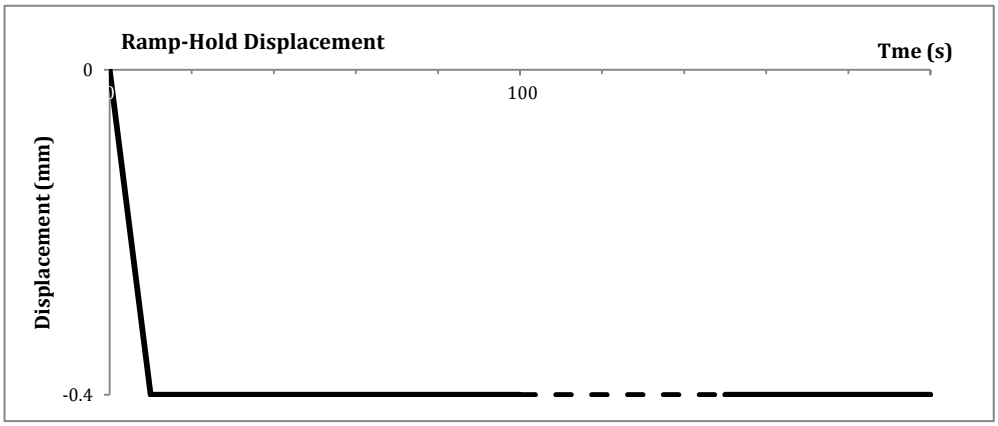

Figure 13 - Ramp-Hold Input for 5% Compression Displacement Input

Similar to Section 3.3.2, for each of the seven models created 25 different stiffness circumstances were applied, using the five different E and k values defined in Table 8 and Table 6 respectively. This gives a total of 176 runs (including the control experiment for the new parameters). The files were exported and ran in FEBio and the outputs, of each of the 176 models, were processed in MATLAB (see Appendix 5 for code used) in order to gain the peak and equilibrium stress values. The values were then compared in order to determine if 'tumour' depth or stiffness has an effect on the biomechanical force response of the tissue in confined compression.

4. Results

4.1 Model Validation

4.1.1 Validation of *PreView* Biphasic Material

After the $10x10x10$ box of homogeneous biphasic material was created, a 10% compression, under displacement control, was initiated in the z-direction. The output force response, recorded at the platen, is illustrated in Figure 21 below. As can be seen, the confined compression test in *FEBio* of this biphasic material has provided a force response with well-defined ramp and hold phases. The ramp phase is between $0 - 100s$, the same as the prescribed displacement ramp input; and the end of the ramp phase creates a peak, which is an important point to analyses when looking at biphasic behaviour.

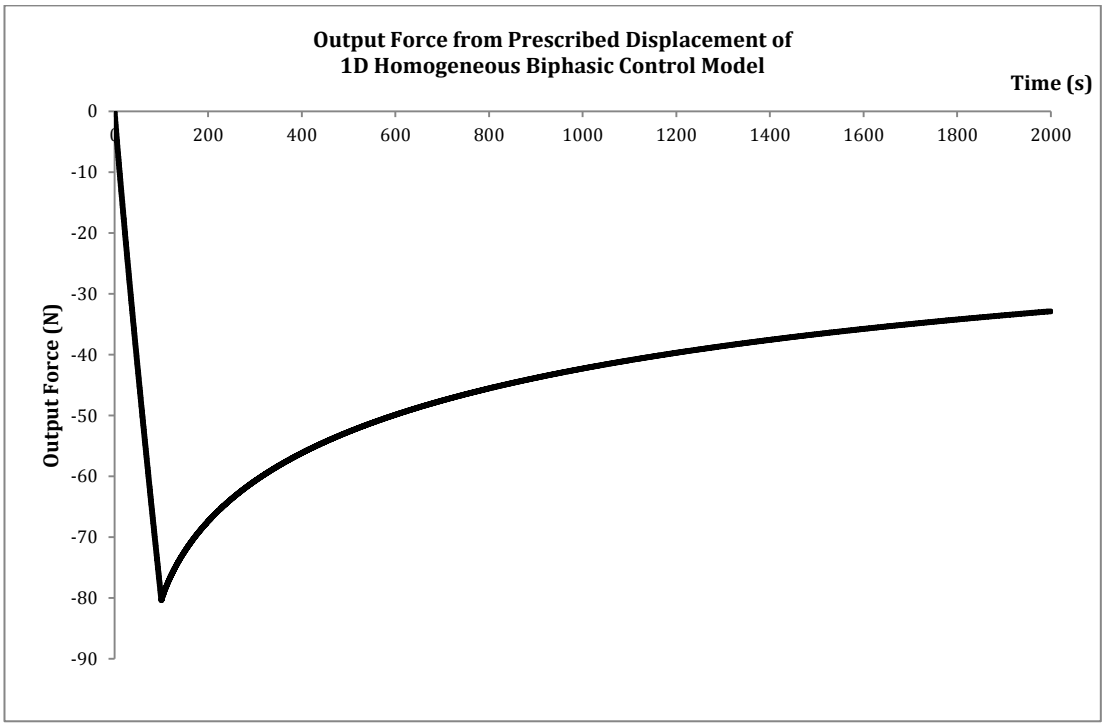

Figure 14 – 1D Control Model Output Force from Prescribed Displacement Test

In order to visualise whether the biphasic material functions correctly, the analysis of fluid flux was viewed in *PostView* (Figure 22). *PostView* has dynamic analysis, and therefore the appropriate legend is given with each time frame – irregular time intervals are shown for the full length of the analysis. Through explanation of the material behaviour, it should be clear whether or not the material is biphasic. Note that the red sections illustrate an area of high fluid flux, and dark blue an area of little, or no, fluid flux.

Figure 15 - *PostView* Analysis of *z-fluid flux* for the 1D Control Model, at Irregular Time Intervals, for the Full Length of the Analysis (2000s).

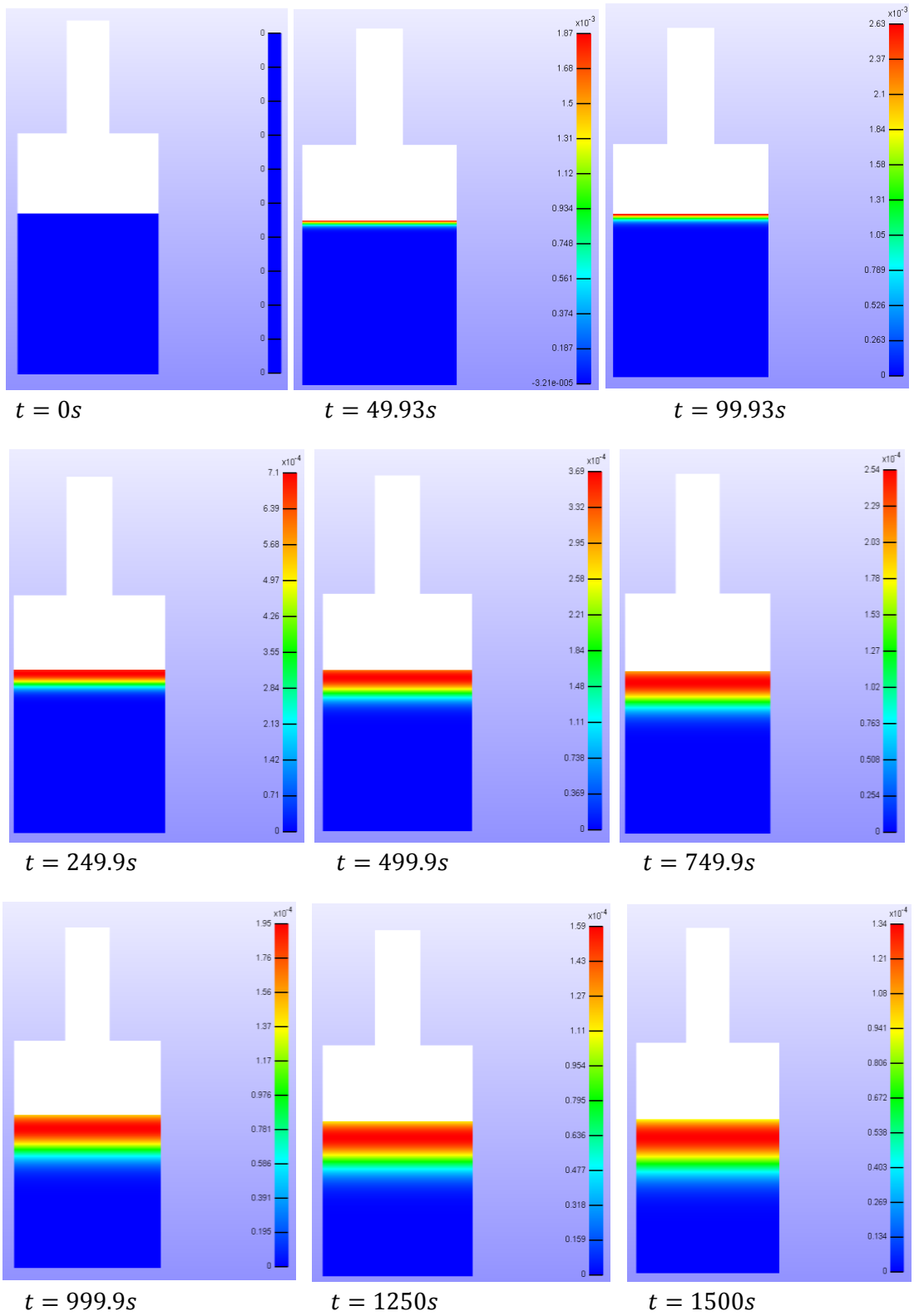

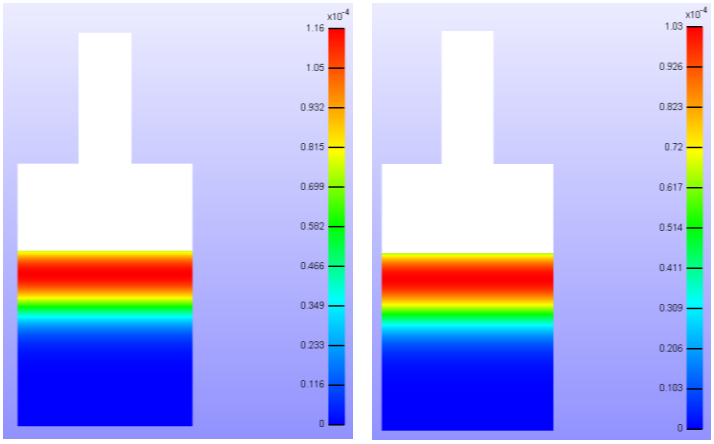

$t = 1750s$ $t = 2000s$

4.1.2 Validation of *PreView* Tied-Biphasic Contact Interface

After the two-layer biphasic material was created, a 10% compression, under displacement control, was initiated in the z-direction. The output force response, recorded at the platen, is illustrated in Figure 23 below. As can be seen, the confined compression test in *FEBio* of this two-layer biphasic material illustrates a similar force response to that described in Section 4.1.1 - the force response shown below also has well-defined ramp and hold phases. In addition to this, Figure 23 also effectively displays tissue relaxation as the output force response is seen to reach a constant equilibrium value as $t \rightarrow 1000s$.

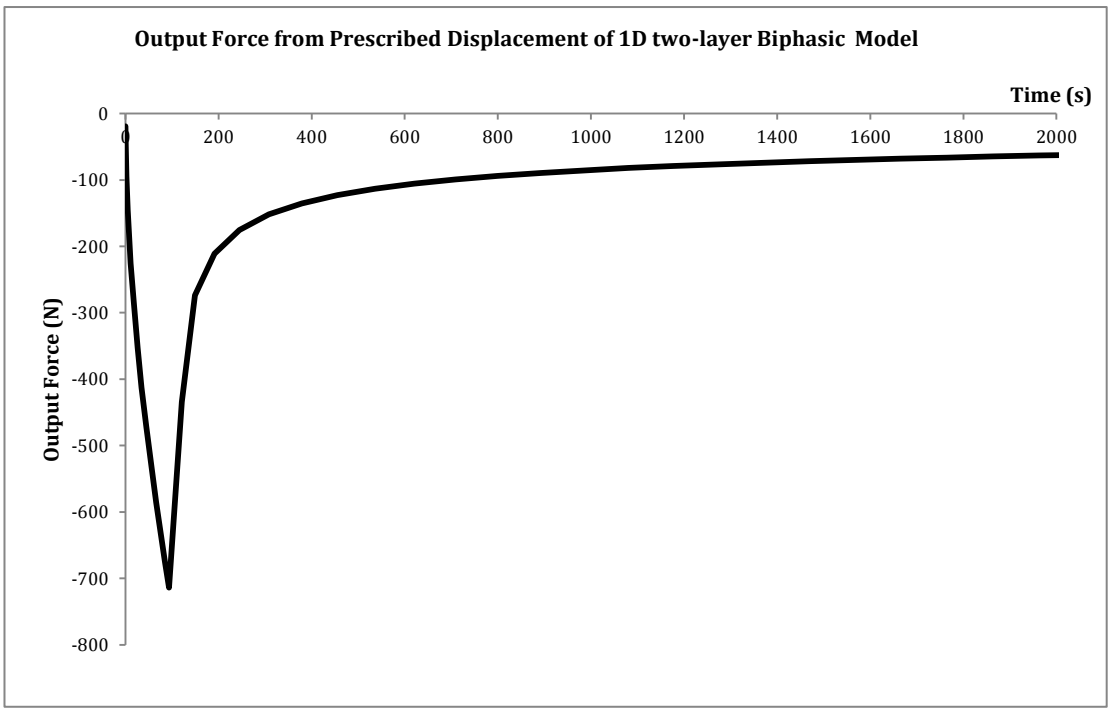

Figure 16 – Two-Layer Biphasic Model Output Force

In order to confirm that the biphasic interface functions correctly, the analysis of fluid flux was again viewed in *PostView* (Figure 24). As stated, *PostView* has dynamic analysis, and therefore the appropriate legend is given with each time frame – irregular time intervals are shown for the full length of the analysis ($0 - 200{,}000s$.) Through explanation of the material behaviour, it should be clear whether the biphasic interface functions properly or creates any unwanted effects. The red and blue sections are as defined in Section 4.1.1.

Figure 17 - *PostView* Analysis of *z-fluid flux* for the Two-Layer Biphasic Model, at Irregular Time Intervals, for the Full Length of the Analysis (200,000s).

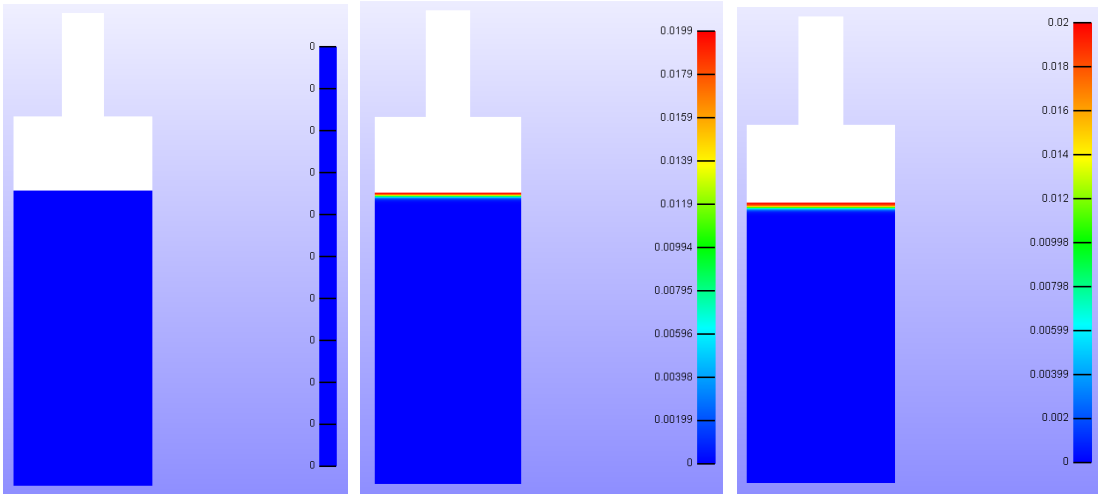

$t = 0s$ $t = 44.55s$ $t = 93.81s$

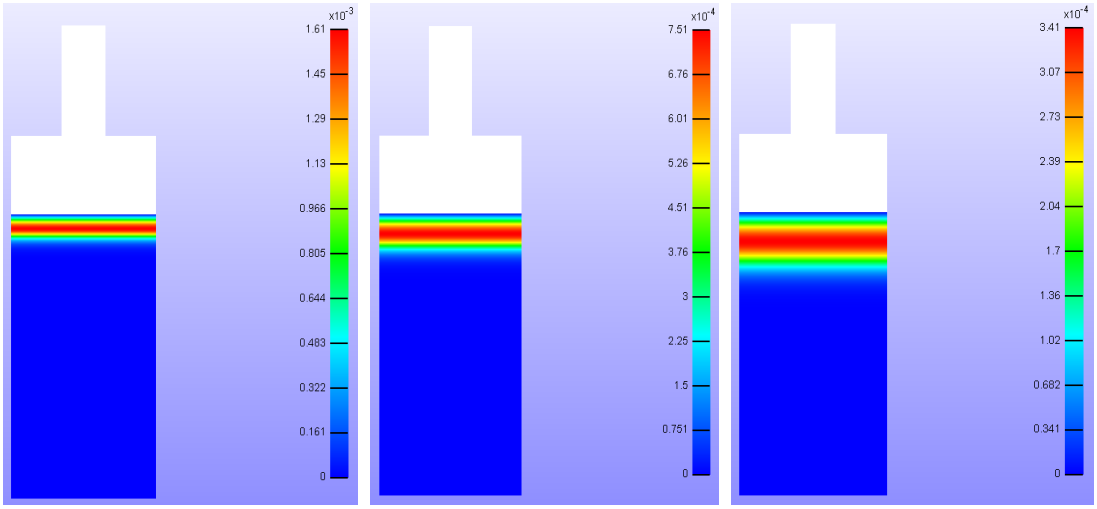

$t = 245.1s$ $t = 455s$ $t = 985.3s$

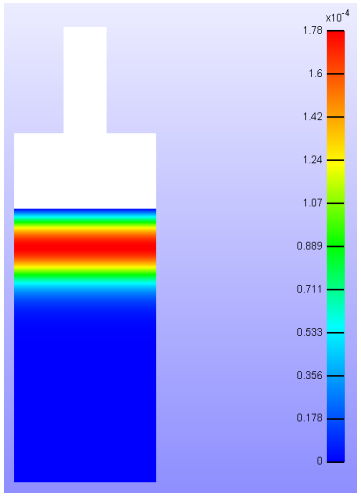

$t = 4961s$

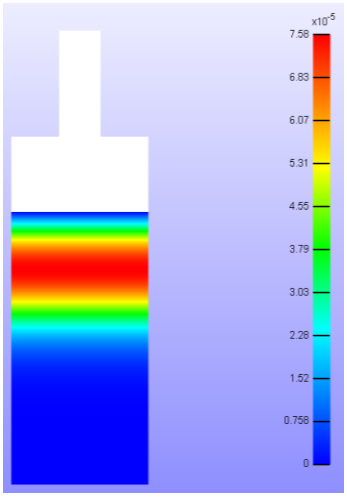

$t = 9961s$

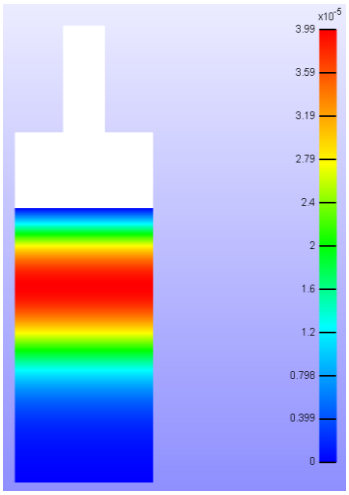

$t = 19{,}960s$

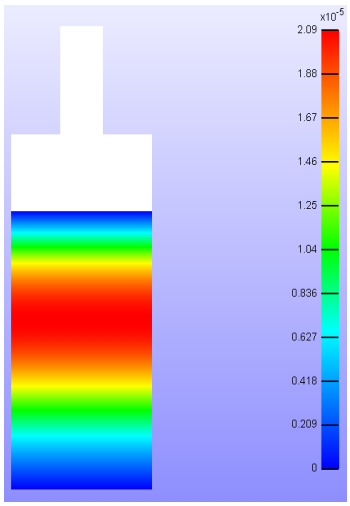

$t = 49{,}960s$

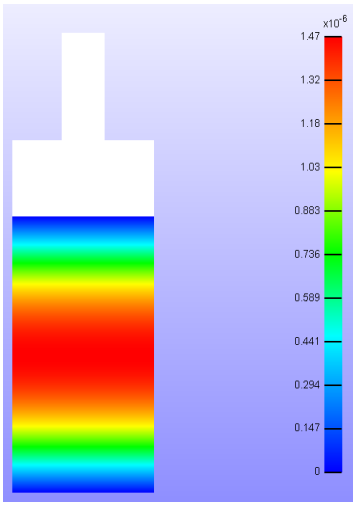

$t = 99{,}960s$

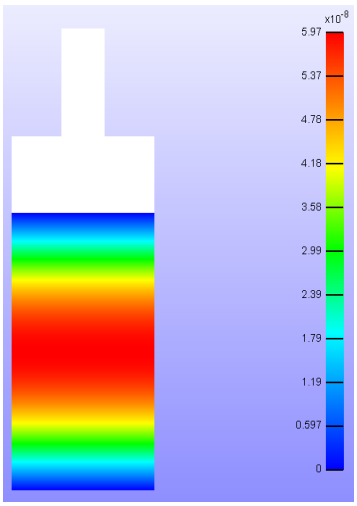

$t = 200{,}000s$

4.1.3 Validation of *FEBio* Coding

If the coding in *FEBio* is not correct, or there is a problem with the model created, using the output force as an input will not return the original displacement graph. In Section 3.1.3 four methods were attempted in order to create an appropriate force input for *PreView* that in turn validates the *FEBio* coding.

In Method 1, the force output graph shown in Figure 6 was used directly as a prescribed force input. This produced the displacement output curve shown in Figure 25 below. It can be seen that the displacement effectively illustrates a 10% compression ($-0.8mm$) of the platen COM from $9mm$ to $\cong 9.2mm$ in $\cong 100s$. However, looking at the end of the ramp phase there is a slight dip.

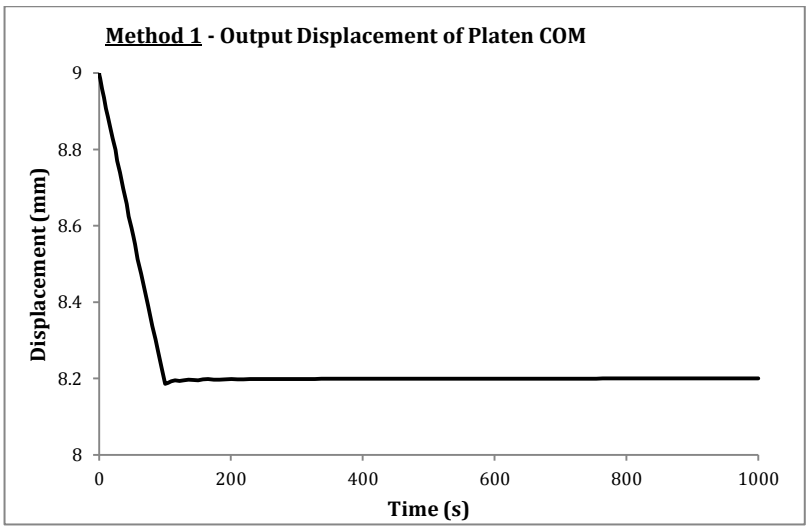

Figure 18 - Displacement Output for Method 1

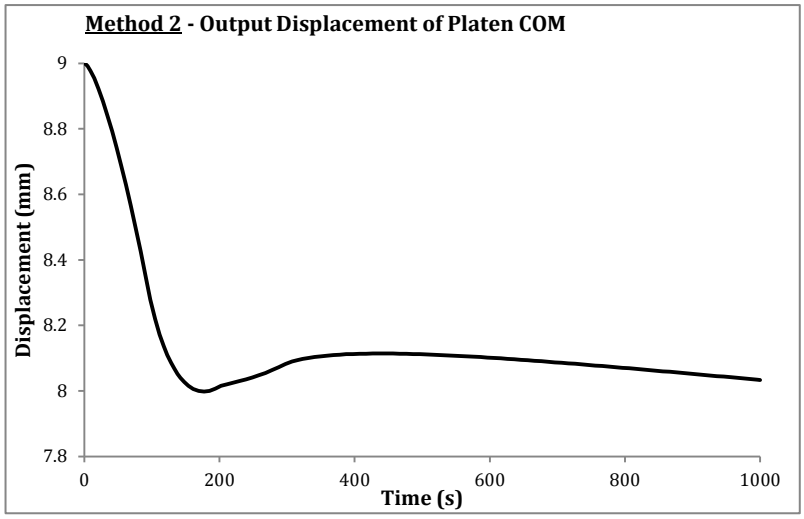

Figure 19 - Displacement Output for Method 2

In Method 2, the force curve points were approximated manually and the *.feb* file was edited appropriately. It can be seen from Figure 7 that this simplifies the curve drastically. The output displacement when using the curve illustrated in Figure 7 as an input is shown in Figure 26 on the previous page. Initially it can be seen that this output curve does not have the correct form. However, the output displacement obtained is slightly better than the one obtained in Method 1 as it reaches its maximum displacement at the correct peak position ($t \cong 100s$). However, the displacement goes beyond a 10% compression, and doesn't look to have the same strain rate – the ramp phase goes from $9mm$ to $\cong 8mm$ in $> 100s$. Thus the curve in Figure 7 has to be smoothed to get rid of the disturbances, but not too drastically.

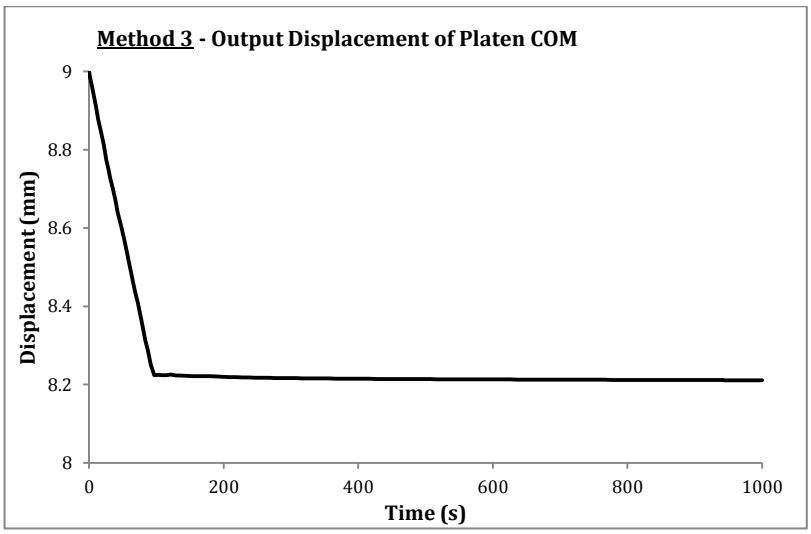

Figure 20 - Displacement Output for Method 3

The next method used (Method 3) was the moving average function in *Excel.* Figure 8 illustrates that the curve has efficiently been smoothed. However, the maximum force of the curve has been significantly reduced from $\cong -580N$ to $\cong -500N$. This is a problem as, shown in Figure 27, the output displacement does not reach a 10% compression – the position of the platen COM during the ramp phase goes from $9mm$ to $< 8.2mm$ in $< 100s$. Additionally, 'kinks' are apparently in the hold phase of Figure 8, which should not happen as the displacement/force should be a constant value (as $t \to 100s$).

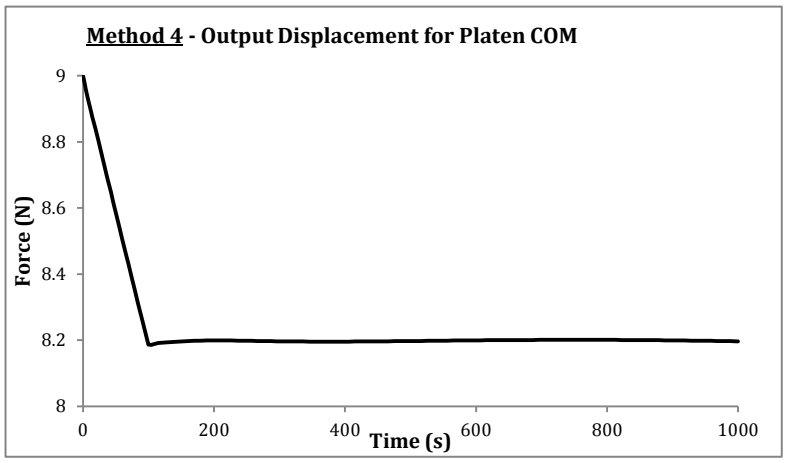

Figure 21 - Displacement Output for Method 4

Method 4 appears to produce the best approximation of the force curve (Figure 9) via *Excel*'s curve fitting technique. The graph has been efficiently smoothed but still reaches the same peak and equilibrium force values. The curve was manually adjusted by inspection and to ensure the boundary conditions were met the data was spilt into

two sections: ramp $(0 - 100s)$ and hold $(100s +)$. By constraining the two sections to meet at the peak point, $t = 100s$, the output displacement graph in Figure 28 was obtained.

The displacement curve shown in Figure 28 is very similar to the original in Figure 6. It has a slight 'kink' after the peak point, however, it was assumed small enough to disregard.

Therefore, by smoothing a force output curve and using it as an input to simulate a prescribed force experiment, the original prescribed displacement graph was found. This shows that the coding within the *FEBio* programme works correctly, and that the model created is fully operational. Accordingly, any of these methods can be used in the following sections to create a curve input accurately.

4.2 Parameter Sensitivity Analysis

4.2.2 Force Control Testing

Using the input curve shown in Figure 19, a force control test was carried out on the 175 model set-ups defined in Section 3.2.1. The output displacement responses were obtained for each model, and compare to each other and the control. It is unrealistic to compare each individual output displacement graph; as a result the end of ramp (t = 100s) and the equilibrium positions of the platen COM for each model were compared. The graphs (Figures 29 and 37) illustrate the change in position at the end of the ramp phase and at equilibrium compared to the equivalent value taken from the control model.

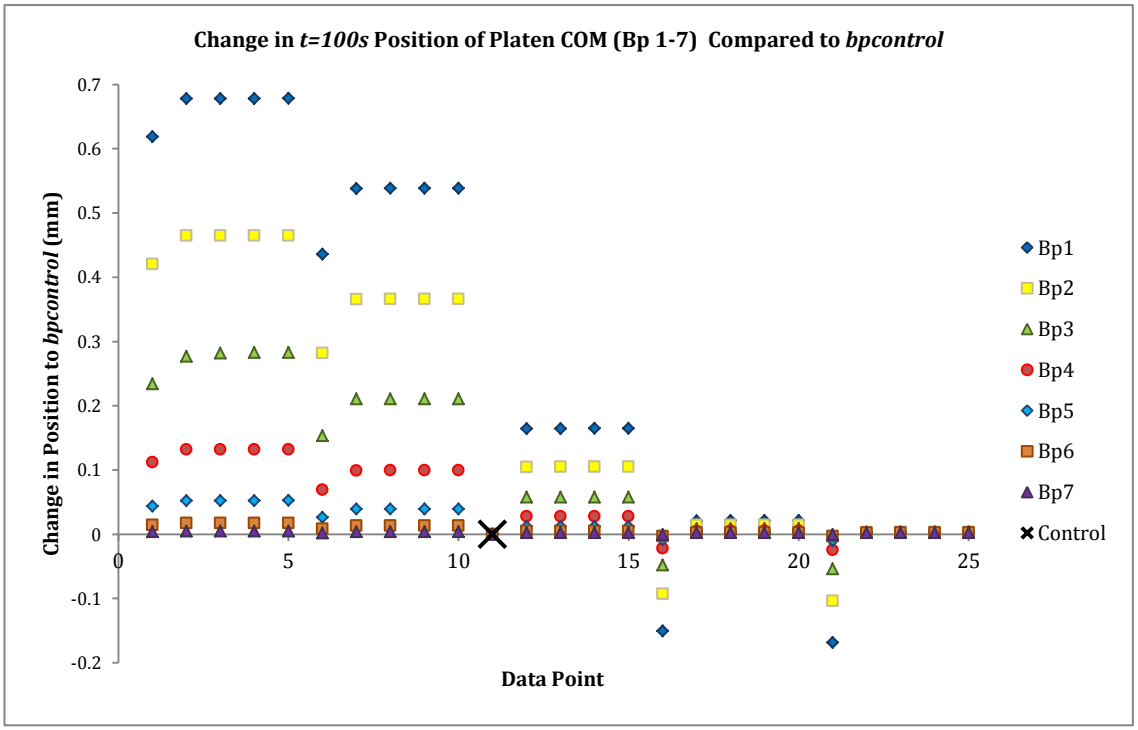

Figure 22 - Comparison of Peak Output Positions to Control

Figure 29 illustrates the difference in 'peak' position of the output curves for all biphasic models. The x-axis displays the data points, which are defined in Appendix 6; and the y-axis gives a numerical measurement of the change in position of the platen COM at $t = 100s$ for each model when compared to the control model. This plot of points is difficult to comprehend when considering the stiffness parameters (E and k), but visibly demonstrations the relationship between output response and distance of 'tumour' layer to the platen. *Bp1* demonstrates the model where the 'tumour' layer is

closest to the platen, and *Bp7* is when it is furthest away. Therefore it can clearly be seen that the closer the 'tumour' layer is to the platen, the larger the difference in the output displacement response is. A positive change in displacement reveals that the platen COM of the model under investigation has not changed in position as much as the platen COM of the control model – this suggests that the tissue is stiffer. Therefore, a negative change in displacement shows that the platen COM has went beyond the position of the platen COM of the control model - suggesting that the tissue deforms easier, implying that the tissue is softer.

In order to understand the relationship between the stiffness parameters and the output displacement response, the data points and the corresponding permeability (k) values are defined below in Table 9.

Data Points	Permeability Magnitude	Permeability Value, k (N/mm^2)
1-5	-x100	1
6-10	-x10	10
11-15	1	100
16-20	+x10	1000
21-25	+x100	10,000

Table 9 - Data Points For Figure 29 and Corresponding Permeability Parameters

By associating the correct permeability value to the corresponding data points in Figure 29, it can be noted that a lower permeability magnitude has a greater effect on the mechanical response of the tissue, as the tissue does not deform as much (a positive change in displacement).

It is difficult to directly read off this chart what relation the stiffness parameter E has in relation to the output response. Consequently graphs for each biphasic model have been created (Figures 30-36) displaying the relationship between Young's modulus, permeability and output position of the platen COM. Each graph was created with the same scale in order to compare the corresponding changes with each biphasic model. The x-axis in each figure represents the different magnitudes of Young's modulus (defined in Table 3); and the y-axis shows the difference in platen COM position at $t = 100s$ of the each model compared to the corresponding value for the control. The legend in each figure describes the different permeability magnitudes (defined in Table 4). Therefore each line in the figures represents a different permeability value for the same model.

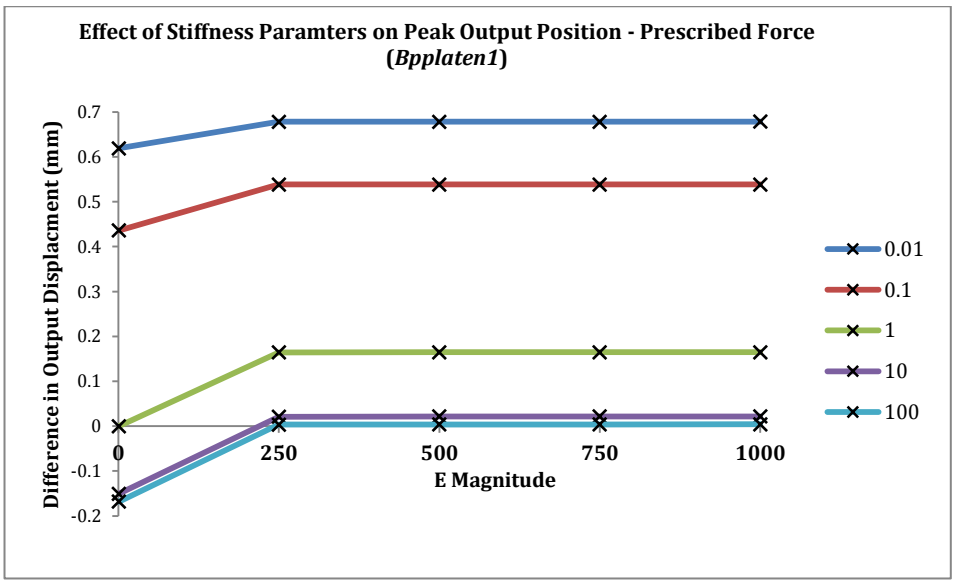

Figure 23 - Difference in Peak Position for *Bp1*

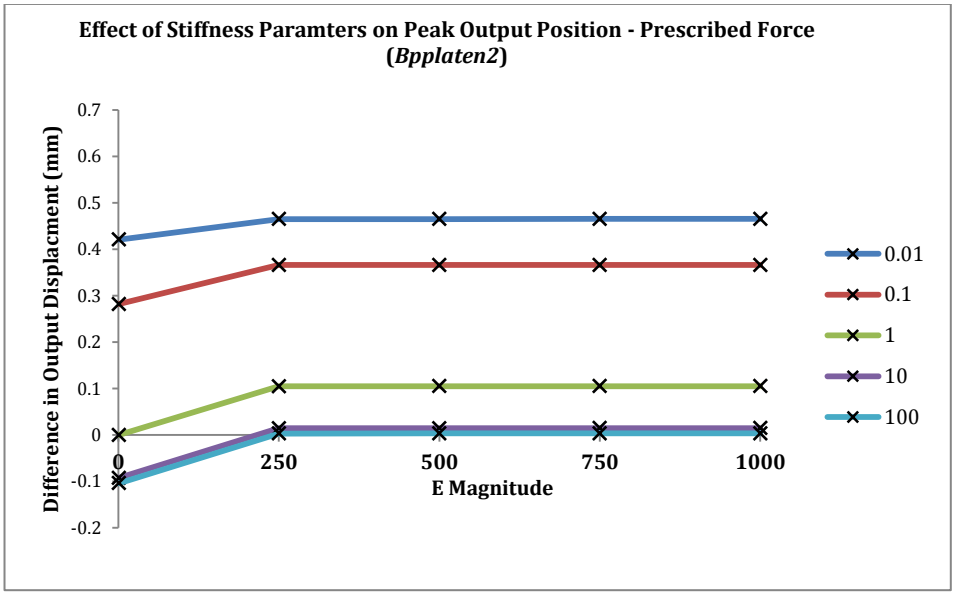

Figure 24 - Difference in Peak Position for *Bp2*

It can clearly be seen for *Bp1* and *Bp2* that the increase in Young's modulus (E) value causes a change in the output response. It illustrates that with an increase in E the model appears stiffer, as it does not deform as much. Additionally it can be noted that above a magnitude of $x250$ there is insignificant change in the output displacement response, meaning that the increase in E only affects the output up to a certain value. Furthermore, it can be seen that the change in E has less of an effect on the output in the models with a lower permeability magnitude.

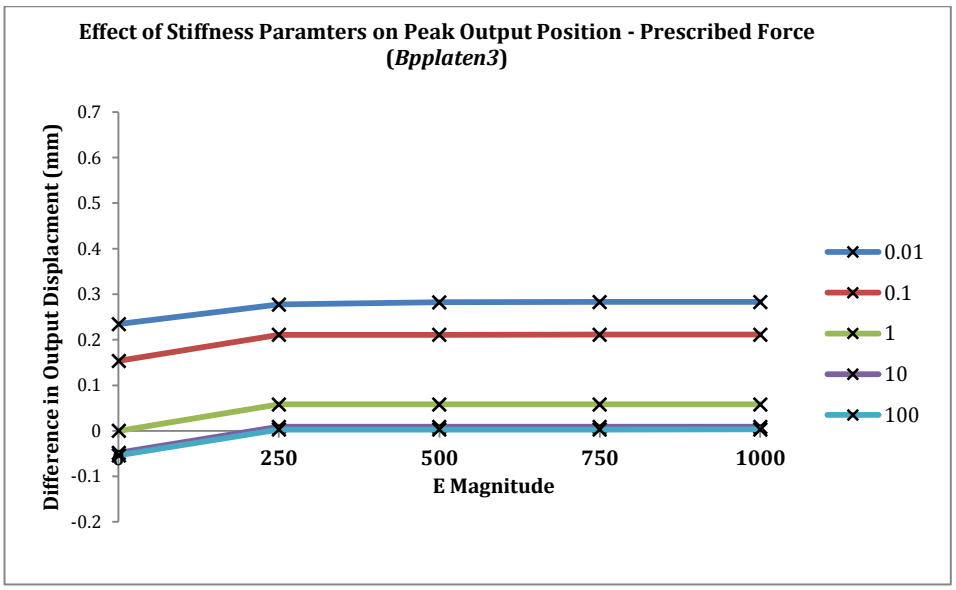

Figure 25 - Difference in Peak Position for *Bp3*

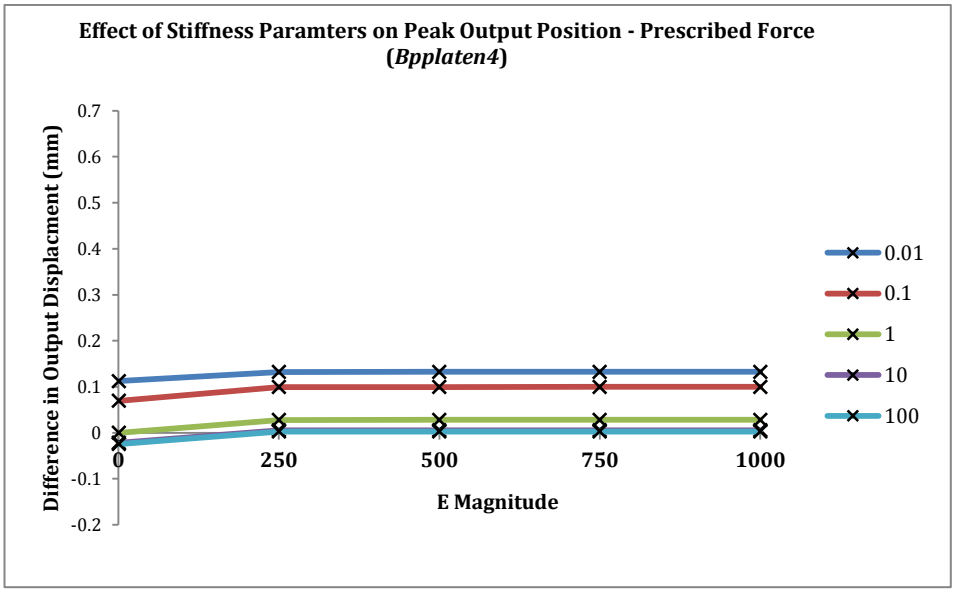

Figure 26 - Difference in Peak Position for *Bp4*

The same output response described for Figures 30 and 31 is seen in Figures 32 and 33. However, by comparing Figure 32 to Figure 33 it is implied that as the 'tumour' layer moves further away from the platen, the stiffness parameters have less of an effect on the output. By further comparison with Figures 34, 35 and 36 on the proceeding page, this relationship between distance from platen and effect of the change in parameters is obvious and can be confirmed. Therefore, the changes in stiffness parameters are only important when the 'tumour' layer is in the half of the tissue closest to the platen (*Bp1* to *Bp4*).

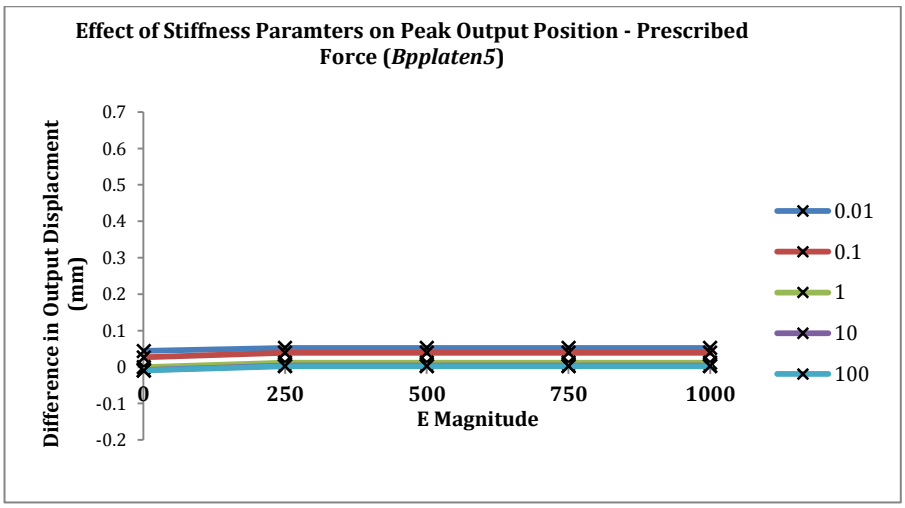

Figure 27 - Difference in Peak Position for *Bp5*

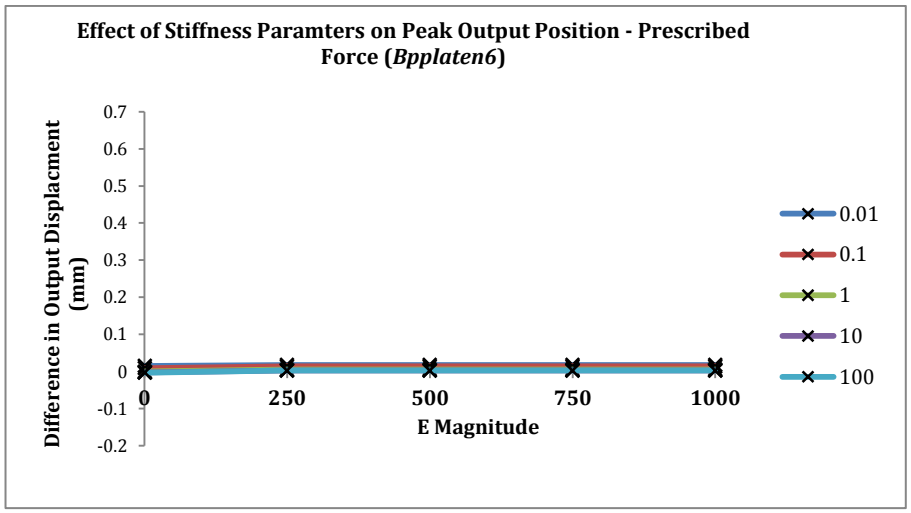

Figure 28 - Difference in Peak Position for *Bp6*

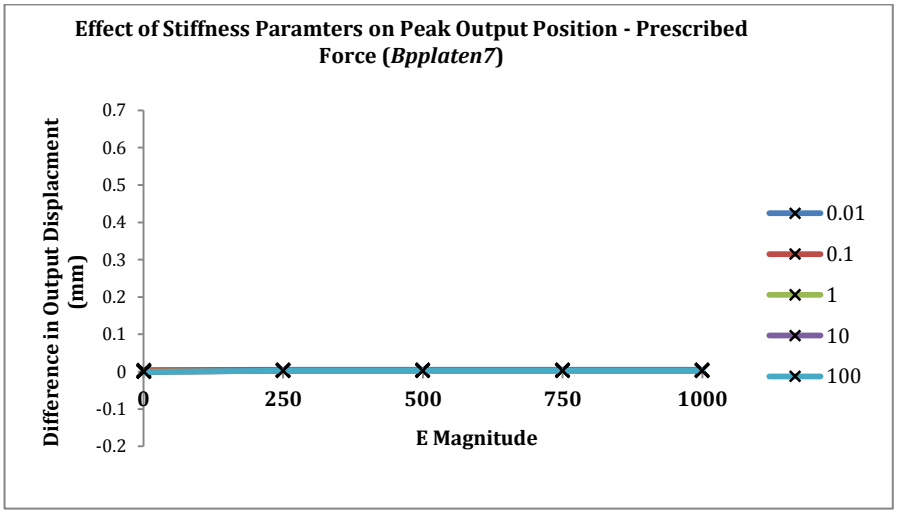

Figure 29 - Difference in Peak Position for *Bp7*

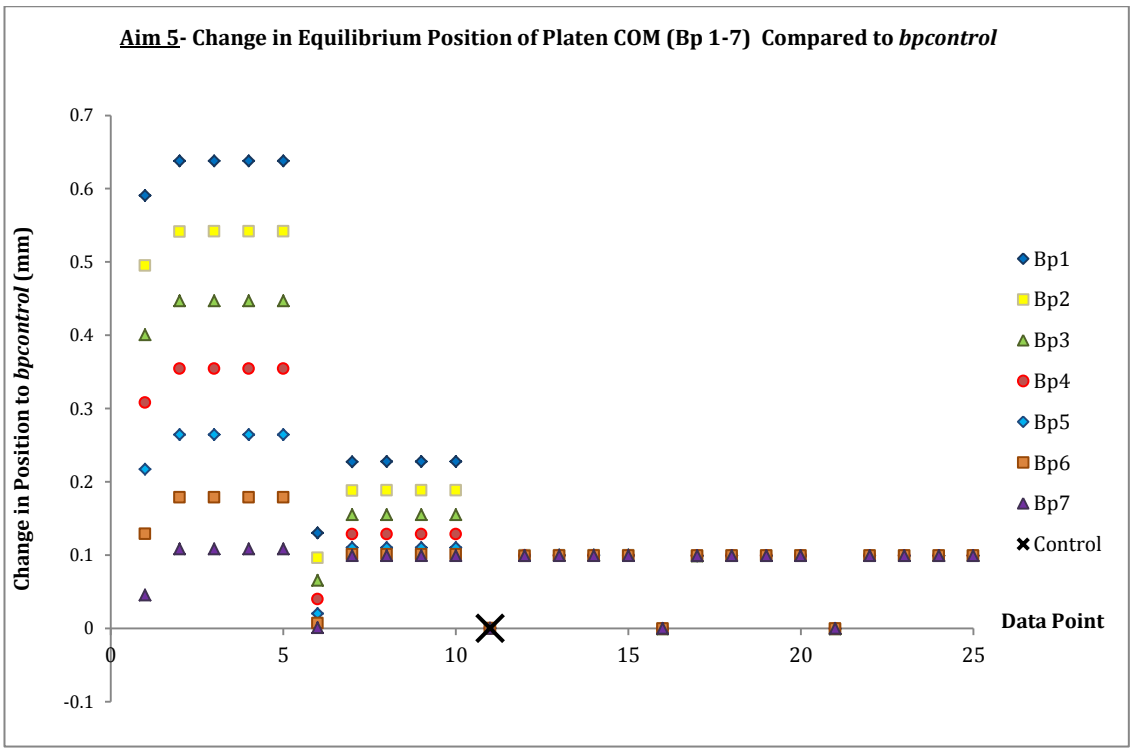

Figure 30 - Comparison of Equilibrium Output Positions to Control

The change in equilibrium position of the output displacement of the platen COM of the model under investigation relative to the control model is displayed in Figure 37. The x-axis displays the data points, which are defined in Appendix 6; and the y-axis gives a numerical measurement of the change in position of the platen COM equilibrium, $t = 1000s$, for each model when compared to the control model. Similar to Figure 29 this plot is difficult to comprehend when trying to directly relate the stiffness parameters and the output response. Analysing the graph it can clearly be seen that the correlation between distance of the 'tumour' layer away from the platen and output displacement response is still apparent for the equilibrium response. By comparison with the permeability values defined for each data point given in Table 9, it can be seen that the output response for permeability magnitudes of $k(0), k(+x10)$ and $k(+x100)$ are all the same for all models. Therefore, a change in equilibrium position can only be recorded for models whose 'tumour' layer has a low value of permeability. Thus it can be repeated that a lower value of permeability has a greater effect on the output response.

Alike Figure 29, the relationship between E and the output displacement response is not very clear. Therefore, graphs for each biphasic model have been created (Figures 38-44) illustrating the correlation between E, k and the change in equilibrium position

of the platen COM compared to the control model. Each graph was created with the same scale in order to compare the corresponding changes with each biphasic model. The x-axis in each figure represents the different magnitudes of Young's modulus (defined in Table 3); and the y-axis shows the difference in equilibrium platen COM position of the each model compared to the corresponding value for the control. The legend in each figure describes the different permeability magnitudes (defined in Table 4). Therefore each line in the figures represents a different permeability value for the same model.

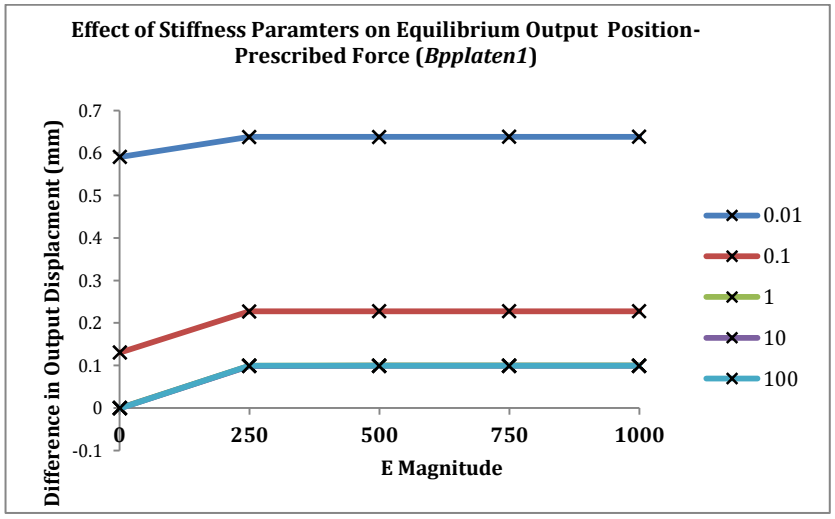

Figure 31 - Difference in Equilibrium Position for *Bp1*

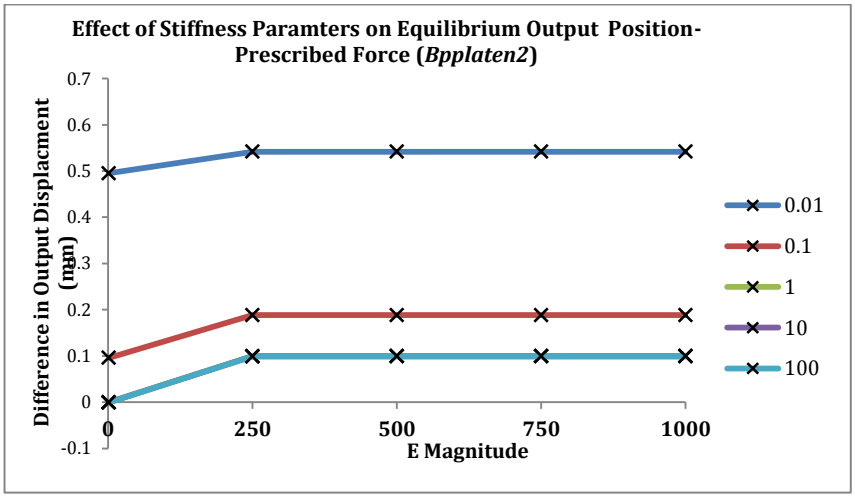

Figure 32 - Difference in Equilibrium Position for *Bp2*

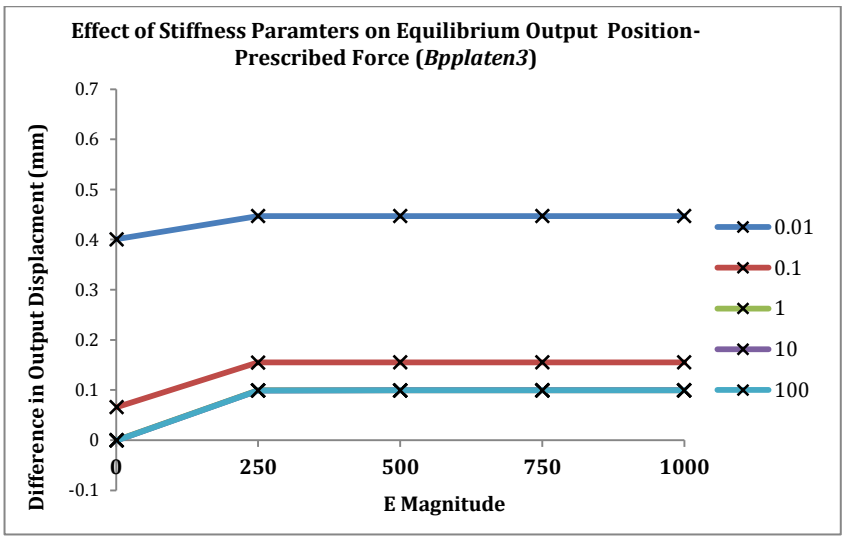

Figure 33 - Difference in Equilibrium Position for *Bp3*

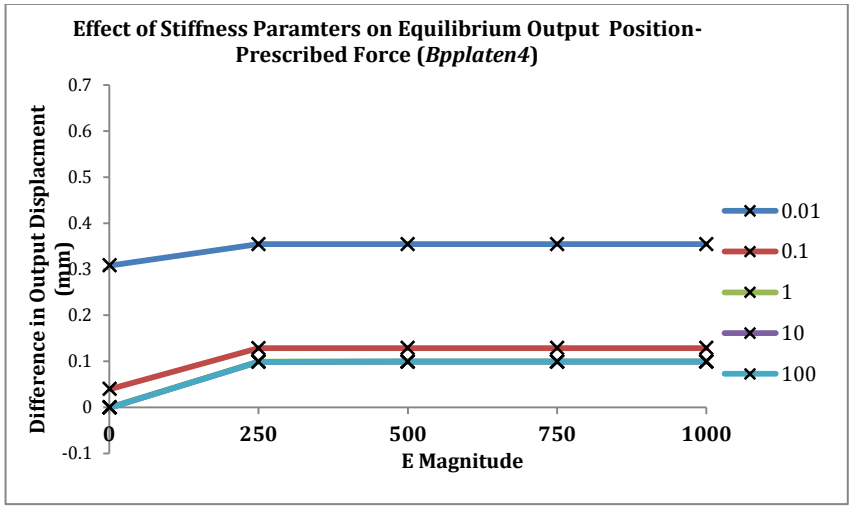

Figure 34 - Difference in Equilibrium Position for *Bp4*

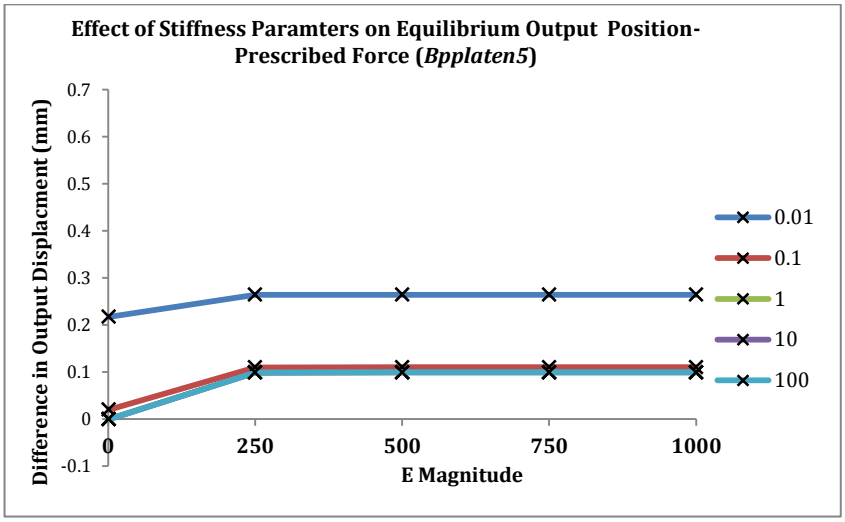

Figure 35 - Difference in Equilibrium Position for *Bp5*

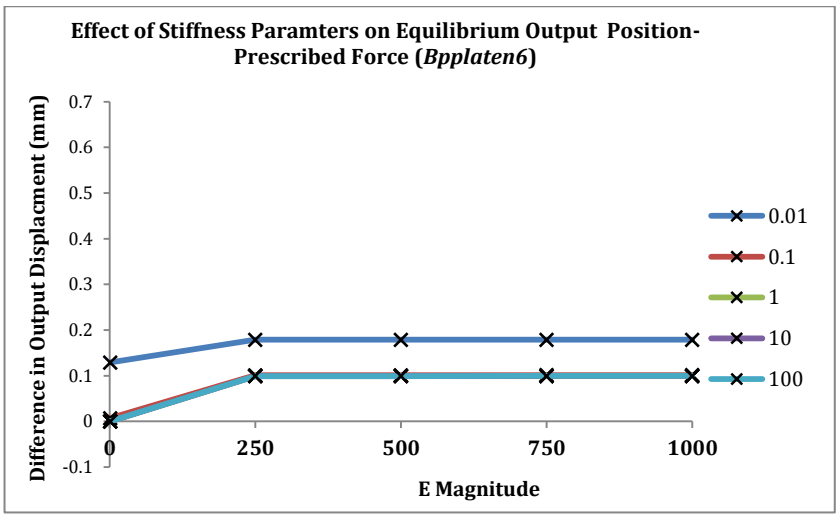

Figure 36 - Difference in Equilibrium Position for *Bp6*

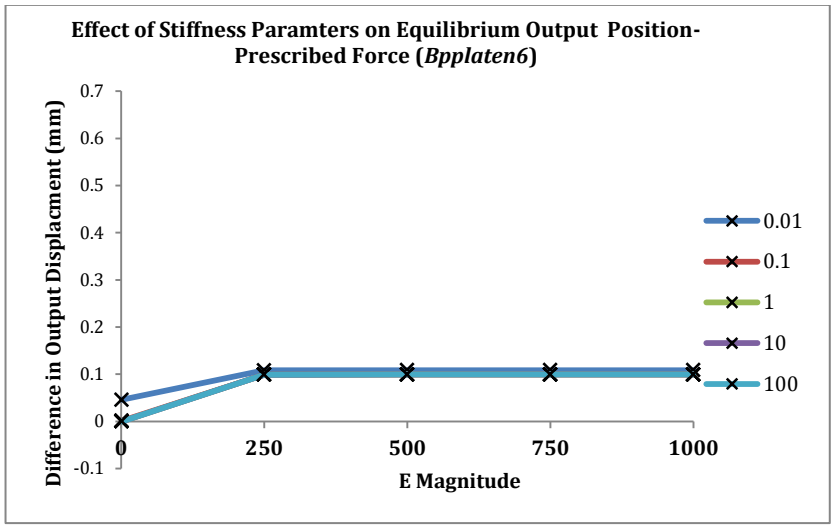

Figure 37 - Difference in Equilibrium Position for *Bp7*

It can clearly be seen in all figures (38-44) that the parameter that has the biggest effect on the output equilibrium position is the permeability, namely the permeability that has a magnitude of $-x100 = 0.01$ creates the biggest change in the stiffness of the model. Similar to the previous graphs (Figures 30-36) it can be noted that the response dependent on the stiffness parameters is less noticeable as the 'tumour' layer gets further away from the platen. Additionally, the Young's modulus had the same relationship with the output response as found previously for the peak response, and creates the greatest difference when increased to a magnitude of $x250$ with no extra effect incurring with further increase in value.

4.2.3 Displacement Control Testing

For each of the models created in Section 3.2.2, the permeability stiffness parameters were updated to those stated in Table 6, taken from a study by Busby *et al.*[4]. The other parameters defined in Tables 7 and 8 were used and the 175 models created. An additional model *bpcontrol* was also generated, using the parameters defined in Table 7, using Young's modulus $E(0)$ and permeability $k(0)$. The control was created with the purpose of accurately comparing all the outputs.

Each model was applied a prescribed displacement of $-0.4mm$ with in $10s$ illustrating a 5% compression ($0.5\%/s$ strain rate, see Figure 20). The reaction force at the plunger was recorded for each model, and the peak and equilibrium force values were compared to the corresponding values of the output force from the control model (Figure 45). The differences between these values and the equivalent value taken from the control model are given in Figures 46 and 48. (See Appendix 7 for a definition of data points and corresponding parameters).

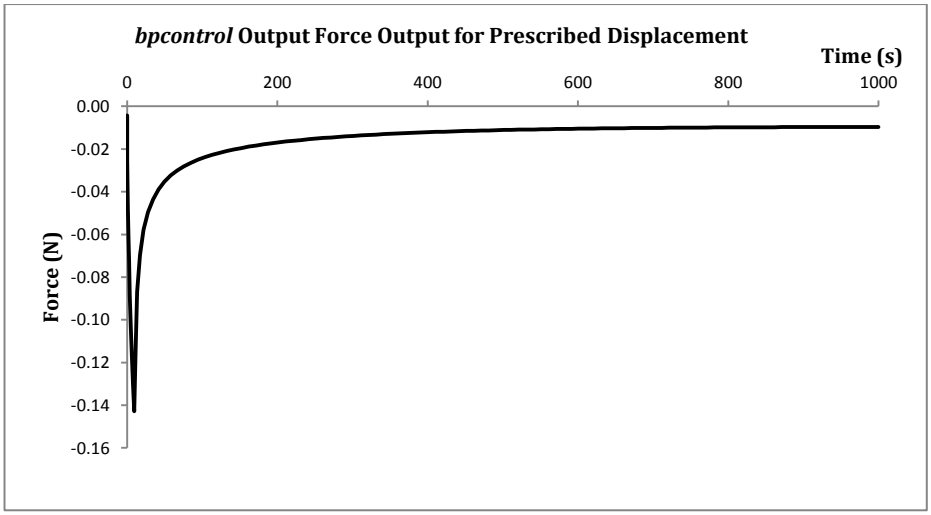

Figure 38 - Output Force Graph for *bpcontrol* in Under Prescribed Displacement

It can be seen from Figure 46 that the control model effectively illustrates a biphasic material (see Section 4.1.1). Therefore it is assumed that by adjusting the stiffness parameters that the peak force (at $t = 100s$) and the equilibrium force (at $t = 1000s$) will change.

On the next page, Figure 46 displays the values of peak force for all 176 models created. As noted in Section 4.2.2, this graph can be hard to comprehend if focusing on the stiffness parameters. However, by considering the relationship between the depth of

the 'tumour' layer and the mechanical peak response, it can clearly be seen that the peak force response is only notably affected if the 'tumour' layer is significantly close to the platen.

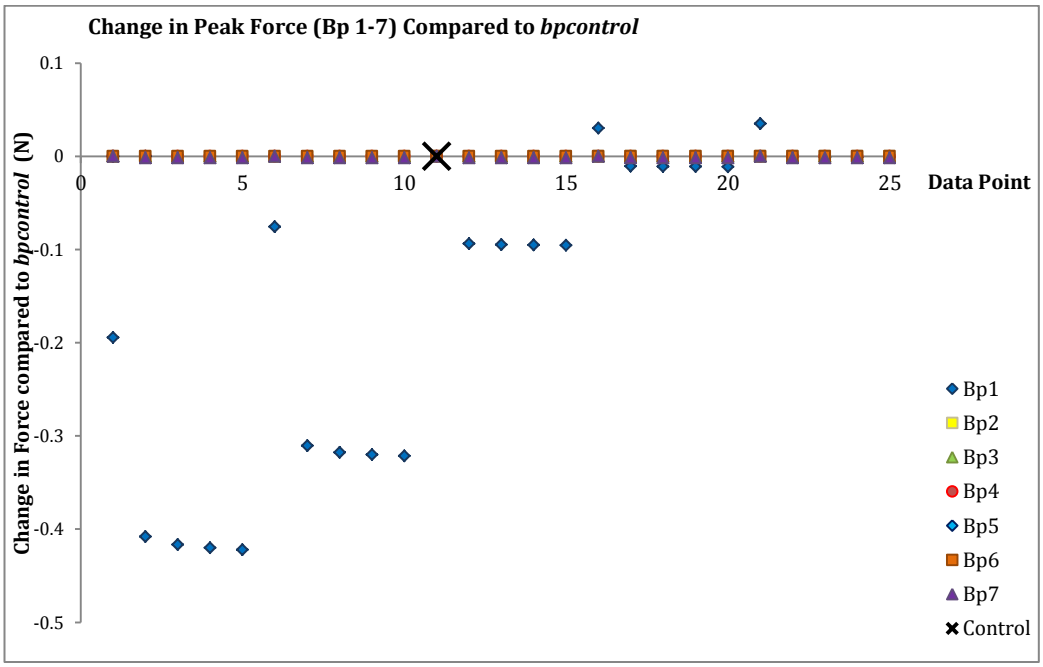

Figure 39 - Comparison of Peak Force Output Values to Control

The only remarkable different in the peak force output is seen in the *Bp1* model where the 'tumour' layer is positioned only 0.5*mm* away from the platen. The stress response of this model is analysed further in Figure 47 below.

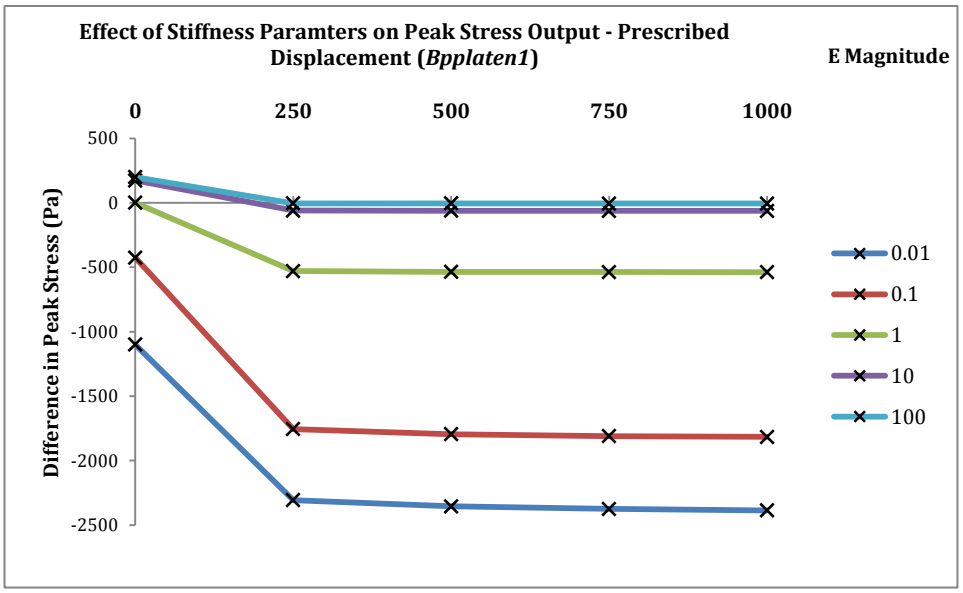

Figure 40 - Difference in Peak Stress for *Bp1*

In Figure 47, the x-axis displays the different magnitudes of Young's modulus, defined in Table 8; the y-axis is a measure of the difference in peak stress response of this model compared to the control; and the legend displays the different permeability magnitudes (see Table 6), with each line representing a different permeability. It can clearly be seen that the most significant change is peak stress response is found when the permeability is at its lowest magnitude ($k(-x100)$), and the Young's modulus is at a magnitude greater than $E(x250)$ – this re-iterates the results from the previous section (Section 4.2.2). Therefore, it can be concluded that a low permeability and a high Young's modulus value are key parameters to illustrate a stiffer material. It can also be seen from this displacement control experiment that the increase of E above a magnitude of $x250$ creates no additional effects. However, unlike the results from Section 4.2.2, an increase in E value causes a greater effect on lower permeability values, rather than high permeability values. The other biphasic models graphs have not been included as the change is peak stress response is $\leq 0.5Pa$ which would not be significant when determining a change in stress at the surface.

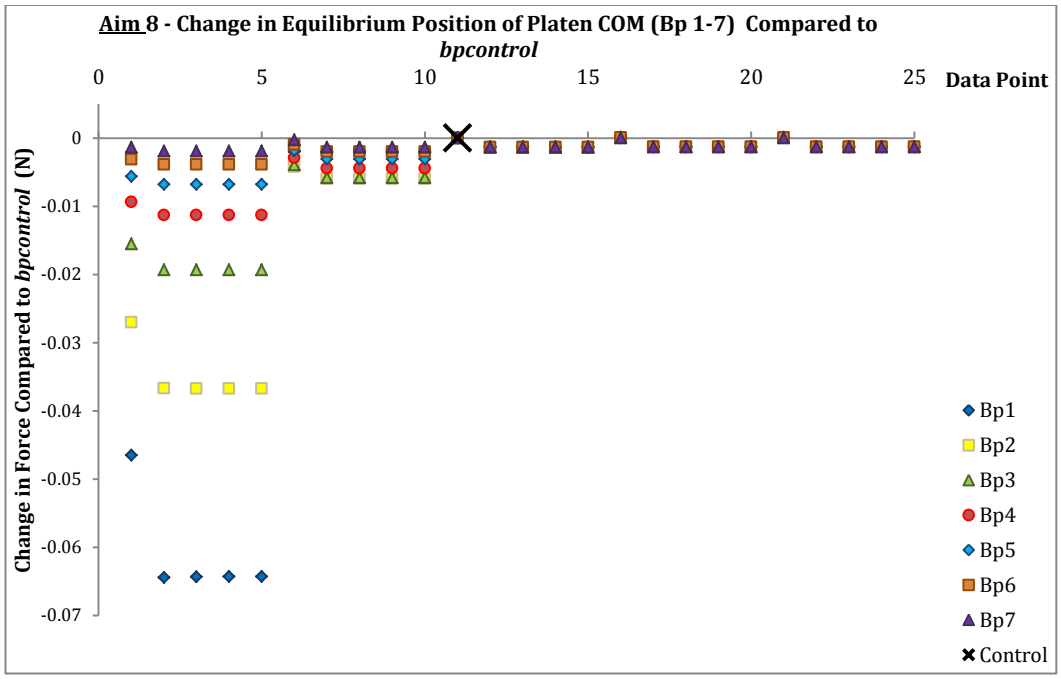

Figure 41 - Comparison of Output Equilibrium Force Values to Control

Figure 48 above displays the equilibrium force response for the 176 models in the displacement control test. Similar to Figure 37, it can be seen that a difference in equilibrium response is only noticeable for higher magnitudes of permeability. However, even for the 'tumour' layer being close to the platen (*Bp1*), and high values of

E and k being used, the difference in equilibrium force response is still relatively small, $< 0.07N$. In an attempt to create a measureable outcome the stresses corresponding to each recorded force was calculated. The graphs of the mechanical stress response for each model are in Figures 49-55. The explanation of the parameters of these graphs is the same of that previous stated for Figure 47, but for equilibrium stress.

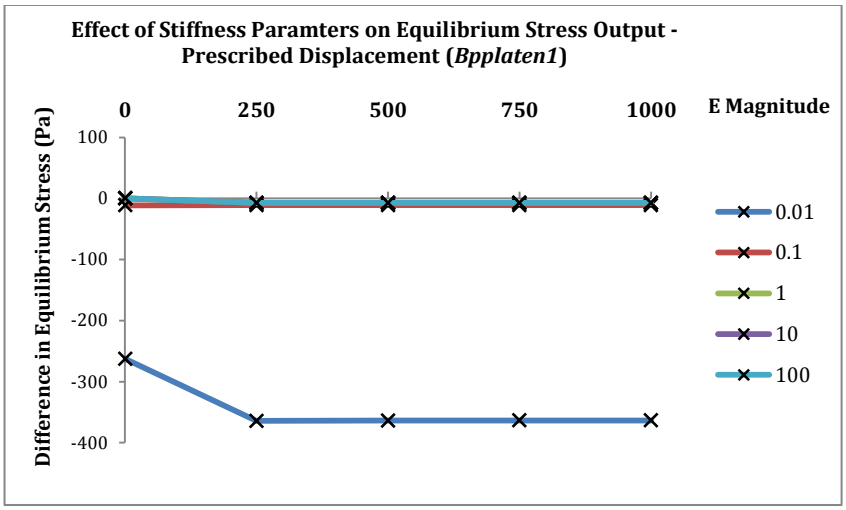

Figure 42 - Difference in Equilibrium Stress for *Bp1*

Figure 49 illustrates the difference stress response for *Bp1* compared to the control model. As can be seen from Figure 48, this model is the one in which creates the largest difference in output equilibrium force recorded at the platen. It can clearly be seen from this graph that the model with permeability $k(-x100)$ and Young's modulus $E(250)$ or above creates the largest different in mechanical stress response.

Figures 49-55 (Figures 48-55 presented on the next two pages) clearly show that the closer the 'tumour' layer is to the platen, the larger the difference in output stress. Each biphasic model displays the same relationship between E and k described in Section 4.2.2 for the equilibrium response, with the stiffness parameters again becoming less significant as the distance from the platen increases (compare Figure 49 for *Bp1* to Figure 55 for *Bp7*).

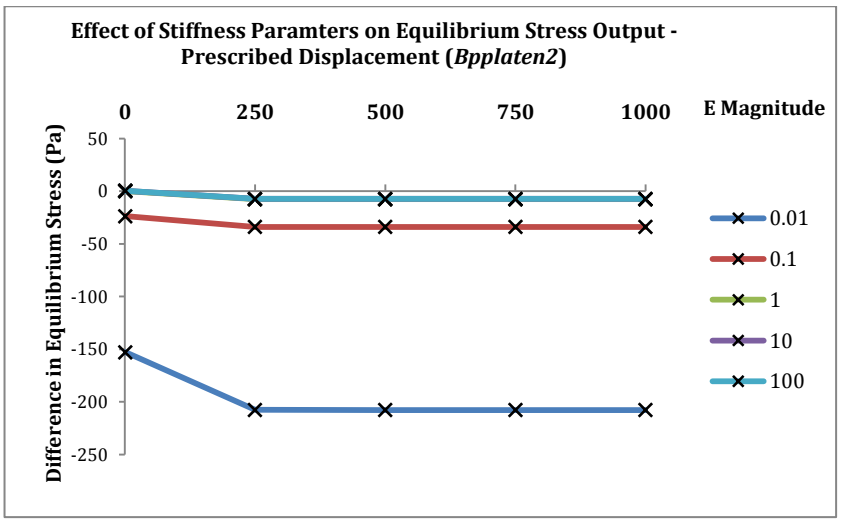

Figure 43 - Difference in Equilibrium Stress for *Bp2*

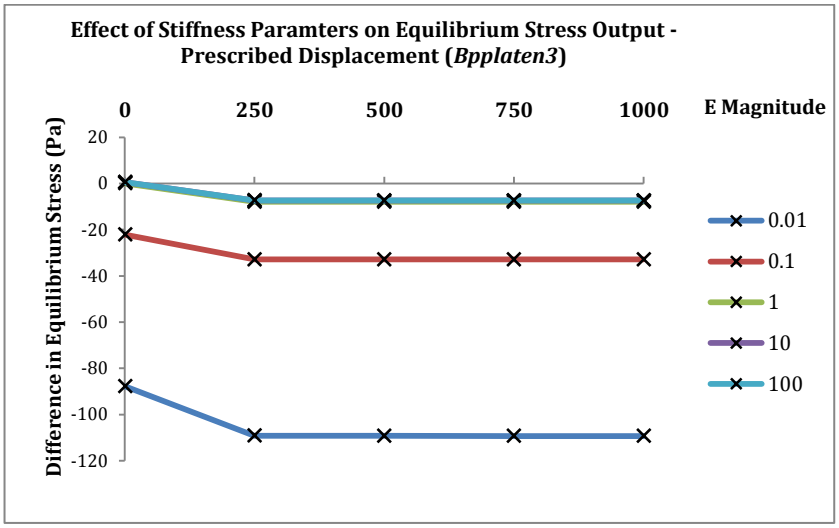

Figure 44 - Difference in Equilibrium Stress for *Bp3*

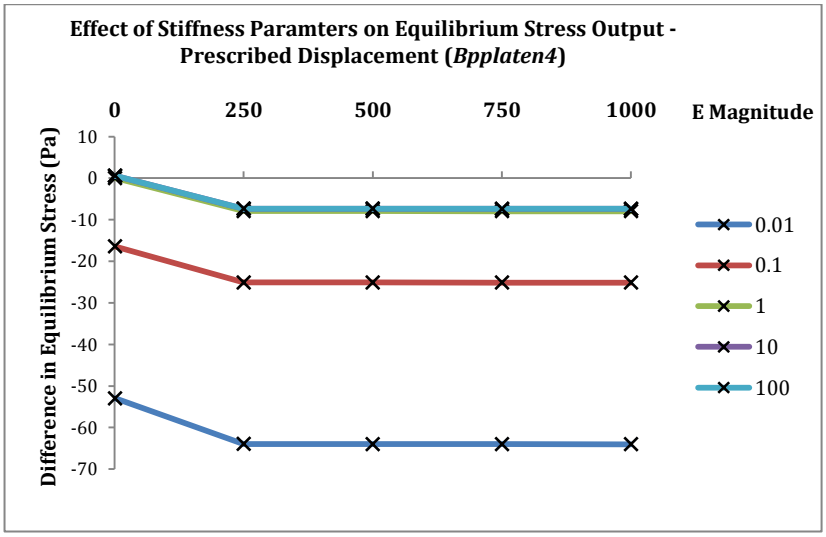

Figure 45 - Difference in Equilibrium Stress for *Bp4*

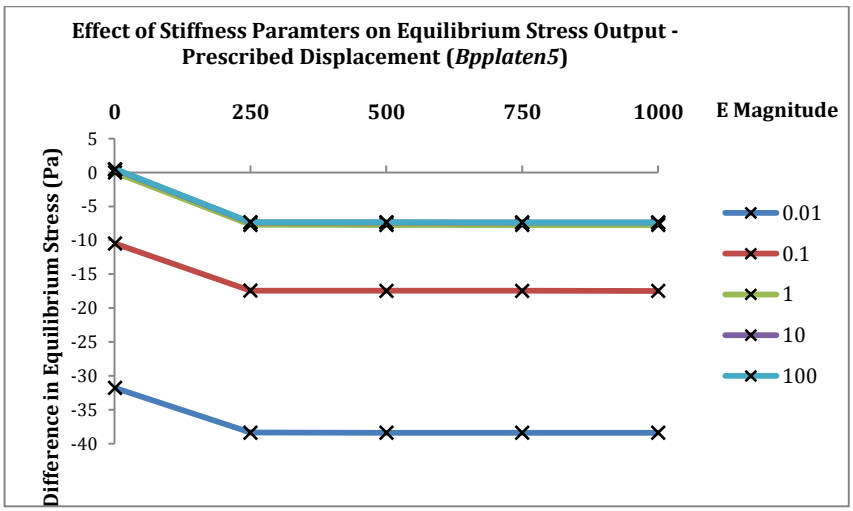

Figure 46 - Difference in Equilibrium Stress for *Bp5*

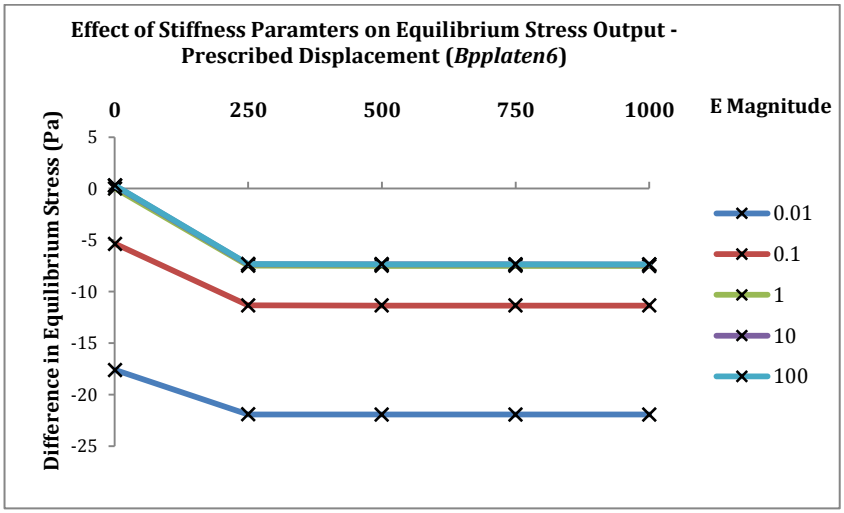

Figure 47 - Difference in Equilibrium Stress for *Bp6*

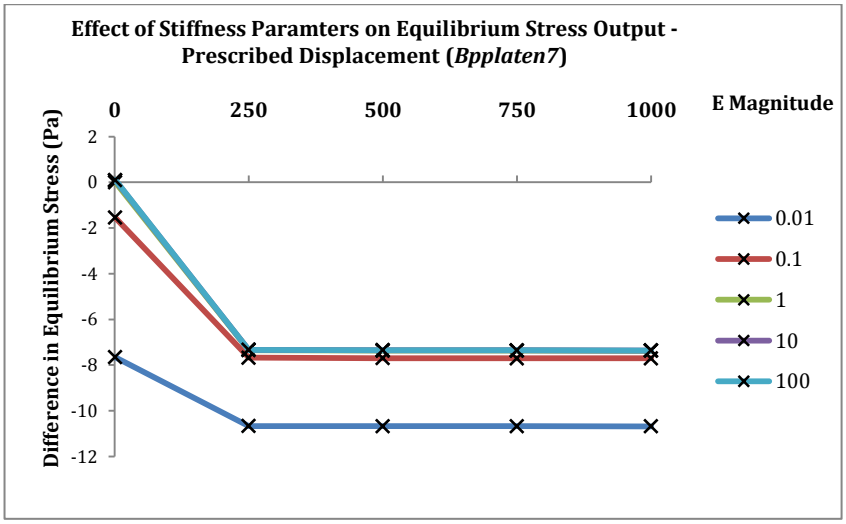

Figure 48 - Difference in Equilibrium Stress for *Bp7*

In order to visualise the influence of the layer within the 'tissue' on the *bpplaten2* model with Young's modulus value of $E(x1000)$ and permeability $k(-x100)$ was ran through *PostView*, and the summary of the z-stress output was obtained (Figure 56).

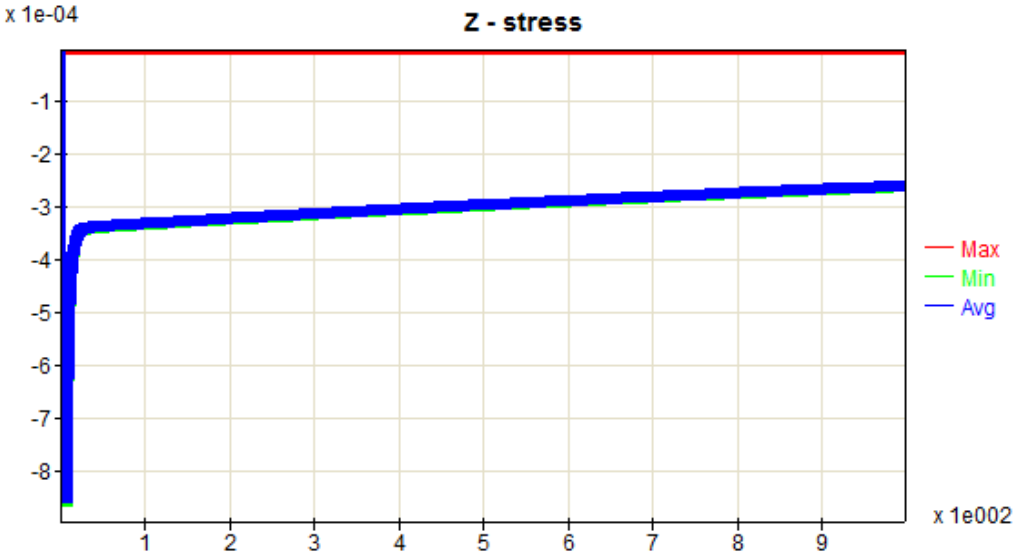

Figure 49 - Stress Response in the Vertical Direction (*PostView* Output)

Figure 56 illustrates the z-stress of the whole model, measured at the platen level. The x-axis represents time (s) and y-axis displays the output stress in the vertical direction (MPa), the direction of compression. Considering the blue line (average stress) the curve demonstrations that the stress increases linearly as time proceeds. This stress curve reaches a maximum at $t = 1000s$, which is regarded as the equilibrium point in the previous graphs. However, as can be seen it does not seem to reach a constant value, which is representative of an equilibrium point.

This point is re-iterated when the z-fluid flux is visualised in *PostView*, similar to Section 4.1. By comparison with Figures 22 and 24 the influence of the additional layer should be apparent. The *PostView* output at irregular time intervals is displayed in Figure 57 on following pages. Similar to the previous *PostView* figures, the red sections illustrate areas of high fluid flux and the dark blue section illustrates area of little, or no, fluid flux.

Figure 50 - PostView Analysis of *z-fluid flux* for the *bpplaten2* model (with *E(x1000)* and *k(-x100)*), at Irregular Time Intervals, for the Full Length of the Analysis (1000s).

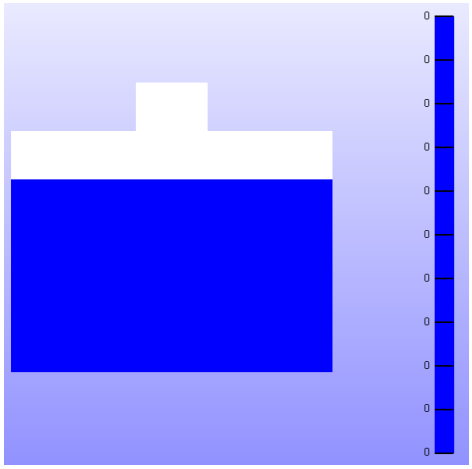

$t = 0s$

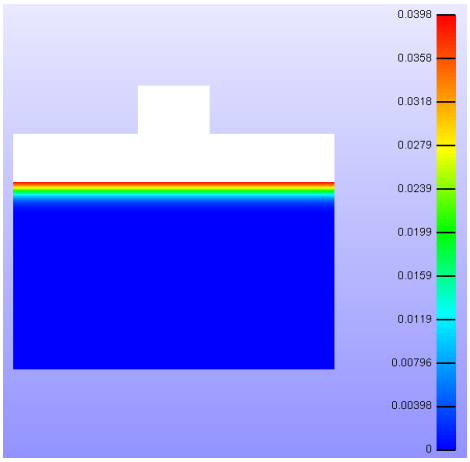

$t = 4.999s$

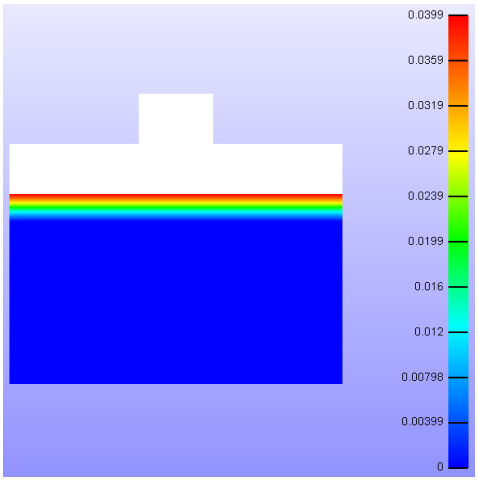

$t = 9.997s$

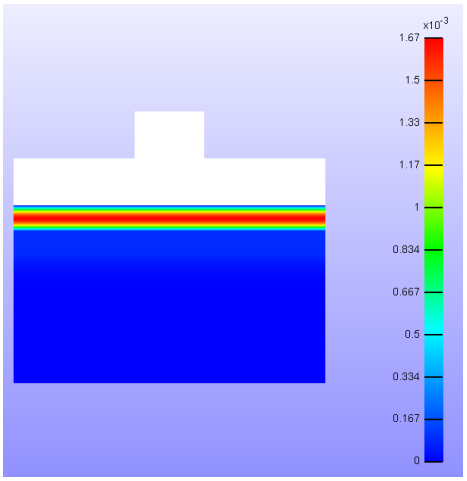

$t = 19.99s$

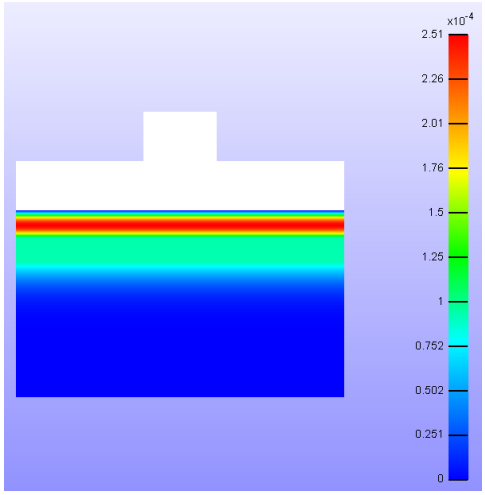

$t = 28.38s$

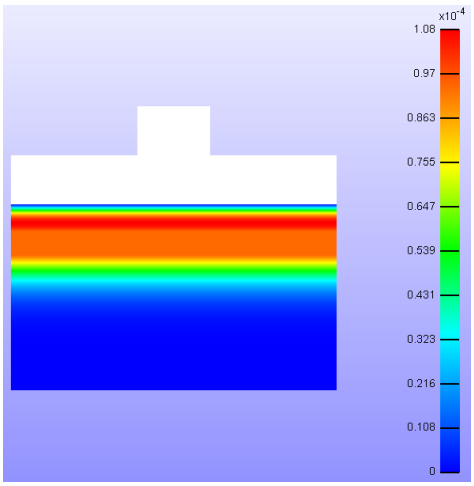

$t = 35.52$

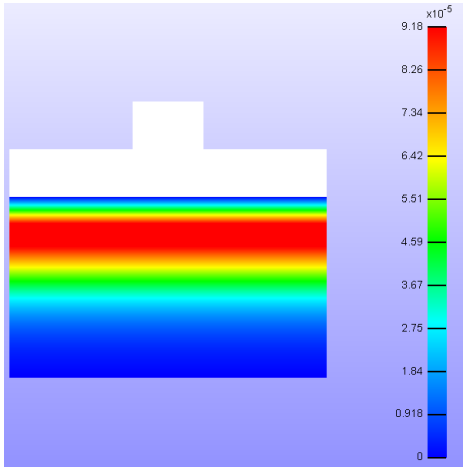

$t = 45.95s$

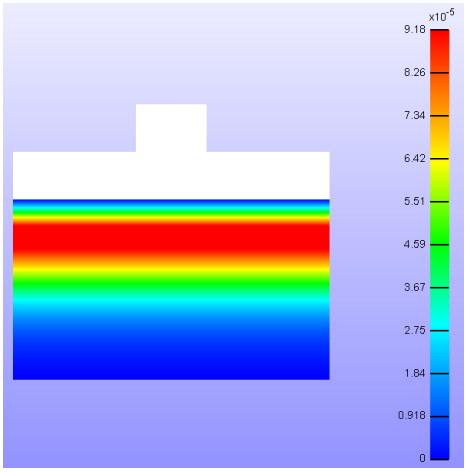

$t = 93.4s$

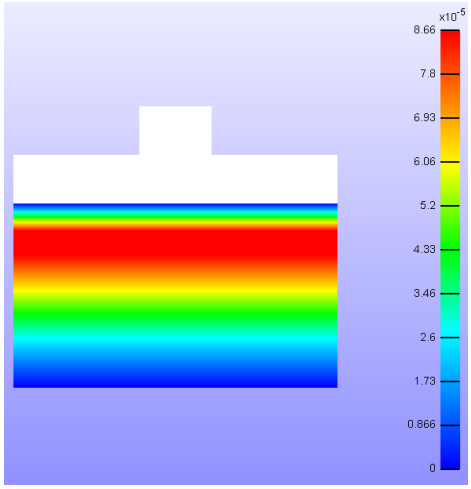

$t = 249.1s$

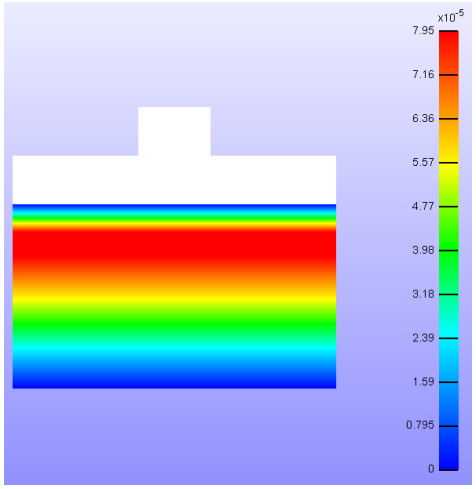

$t = 498.9s$

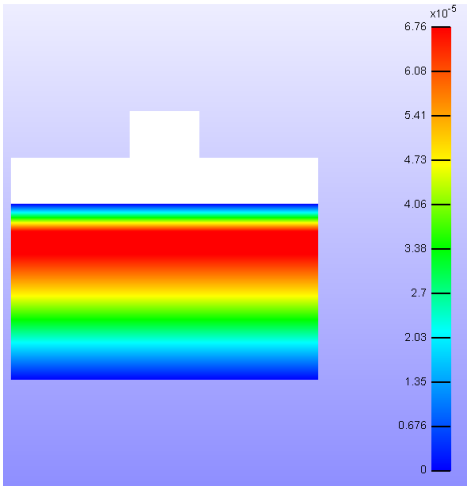

$t = 748.9s$

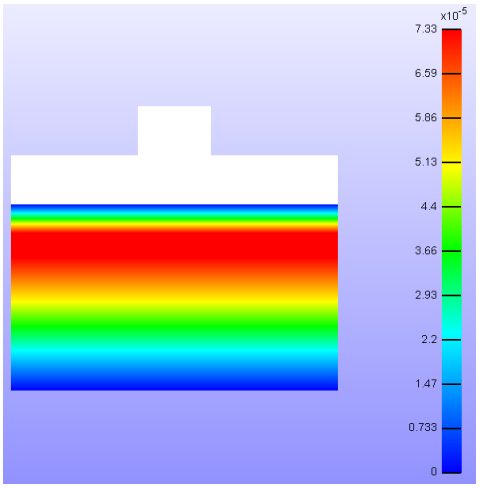

$t = 998.9s$

5. Discussion

5.1 Model Validation

5.1.1 Validation of *PreView* Biphasic Material

As can be seen in Figure 2, the mesh nodes were only created in the vertical, z-direction. This is because the test being simulated is a confined compression where all the movement will be in the vertical direction, and thus analysis is only required along this axis. The simplest measurement of mechanical properties is said to be a step-stress or step-strain experiment[10]. However, the sudden application of a load can result in many problems, including creating severe strain gradients near the surface and significantly affecting the relative fluid flow within the tissue under investigation[15]. Additionally, a step input is not realistic experimentally, and since the overall results should be applicable to experimental procedures, with the purpose of comparing the results accurately, a ramp-hold input was used.

The purpose of the model created in this section was to validate the biphasic material choice in *PreView* so that the model created can go on to act as a control model in future sections of this project. It is therefore important to analyse the properties of a biphasic material correctly.

Figure 21 displays the recorded output force at the platen. As can be seen, the confined compression test in *FEBio* of this biphasic material has provided a stress response with well-defined ramp and hold phases. The ramp hold is between $0 - 100s$, the same as the prescribed displacement ramp input. The end of the ramp phase creates a peak, which is an important point to analyses when looking at biphasic behaviour. This is because the peak is said to increase with increasing collagen content[4]. After the peak, the curve then starts to levels out to an equilibrium value. This value is also of importance as it shows that there is no longer any fluid pressure gradient within the material and is the point at which the solid matrix resists the applied load. However, the analysis in this section is not long enough for the correct equilibrium value to be defined. Therefore in other *FEBio* models the analysis step should be sufficiently extended in order for the equilibrium value to be reached.

Figure 22 illustrates the progression of fluid flux through the medium. These time frames are obtained from *FEBio*'s post-processor software *PostView.* In *PostView* the analysis is dynamic, and thus a corresponding colour key has been provided for each

time step. Through explanation of this fluid flow (units: m/s), it should be clear whether or not the material is biphasic.

Looking at t = 0s, the material is homogeneous, shown as there is 0 fluid flux, and therefore is no strain at any point within the 'tissue'. Under application of a load, in confined compression, the 'tissue' can't deform immediately[16] and the fluid pressure rises to balance said applied load. Initially, under this compressive load the fluid stress supports the applied stress, as can be seen in Figure 22 between the time steps t = 0s and t = 49.93s, as a small fluid flux appears at the top of the 'tissue'. These time steps demonstrate the first half of the ramp phase where the load (prescribed displacement) is applied. The application of this load causes a vertical displacement to occur. In response to this vertical displacement the fluid pressure rises, creating an induced fluid flow out of the porous platen. Between the stated time steps a thin red line appears, illustrating an area of high fluid flux ($\cong 1.87\mu m/s$). Through the dynamic analysis it can be seen that at $t = 99.93s$ the fluid flux measurement at the platen has increased to a value of $\cong 2.63\mu m/s$ (this area of red also increases slightly in size). This implies that during the ramp phase of the simulation, the fluid part of the biphasic material is modelled to dissipate out through the porous platen. This demonstrates the fluid flow down the pressure gradient (between the outside atmosphere and the tissue) out of the tissue at the boundary, namely the platen-tissue interface.

After the ramp phase, during the hold phase, the measurement of fluid flux in the high fluid flux area has decreased to $\cong 0.7\mu m/s$ at $t = 249.9s$ to $\approx 3\mu m/s$ for times steps $t = 499.9s$ and $t = 749.9s$. This suggests that as the time progresses a localised compression starts to appear at the platen-tissue interface, causing the fluid to no longer dissipate out of the 'tissue'. This in turn causes a fluid pressure gradient to arise and the fluid beings to dissipate down through the tissue in the direction of compression - this is illustrated by the increase in size of the high fluid flux area (red part in all time frames of Figure 22). The permeability value governs the rate of this fluid flow through the 'tissue'. Since the permeability has been modelled to be a constant value it means that the fluid part will travel vertically downwards at a consistent speed.

Beneath the red section in the pictures of Figure 22, there are also yellow, green and light blue sections. At the end of the analysis, t = 2000s, these colours are seen to appear directly beneath the platen, between the platen and the red section. This

illustrates that majority of fluid flow is now within the 'tissue'. At this stage, in the hold phase, the load remains constant and the developed fluid pressure drives the fluid down the 'tissue'. The fluid is expected to diffuse through the 'tissue' until the equilibrium solution is reached. Unfortunately, this analysis is not long enough to exhibit tissue relaxation but it efficiently displays all the steps up until this point.

At equilibrium the stress and strain throughout the whole 'tissue' should be constant, and there should no longer be a fluid pressure gradient.

Referring to Equation 2, at equilibrium $\frac{\partial \mathrm{u^s}}{\partial \mathrm{t}} = 0$ and therefore the equation reduces to $\frac{\partial^2 \mathrm{u^s}}{\partial \mathrm{x}^2} = 0$. Integrating this verifies that at equilibrium, $\mathrm{t} \to \infty$, the strain is constant throughout the 'tissue'. Thus, with reference to Figure 22, the 'tissue' should appear all dark blue as in the $t = 0s$ time frame. At equilibrium, the solid part of the material resists the applied load, meaning that the Young's modulus stiffness parameter plays an important role into how much load the solid phase of the model can withstand.

Therefore, it can be said that under load the tissue has more fluid-like behaviour, but it is the solid part that implements the boundary conditions, maintaining its mechanical compressive strength. This explanation of the fluid flux in the different time steps of Figure 22 proves that the material assigned to this model can be regarded as a fully functioning biphasic material. This is because it has been shown to co-exist as both solid and fluid phases. Therefore, this material and properties can continue to be used in the proceeding aims to model collagen gels, but the analysis time should be extended.

In the set-up of the model, a tied-interface contact was assigned between the 'tissue' and the plunger. Additionally, a boundary condition of pressure equal to zero was given along this interface. This shows that the platen is modelled as being porous, allowing the free flow of interstitial fluid out of the 'tissue'. If the biphasic model functions correctly the fluid will initially flow out of the porous plunger and then dissipate through the medium to create a zero pressure gradient. This is illustrated clearly in Figure 22 during the ramp phase time steps.

5.1.2 Validation of *PreView* Tied-Biphasic Contact Interface

The model in this section was created with the intention to prove that the biphasic interface available in *PreView* did not alter the output in any way. Section 5.1.1 effectively showed that the biphasic material selected functions properly for the

defined parameters. Therefore by defining two blocks connected by a biphasic interface and having the same material parameters, if there are any changes in the output then it will be due to the contact between the two parts.

When applying the mesh nodes to the geometry there is an option to have a 'z-ratio' which increases the mesh density at one or both ends of the material. This would be beneficial as it means more analysis will be undertaken at the interface and boundaries. However, as can be seen from Figure 4, the nodes assigned are close enough together that a mesh ratio is not required. One change that was implemented was that the analysis time was extended. This was done to allow the fluid to dissipate the full way down the model, meaning it will cross the interface and, hopefully, reach equilibrium. Extending the analysis so that the fluid flux passes the contact ensures that the biphasic-interface works correctly, or if it creates any unwanted effect on the fluid flux.

By comparing Figure 23 to Figure 21, it can be seen that the same ramp and hold relationship exists. Furthermore, as the analysis time has been extended, the tissue now reaches full relaxation through the hold phase, and levels off to a constant equilibrium value. Therefore as there are no discontinuities in the output force, it can be suggested that the biphasic-interface contact provided in *PreView* functions efficiently. In order to confirm this hypothesis the two-layer biphasic model was analysed in *PostView* and compared to the theory described in Section 5.1.1.

Figure 24 illustrates the *PostView* images obtained for the 1D confined compression of the two-layer biphasic material. The time steps $t = 0s$ to $t = 2461s$ display an equivalent pattern to the images in Figure 22. Therefore the same analysis applies to these time steps. However, as the analysis in this section has been extended in time, after $t = 2461s$, the fluid flux can clearly be seen to dissipate down the 'tissue' further in the direction of compression displaying the start of tissue relaxation - this is illustrated by the red section becoming larger, showing the area of maximum fluid flow. Additionally, in the time-step frames for $t \geq 49{,}960s$ the tissue can be regarded to have reached equilibrium. This is because the difference between the maximum fluid flux (red section) and minimum fluid flux (dark blue section) is $\leq 59.7nm/s$. This is a magnitude of $x10^{-6}$ smaller than the difference in fluid flux illustrated initially at $t = 44.55s$, where the difference is $0.02m/s$. Therefore the difference can be regarded as negligible, and thus the 'tissue' is said to have effectively reached equilibrium as there is no longer any fluid flux, a result of there being no fluid pressure gradient. This

demonstrates the tissue's attempt to regain its initial shape. As this re-iterates what was found when evaluating Figure 23, and there is no disturbance in the fluid flux across the boundary (see $t = 19{,}960s$) it can be said that the biphasic interface functions correctly and does not cause any irregularities in the output. Hence, it can be used in all proceeding models to create a fully functioning 'tumour' layer.

5.1.3 Validation of *FEBio* coding

The *bpcontrol* model in *FEBio* did not take as long a time as the other models, and therefore it was ideal to use to determine the correct force input. Nonetheless, as can be seen the reaction force of *bpcontrol* under prescribed displacement (Figure 6) is not very smooth in the ramp phase, or the initial section of the hold phase. Therefore four different methods were used in order to 'smooth' the curve and still obtain the correct output displacement - which will be the same as the initial displacement input (Figure 5).

In Method 1, where the force output graph is used directly as an input for a force control test, the output displacement graph (Figure 25) can be seen to illustrate the correct strain rate. This is important as strain is time dependent so a difference strain rate could affect the output results obtained. However, the displacement is seen to go slightly beyond the maximum after the peak position ($t = 100s$). This suggests that the disturbances in the original force input (Figure 6) has cause a disturbance to the output response recorded. This is because after the peak position the displacement should be constant, illustrating the hold phase of the original displacement input. Therefore, the proceeding methods were attempted in order to smooth this force curve and create a more appropriate force input curve that produces the required output.

In Method 2 the load curve points were approximated manually. However as only 4 points were created on the load curve (Figure 7), the force input is simplified drastically. This causes the output displacement (Figure 26) to take on the incorrect form. The hold phase of the output should be a constant value, but it is seen to creases and then level out to an equilibrium value. This causes a problem as this input is not very applicable in real experiments. Additionally, the displacement goes beyond a 10% compression within the ramp phase causing a slower same strain rate. Thus, the solution was to smooth the curve in Figure 6 to get rid of the disturbances and discontinuities, but not drastically simplify it.

The next method (Method 3) used was the moving average function in *Excel*. It was assumed that this method would just smooth the disturbances. However, as can be seen in Figure 8, it kept in one of the discontinuities and also reduced the maximum force. This caused the output displacement (Figure 27) to not reach a full compression of 10%, meaning that the strain rate was slightly reduced. The advantage of this method was that the peak position remained at $t = 100s$. Therefore, one additional method was attempted with the intention of defining the correct time at which the ramp phase should end, but ensuring the maximum force is also reached.

Method 4 used the curve fitting technique available in *Excel.* To ensure the end of the ramp phase remained at $t = 100s$, the curve was split into two sections and they were constrained to meet at this time position. Method 4 appeared to produce the best approximation of the force curve (Figure 9), suggesting that the best displacement output would also be obtained. The output displacement response recorded at the platen (Figure 28) is considerably similar to the original ramp-hold input (Figure 5). This implies that the coding within the *FEBio* programme is

Method 4 appeared to produce the best approximation of the force curve (Figure 25) via *Excel*'s curve fitting technique. The graph has been efficiently smoothed but still reaches the same peak and equilibrium force values. The curve was manually adjusted by inspected and to ensure the boundary conditions were met the data was spilt into two sections: ramp $(0 - 100s)$ and hold $(100s +)$. By constraining the two sections to meet at the peak point, $t = 100s$, the output displacement graph in Figure 26 was obtained. The displacement curve in Figure 26 is very similar to the original in Figure 6. It has a slight 'kink' after the peak point, however, it was assumed small enough to disregard.

Therefore, by smoothing a force output curve and using it as an input to simulate a prescribed force experiment, the original prescribed displacement graph was found. This shows that the coding within the *FEBio* programme works correctly, and that the models created are fully operational. Consequently, any of these methods can be used in the following aims to create a curve input accurately.

5.2 Parameter Sensitivity Analysis

5.2.1 Stiffness Parameter Specification

In consideration of the biphasic material, tied-biphasic interface, and consequently the coding, in the *FEBio* programme being validated in Section 5.1, a hierarchy of three-layer biphasic models of experimental dimensions were created. The models all contained an intermediate of $1mm$ thick that represented a 'tumour' layer within the 'tissue'. This 'tumour' layer was modelled at varying positions, all increasing in distance from the platen. When creating the models it was imperative to ensure that the *bp-top* and *bp-bottom* layers were not non-existent, i.e. that there should be some 'tissue' either side of the 'tumour' layer. Therefore, using a $1mm$ layer, seven different models were created, as can be seen in Figures 12-18. A control model of the same dimensions of the full 'tissue' was also created (Figure 11).

The various values chosen for Young's Modulus (E) and permeability (k) are shown in Tables 3 and 4 respectively. The value of E was increased to illustrate a stiffer solid part of the biphasic material, as it is well known that as E increases, the stiffness of the material increases. However, there is little previous investigations into the relationship between k and the equivalent stiffness of a biphasic material, only the relationship with fluid flow is known[16] – for this reason the magnitudes of k both larger than and smaller than the reference value, $k(0)$, were taken.

Additionally, there are limited investigations into the Poisson's ratio (ν) of a collagen hydrogel that represents normal body tissue. For this reason, a reliable source was used. The value of ν was taken from a study on nucleus pulposus by Farrell and Riches[31]. Through the literature review it was observed that in nucleus pulposus investigations, if a computational model is required it is modelled using a collagen hydrogel. Furthermore, as Poisson's ratio can be considered to 'scale' the value of the Young's modulus, it is not required to change both these parameters. Even though the value of ν used is not for the correct tissue, as long as it is kept constant it should not affect the results in any way.

It is expected that for the models created with a stiffer middle layer in different positions within the 'tissue', that the output response will change from that shown in the original displacement input, Figure 5. If a change in output displacement is seen then it can be concluded that the subsurface (*bp-middle*) does have a mechanical effect

that can be seen on the surface. This will determine whether or not the investigation of a biomechanical biomarker is possible. Additionally, the mechanical effect perceived may be dependent on the stiffness parameter E and k, and the distance of the 'tumour' layer away from the platen – where the response is being recorded. Busby *et al*. noted that as collagen content increased the peak and equilibrium stress values also increased. Therefore there is already an apparent relationship between tissue stiffness and mechanical response, but there is no definite relationship specific to the different stiffness parameters of the tissue under investigation.

The exported *.feb* files (Appendix 9) for each model can be altered in order to edit the input parameters of stiffness (E and k) of the biphasic material used for *bp-middle*.

5.2.2 Force Control Testing

It was discovered that the prescribed displacement runs analysed in Section 5.1 took a substantial amount of time to run (some over 3 hours). Therefore, since the use of force control testing was validated through validation of the *FEBio* code, a prescribed force simulation was carried out, in an attempt to reduce computation time.

The 25 different stiffness circumstances specified in Section 4.2.1 were applied to all seven different models created. The 175 different models were then run through *FEBio* under a prescribed force, using the curve shown in Figure 19. This curve was obtained by inputting a prescribed displacement (Figure 5) to the control model (*bpcontrol*) using the parameters specified in Table 3 along with $E(0)$ from Table 4 and $k(0)$ from Table 5. The curve illustrates the reaction force at the plunger. It can clearly be seen that this force is significantly smoother than the one found in the previous aim, shown in Figure 6. Therefore, this force output can be used directly as an input for a prescribed force simulation (Method 1 in Section 4.2.1).

The displacement outputs from the 175 different models were then compared to the control in order to determine the effect of position and stiffness of the 'tumour' layer under a force control test - the results are shown in Figures 29-44. They display plots of the position of the platen COM of the model under investigation relative to the equivalent position of the control model. Two different positions of the platen were analysed: the peak position ($t = 100s$) and the equilibrium position ($t = 1000s$). The peak position was taken as the position of the platen COM at $t = 100s$, as from the results in Section 5.1.3 some output displacement graphs were seen to have a small

'kink' after the end of the ramp phase which could disrupt the results for peak displacement. Therefore, through interpolation techniques the position at $t = 100s$ was approximated and assumed to be the position of the platen COM at the end of the ramp phase, i.e. the peak position.

Figure 29 illustrates the difference in 'peak' position of the output curves, with the y-axis shows the difference in platen COM position of the each model compared to the corresponding value for the control. From the analysis in Section 4.2.2, and considering the corresponding data point parameters given in Appendix 6, it can clearly be seen that with a lower magnitude of permeability (k) and a higher magnitude of Young's modulus (E), a 'stiffer' material is illustrated. This relationship is more apparent in Figures 30-33, where the relationship between E and k is directly related to the output displacement position. It can also be noted from these figures that the permeability value has the greatest effect on the output peak response. It can be seen that as the permeability of *bp-middle* is increased, the tissue appears 'softer'. With a decrease in magnitude of k, the peak position recorded is not as low as that recorded for the control, giving a positive change in displacement. This reveals that the platen of the model under investigation has not changed in position as much as the platen of the control model. Therefore it implies that a full 10% compression is not reached, suggesting that the model under investigation is 'stiffer' than the control and thus cannot be deformed as easily. Subsequently, with an increase in magnitude of k the peak position is lower than that recorded for the control, represented by a negative change in displacement. This shows that the platen of the model under investigation has caused a compression greater than 10%, meaning the model has deformed easier than the control. This indicates that a model with a negative change in displacement is 'softer' than the control. Focusing on data points 1 to 5 in Figure 29, the parameters of each point are shown in Table 10 below:

Data Point	Permeability value, k	Young's Modulus Value, E
1	-x100 = 1 N/mm^4	0 = 0.001 mm^4/Ns
2	-x100 = 1 N/mm^4	x250 = 0.241 mm^4/Ns
3	-x100 = 1 N/mm^4	x500 = 0.482 mm^4/Ns
4	-x100 = 1 N/mm^4	x750 = 0.723 mm^4/Ns
5	-x100 = 1 N/mm^4	x1000 = 0.96429 mm^4/Ns

Table 10 - Data Points 1-5 and Corresponding Parameters for Figures 29 and 37

If data points 1-5 (representing $k(-x100) = 1$) are compared to data points 20-25 (representing $k(+x100) = 10{,}000$). It can be perceived that for the $E(0)$ data points, points 1 and 20, where only the permeability has changed, there is a significant difference in peak displacement at the end of the ramp phase. Data point 20 is a negative value; this means that the tissue has been compressed beyond a 10% compression. This re-iterates that a lower magnitude of k represents a softer biphasic material. Therefore, by comparing permeability directly with model stiffness, it can be established that a permeability of magnitude lower than reference ($k(-x100)$) illustrates a more 'solid-like' material, and a permeability of magnitude higher than the reference ($k(+x100)$) signifies a softer material. Consequently, it confirms that a biomechanical biomarker conditional of known stiffness parameters is possible.

Furthermore, when comparing the different models under investigation in Figure 29, it is visible that a greater response is seen when the 'tumour' layer is positioned closer to the platen. This proves that tumour depth would have an effect on the biomechanical biomarker found as the change in response of the tissue is not as significant as when the 'tumour' layer is closer to the surface – seen by comparing *Bp1* to *Bp7*. It can also be understood that with an increasing distance from the platen, the stiffness parameters of the 'tumour' layer are less noticeable. Therefore, in determination of a biomechanical biomarker, the distance between the surface and the tumour under investigation has to be relatively small. From analysis of Figures 30-36 it can be seen that as the 'tumour' passes half way through the full depth of the model, *Bp4*, the response is significantly less noticeable. This is clear in Figures 34-36 as the responses all appear as equivalent for each value of E and k, and the difference in output peak response is negligible. Therefore, in proceeding tests only the first few biphasic model set-ups will be analysed further as the closer the layer is to the platen, the greater the biomechanical effect visible. Moreover, the variations noted above for E and k are not as evident as the 'tumour' layer moves further away from the platen. Therefore, a biomechanical biomarker would be most effective for tumours close to the surface of the tissue

From Figures 30-33 it can also be seen that the Young's modulus value has less of an effect on the output with a decrease in permeability value. Therefore it can be recognised that the permeability parameter has the greatest effect on the stiffness of the material. Furthermore, above a Young's modulus magnitude of $x250$ the response does not change. This suggests that the value of E that causes a difference has a

maximum value, and past this point an increase in Young's modulus has no effect on output response of the biphasic material.

Figure 37 displays a plot of the difference in equilibrium position of the output displacement of the platen COM of the model under investigation relative to the control model. The corresponding data point parameters are also given in Appendix 6. It can be noted that there is an equivalent response to that found for the peak values at $t = 100s$. That is, there is a change in response when the magnitude of E of the middle layer is increased, causing the 'tissue' to appear stiffer; and that for $E(x250)$ to $E(x1000)$ the change in displacement recorded are relatively similar. This relationship is clearly seen for all permeabilities and is confirmed by Figures 38-44. In these figures it can be seen that by increasing the magnitude of the permeability it has no effect on the output equilibrium response. However, compared to the output peak response, the equilibrium response is more apparent when the 'tumour' layer is further from the platen. This proves that both the equilibrium and peak positions of the output response are important in determination of a biomechanical biomarker for a force control test.

It can be noted that the *Bp1* model gives the stiffest equilibrium response, for a permeability magnitude of $k(-x100)$ and a Young's modulus magnitude of $E(x250)$ or greater. The higher equilibrium response seen for this model (Figure 38) suggests that the tissue has yet to reach the point of relaxation – this confirms the theory that this model demonstrates a more 'solid-like' material.

Comparing each model for permeability values of $k(0)$, $k(+x10)$ and $k(+x100)$, there is infinitesimal difference between the models, proposing that the 'tissue' has reached the point of full relaxation. This reiterates the point that a lower permeability value illustrates a 'softer' material, as a softer material would reach equilibrium faster and therefore explains why they all have the same final value after a time of $1000s$. Furthermore, this demonstrates that a 'stiffer' biphasic tissue does not reach full tissue relaxation within the allotted time, suggesting that a biomechanical biomarker relating to equilibrium time is time dependent.

In conclusion, it is believed that determination of a biomechanical biomarker is possible, based on the stiffness parameters of E and k, and the difference in tissue response can be analysed both at peak or equilibrium positions.

The table of values in Appendix 6 provides the parameters of each data point as well as the corresponding position measurement in mm. The first column, labelled 'Bp', provides the model number for *bpplaten1* to *bpplaten7*. $Bp = 0$ illustrates the control model, and provides the reference values. Following this column is the data point column which gives the value corresponding to the x −axis of both Figures 29 and 37. The data point for the control is given as 0, however in the graph it appears at datat point 11. This was done in order to compare the control model to the other models for parameters $E(0)$ and $k(0)$. The two subsequent columns represent the stiffness parameters for the 'tumour' layer, *bp-middle*, where p is the permeability and E is the Young's modulus value. The columns after this are the data points retrieved after running the *FEBio* outputs through MATLAB using the code in Appendix 4 – the positions are all given for the position of the platen's COM in each model.

The 'normal tissue' values of E and k are considered to be the reference values from the Busby *et al*.[4] investigation, namely $E(0)$ and $k(0)$. To ensure the biphasic contacts continue to have no effect on the results obtained when the parameters have been updated, the control model was compared to each model with *bp-middle* stiffness parameter $E(0)$ and $k(0)$, namely these are the models with $E = 0.001MPa$ and $k = 100Ns/mm4$. The objective was to determine whether or not the tied-biphasic interface functioned properly in all models. As is most apparent in Figures 29 and 37, data point 11 falls precisely on the x-axis, illustrating that there is a $0mm$ change in output position compared to the control. This re-iterates what was proven in Section 5.1.2 that the tied-biphasic interface has no effect on the output recorded.

From the literature review it was established that in order to change the stiffness properties of a material the following parameter should be altered: Young's modulus (E), permeability (k), solid volume fraction (φ), and Poisson's ratio (ν). In this section only the E and k values were altered to different values to determine whether the change in parameters affected the tissue's response. It was also noted that ν acted to scale the value of Young's modulus, and therefore would not be required to be under investigation as there is also not definite reference value as the control. Therefore, the only other parameter to investigate is solid volume fraction. φ should not have any effect on the mechanical response as it is a property of fluid flux, and therefore will not alter the solid matrix properties of stiffness. However, to prove that it has no effect on the mechanics of the tissue, 3 set-ups were created for each model of *bpplaten1*, *bpplaten2* and *bpcontrol*.

The three different set-ups created were:

1) $\varphi = 0.2$ for all layers
2) $\varphi = 0.003$ for all layers
3) $\varphi = 0.2$ for *bp-middle* with $\varphi = 0.003$ for *bp-top* and *bp-bottom*

These values for solid volume fraction were applied to all 25 models in *bpplaten1*, *bpplaten2* and the control model, *bpcontrol,* as these are the models where the most significant different is visible. Therefore if no effect is seen in these models it can be proposed that there will be no effect in other models.

All models were simulated with a prescribed force, using the force curve shown in Figure 19. The displacement output graphs were then compared and were seen not to vary at any part. Hence, it was concluded that the solid volume fraction parameter of the biphasic material had no effect on the mechanical response of the tissue at the end of the ramp phase, i.e. the peak position, or at the equilibrium point. This means that the biomechanical biomarker under investigation does not have any relation to the solid volume fraction parameter of the stiffness.

All the figures created in Section 4.2.2 were illustrated as a change in position to the control. This was done so that a direct comparison between the effect on the surface and the parameters used could be viewed, and the difference in output response can be used to determine a biomechanical biomarker relative to the stiffness parameters E and k.

This section of the investigation was very time consuming, as even though prescribed force experiments are faster than prescribed displacement ones, due to the large number of models the computation time was still relatively long.

5.2.3 Displacement Control Testing

Previously it was noted that the prescribed displacement runs took a considerable amount of time in *FEBio* (up to 3 or 4 hours). However, it was found through completion of the force control testing that some of the prescribed force simulations also took an extended amount of time, similar to that of some prescribed displacement tests. Therefore, in order to be able to compare the results directly to experimental investigations a prescribed displacement model was created. This is beneficial as prescribed displacement is easier to achieve experimentally, and by using a similar set-up to that of Busby *et al.* (2013) the results can be verified. If the results are similar it

concludes that the computational programme *FEBio* is fully operational and can effectively model biphasic tissues. It also proves that any changes in the output response compared to the control are due to the change in parameters. Therefore this change can be investigated as a possible biomechanical biomarker.

For the previous sections, a 10% compression was used with a strain rate of $0.1\%/s$. However, a 0.3% collagen gel has a high permeability as it mainly consists of water (solid volume fraction =0.003). Therefore a faster strain rate is required with the aim of seeing better results. The strain rate was increased from $0.1\%/s$ to $0.5\%/s$ – the strain rate value in the investigation by Busby *et al*[4].

By using the experiment set-up from a previous study by Busby *et al.*[4], and the parameters shown in Tables 6, 7 and 8, 25 different stiffness circumstances were created for each biphasic model (*bpplaten1* → *bpplaten7*). Under confined compression with a prescribed displacement of $-0.4mm$ in $10s$ (Figure 20), the output stress response at the platen level was recorded. The force curves obtained were all similar in form to the one shown in Figure 45 for the control model, *bpcontrol.* As it is not suitable to show these for all 176 runs, the values of the peak force, which occurs at the end of the ramp phase ($t = 100s$), and the equilibrium force, which occurs at the end of the analysis ($t = 1000s$), were extracted and comparison plots were created - shown in Figures 46 and 48. Figures 46 and 48 were analysed in order to predict if there was any mechanical effect of varying the 'tumour' depth of stiffness parameters *E* and *k* of the 'tumour' layer through a prescribed displacement experiment.

The different data points and the corresponding parameters for Figures 46 and 48 are found in Appendix 7. The table set-up is similar to that in Appendix 6, described in Section 5.2.2. The only change is the values are now for peak and equilibrium force instead of displacement position. It is good to note that the same relationships between stiffness parameters and output response are found in the prescribed displacement simulations that were found previously in the prescribed force experiment (Section 4.2.2). This is that an increase in *E* and a decrease in *k* exhibit a stiffer appearing tissue at the tissue level, as the output responses are higher. A higher force resistance implies more resistance to compression, and consequently a higher stress at the platen surface. By focusing on data points 1 to 5 (see Table 9 for parameters), it can be seen that the same relationship exists between data point 1 and data points 2-5. This is that the increase of the Young's modulus makes the 'tissue' appear stiffer. This is clearly shown

in Figure 46 for *bpplaten1*, and it is also demonstrated for all biphasic models in Figure 48.

In Figure 46 *bpplaten1* is the only model to show significant difference in peak force for all permeability values. The other models' peak values are within one hundredth of a Newton away from the control (whose peak force value is$\cong -0.14N$, Figure 45). Therefore when analysing the peak force output there is only significant change if the 'tumour' layer is positioned very close to the platen. In order to determine if the stress response has noticeable change that could be regarded as a biomarker, the different in the stress output of each parameter set-up for *Bp1* was compared to the control model, and the results shown in Figure 47. Unlike previous analysis, it is seen that with a decrease in k, the Young's modulus parameter becomes more effective. The difference in peak stress response is significantly better than when considering the force. When analysing Figure 47 it can be seen that the difference in output is best differentiated when there is a lower permeability value. This re-iterates the results found before. The other biphasic models were not presented individually as the change in peak stress $\leq 0.5Pa$, which is not a substantial enough different in order to differentiate different stiffness parameters. Therefore, under a displacement control test, the peak response is not the best position to analyse.

The relationship between stiffness and *bp-middle* position within the model is better displayed in Figure 48, showing the change in equilibrium position of the output force. The relationship displayed is the same as the one found in Figure 37 - the connection is that as the 'tumour' layer, *bp-middle,* moves further away from the platen the stiffness parameters of the layer have less influence on the output response at the surface. It can also be noted that, again, there is little variation in the results for $k(0), k(+x10)$ and $k(+x100)$ when looking at equilibrium response compared to the control. This reiterates what was proven previously, that the higher the permeability value, the softer the biphasic material appears and the quicker it reaches equilibrium after disturbance. Evaluating the equilibrium force output is not very beneficial in the attempt to define a biomechanical biomarker as the difference in force output is still relatively small, $< 0.07N$. In an attempt to create a measureable outcome the stresses corresponding to each recorded force was calculated. The graphs of the mechanical stress response for each model are given in Figures 49-55. The explanation of the parameters of these graphs is the same of that previous stated for Figure 47, but for equilibrium stress. These figures clearly illustrate that the closer the 'tumour' layer is to

the platen, the larger the difference in output stress, with the maximum change in stress varying from $\cong 360Pa$ in *Bp1* to $\cong 10Pa$ for *Bp7*. Nonetheless, each biphasic model displays the same relationship between E and k described in Section 4.2.2 for the equilibrium response, with the stiffness parameters again becoming less significant as the distance from the platen increases (compare Figure 49 for *Bp1* to Figure 55 for *Bp7*). Additionally, it is important to note that even though the change in stress for the other biphasic model set-ups are not as large as that illustrated for *Bp1*, the same relationship is apparent for each model. Therefore if the depth of the 'tumour' layer is known, the mechanical stress output could be used as a biomechanical biomarker. This stress response would correspond to specific values of permeability and Young's modulus for the 'tumour' layer. Consequently, if there was a hierarchy of models with additional stiffness parameters and different thicknesses of layers at various positions, a more specific biomarker could be determined in correlation with 'tumour' layer thickness. This could in turn develop into a biomechanical biomarker of cancer if the stiffness parameters of different tumours are recorded and a direct correlation may be made between the stress response of a displacement control test and the corresponding stiffness parameters of the 'tumour' within the tissue under investigation. However, further research is required in order to define stiffness parameters of different tumours.

As can be seen in Figures 46, 48 and 55, the data points for *bpplaten7* do not differ from the control value by very much. It can be noted that when the files for *bpplaten7* were ran through *FEBio* they were significantly faster than the other models. The speed of the computational simulation was similar to that of the control model, and thus suggests that the 'tumour' layer at this position is too deep within the 'tissue' to considerably affect any results. There is a possibility that if the analysis ran for longer a better change may be viewed, but in combination of the other results found it is unlikely that any significant change in response if the equilibrium time is increased.

The comparison figures (46 and 48) clearly illustrate biphasic behaviour as the peak and equilibrium forces, which are relatable to the peak and equilibrium stresses, display significant increase with increasing stiffness – supposing an increase of stiffness is modelled by a larger E value, a smaller k value and *bp-middle* position closer to the platen. Therefore, a biomechanical biomarker is possible with regards to stiffness parameters E and k, but is dependant of tumour depth within a tissue. This means that

any observed changes in the output force/stress can be regarded as a biomechanical biomarker due to the influence of the 'tumour' layer.

Figure 49 illustrates the difference stress response for *Bp1* compared to the control model. As can be seen from Figure 48, this model is the one in which creates the largest difference in output equilibrium force recorded at the platen. By examining output stress the results are directly relatable to previous experimental studies. It can clearly be seen from this graph that the model with permeability $k(-x100)$ and Young's modulus $E(x250)$ or above creates the largest different in mechanical response. This stress output is significantly different from all other set-ups for the same biphasic model. This graph emphasises what has been proven previously, that the greatest effect is seen with these parameters at this platen level. This provides support to the hypothesis that a biomechanical biomarker can be found.

In order to visualise the influence of the 'tumour' layer the z-stress graph was viewed in *PostView* (Figure 56). The solid and fluid part of the biphasic materials should act as described in Section 5.1.1, however, the stiffer layer is expected to affect this. For example, as permeability influences the rate of fluid flow, the fluid should flow slower through the 'stiffer' layer with an increased permeability. Additionally, a material with an increased Young's modulus value will have a stiffer solid matrix, which implies that it will not compress as easily. By analysing Figure 56 it can be seen that the stress in the vertical direction linearly increases as time goes on. The stress reaches a maximum at $t = 1000s$, which is regarded as the equilibrium point. Therefore it can be noted that the equilibrium stress of the stiffest set-up of a *bpplaten2* model ($E(x1000)$ and $k(-x100)$) is $\cong 2.7x10^{-4}MPa \equiv 270Pa$. By comparison with the Busby *et al.* investigation (see Appendix 8 for graph), this stress value is representative of a collagen hydrogel with percentage greater than 0.3% but less than 0.4%. It can be seen that at $t = 1000s$ the value is not constant, and it therefore is not a correct representation of an equilibrium stress. Hence, this may account for the change in result. However, as the results are of the same magnitude it can be established that the results are in agreement. Thus, the simulations have successfully produced models demonstrating a stiffer 'tumour' layer, and the effect of the stiffer layer can evidently be measured as a surface output. Consequently, there is potential to determine a biomechanical biomarker, but more research into the area is required in order to create a hierarchy of models.

To further visualise the effect of the addition of a stiffer intermediate layer, the *PostView* output of z-fluid flux was analysed. This was done so that the results of the displacement control test could be visually compared to the result in Section 4.1, and the analysis in Section 5.1. By comparison to Figure 22 (*PostView* output files for 1D homogeneous control model), in Figure 57 it can be seen that the fluid flux pattern begins to differ at $t = 28.38$s. Previous to this time frame, at $t = 19.99s$, the pattern beginning to appear at $t = 2000s$ in Figure 22 is apparent. This suggests that there is an obstruction to the fluid flow, causing the rest of the tissue in the Figure 57 analysis to appear dark blue. By comparing the position of this apparent obstruction to the *bpplaten2* model (Figure 13 Section 3.2.1) it can be noted that this barrier appears to be the interface between *bp-top* and the 'tumour' layer. As in Section 5.1.2 it was proven that the tied-biphasic interfaces function efficiently it can be established that the difference in pattern is due to the change in stiffness parameters. Focusing on the time frame $t = 28.38s$ in Figure 57, it can be seen that the fluid flux starts to dissipate through the 'tumour' layer. The speed fluid flow is taken to be $\cong 0.1mm/s$ which is significantly slower than previous time steps. This is expected though as the permeability governs the rate of fluid flow, therefore as this intermediate layer is modelled to have a considerably lower permeability value the corresponding fluid flux will also be reduced. This confirms that the biphasic three-layer model is correctly functioning when demonstrated by the *FEBio* software. It can be seen in later time steps the model is heading for tissue relaxation, but due to the stiffer layer, the time taken to reach a constant value is altered. Therefore it is suggested that the change in equilibrium values recorded for the models with the stiffer layer are only different as they have not yet reached their true equilibrium value. Thus for further mechanical tests, a set time for measurements should be tested and compared, rather than labelling a position 'peak' or 'equilibrium'.

6. Conclusion

In conclusion, it is believed that the possibility of having a biomechanical biomarker is possible. After efficient validation of the biphasic material and tied-biphasic interface in *PreView*, and appropriate authentication of the *FEBio* programme, a hierarchy of models were created with parameters based on studies by Busby *et al.* and Farrell and Riches. Three-layer biphasic models with a 'tumour' layer of varying stiffness were created and simulated under both force control and displacement control tests in *FEBio*. Simulating a 10% confined compression through a ramp-hold force control test, differences in the output peak and equilibrium displacement were illustrated. These differences had a direct correlation with the stiffness parameters under investigation, Young's modulus and permeability. It was found that the stiffness of the 'tumour' layer was increased when a lower permeability and a higher Young's modulus value were modelled. However, force control tests are difficult to carry out experimentally so there are no previous experimental results to compare the findings to. Conversely, the results of the displacement control test can be directly compared to the findings of Busby and colleagues. Under a ramp-hold displacement control test demonstrating a 5% confined compression, differences in the output force were more apparent at the equilibrium position than the peak position. When analysing the peak force output the difference was only apparent for a biphasic 'tumour' layer situated close to the platen edge, where the output was being recorded. However, when assessing the output equilibrium force the difference was apparent for all biphasic models created. It was established that each biphasic model displayed the same relationship between the stiffness parameters and the output stress, and the further away the 'tumour' layer was situated from the platen, the smaller the difference in output stress. Therefore a directly correlation between output stress, stiffness parameters and depth of the 'tumour' layer has been found. This means that if the depth of the 'tumour' layer is known, the equilibrium stress output could be used as a biomechanical biomarker to determine the corresponding stiffness parameters. Thus, if a database of stiffness parameters corresponding to different grades and types of cancerous tumours was available, this biomechanical biomarker would be able to diagnose whether or not a tumour was cancerous.

Hence, the conclusion drawn is that the determination of a biomechanical biomarker is possible but significant research is still required into a wider range of stiffness parameters and a larger hierarchy of models before it is applicable in a clinical setting.

7. Limitations and Recommendations for Further Work

The main goal of this project is to determine an experimentally validated biomechanical biomarker for cancer. In order to do this the computational model will have to be increased in complexity. One simple method of increase the accuracy of the model would be to use a different solid type for the material specification in *PreView.* The *FEBio* Manual[19] states that care must be taken when using the *Neo-Hookean* material to model materials with nearly-incompressible material behaviour in order to avoid element locking. This is because the *Neo-Hookean* model uses a standard displacement-based element formulation. It is suggested that the *Mooney-Rivilin* material is more appropriate for these situations, and therefore may be appropriate to use in this type of investigation.

An additional investigation that could be carried out in order to increase the accuracy of the model would be to alter the thickness of the layer as well as the position within the 'tissue'. This would increase the complexity of the model without making it too advanced, with the aim of determining whether or not a 'minimum' size of tumour is required in order to define a biomechanical biomarker.

Another method of increasing the complexity of the computational model would be to create a three-dimensional (3D) model of body tissue with a spherical, or more complex shaped, 'tumour' inside. This specially shaped tumour could then be increased or changed in size to mimic the metastasis of cancerous cells. This type of modelling can prove difficult with assigning contacts and meshes and that is why the basic rectangular shaped geometry was used first to ensure the code functioned properly, and that the idea was plausible. A 3D computational model requires the mesh nodes to be in all three axes (x, y and z). The advantage of 3D modelling is that it would allow exact representation of specific tumour sizes and location so that the method could directly relatable to diagnostic techniques in cancer research.

Additionally, in order to effectively increase the complexity of the model it would be beneficial to create a model specific to a type of cancer or a certain body region. This is because as mentioned previously, collagen has many different compositions in different tissue types. Therefore by modelling a specific tissue type, accurate parameters could be obtained so that the model is particular in what it is simulating. Additionally, as seen in the literature review, cancer is very specific, so the biomechanical biomarker will most likely be different for different types and stages of cancer.

Furthermore, the variety of stiffness parameters of the models could also be enhanced so that a hierarchy of set-ups could be created for range of different 'tumour' layer stiffness's. This would create a greater number of permeability and Young's modulus values that could be compared, with an intention to determine the exact Young's modulus value after which an increase does not affect the result.

In the set-up of the models, a mesh of 100 elements in the vertical direction was applied to each different section: *bp-top, bp-middle* and *bp-bottom*. However, the depth of each of these sections is varied, and therefore the distance between adjacent nodes is altered in each model. Furthermore, the control had 300 element nodes equally spaced in the z-direction. Therefore the total number of mesh elements is the same is each complete model, but the position of them is not, which could cause dissimilar analysis in *FEBio*. A possible future study could investigate whether or not the control model with 300 mesh elements can be modelled, but different materials applied to different nodes. This would allow the mesh to always be equally spaced on all the models, meaning every part in each model is under the same amount of analysis; however, it would only work if the node positions on the model were known. Nonetheless, this technique appears advantageous as it could take away the need to create contact interfaces.

Another potential addition to the investigation would be to verify that the Poisson's ratio and density values do not alter the stiffness, and thus the mechanical output response of a tissue. A similar method to that used to determine the effect of solid volume fraction should be used. Even though it is understood from the literature review that these parameters do not affect the results, in order to determine the exact influence of the output response with regard to finding a biomechanical biomarker, it would be valuable to investigate them as well.

When trying to compare the results of this study to those of Busby *et al*., the solutions were found to differ slightly. This may be due to a number of factors. The leading problem is presumed to be that the samples in the paper are cut into cylindrical discs of diameter $15mm$ and depth$4.79 \pm 0.06mm$; and the computational models created were rectangular in shape with sides of $13.3mm$ and a depth of $8mm$. The computational models' volume was modelled from a cylindrical tissue of depth 8mm and diameter 16mm. Therefore the diameters are only 1mm different. Even though this difference appears small, it can cause a significant change in the output stress calculation.

Therefore, if this research were to be continued it would be helpful to model cylindrical discs of the exact dimensions of the paper, in order for direct comparison of results.

The main limitation in this project was the length of time it took to run the model through *FEBio*. It was thought that the prescribed force simulations would run faster than prescribed displacement, which was true for some models. However, as the parameters were updated some of the force input experiments took just as long computationally. Therefore, in the final section it was decided to revert back to prescribed displacement so that a similar experiment could be set-up experimentally and the results would be directly comparable.

A consequence of the long running times was that the output data was contained in large files. This was a problem as it meant that the output files could not be opened in *PostView* in order to visualise the result. It also meant if there was a problem, you could not physically see it to correct it, the code had to be deciphered instead.

During this study the only mechanical test under investigation was a ramp-hold confined compression. This is only one type of mechanical test, and therefore limits the results that can be found. Thus, in order to determine a clearer distinction between the tissue parameters and the mechanical response different dynamic tests such be investigation, such as oscillatory force or displacement tests. Comparing a different testing procedure may be able to assist in determination of a biomechanical biomarker that could distinguish between tissues with and without a rigid inclusion, and determine when the intermediate stiffer layer becomes mechanically important.

8. References

1) Cancerresearchuk.org (2014) *All cancers combined Key Facts: Cancer Research UK* [online] Available at: http://www.cancerresearchuk.org/cancer-info/cancerstats/keyfacts%20/Allcancerscombined/ [Accessed: July 2014].

2) Smith, J. D. and Conlon, K. C. P. (2010) 'Biopsy and Staging: Technical Issues', in Greene, F. L. and Heniford, B. T. (ed.) *Minimally Invasive Cancer Management*, 2nd Edition: Springer.

3) Villanueva, A. L. (2012) 'Biomedicine, Biomarkers, Biomechanics and Predictive Medicine' *Trébol*, 60: 5-10.

4) Busby, G. A., Grant, M. H., MacKay, S. P. and Riches, P. E. (2013) 'Confined Compression of Collagen Hydrogels', *Journal of Biomechanics*, 46: 837-840.

5) Sci.utah.edu (2014) *FEBio* [online]
Available at: http://www.sci.utah.edu/software/40-mrl/39-febio [Accessed: July 2014]

6) NHS (2012) *Cancer - Information on Cancer and useful links* [online]
Available at: www.nhs.uk/conditions/cancer [Accessed: July 2014].

7) Sarg, M. J. and Gross, A. D. (2007) *The Cancer Dictionary,* 3rd edition, New York: Facts on File.

8) Unnikrishnan, V. U., Unnikrishnan, G. U. and Reddy, J. N. (2012) 'Biomechanics of Breast Tumor: Effect of Collagen and Tissue Density' *International Journal of Mechanics and Materials in Design*, 8: 257-27.

9) NHS (2013) *Biopsy – Information* [online]
Available at: www.nhs.uk/conditions/biopsy [Accessed: July 2014]

10) Guck, J., Schinkinger, S., Lincoln, B., Wottawah, F., Ebert, S., Romeyke, M., Lenz, D., Erickson, H. M., Ananthakrishnan, R., Mitchell, D., Käs, J., Ulvick, S. and Bilby, C. (2005) 'Optical Deformability as an Inherent Cell Marker for Testing Malignant Transformation and Metastatic Competence', *Biophysical Journal*, 88(5): 3689-3698.

11) Eyre, D. R. (1980) 'Collagen: Molecular Diversity in the Body's Protein Scaffold', *Science*, 207: 1315-1322.

12) Chandran, P. L. and Barocas, V. H. (2004) 'Microstructural Mechanics of Collagen Gels in Confined Compression: Poroelasticity, Viscoelasticity, and Collapse', *Journal of Biomechanics*, 126(2): 152-166.

13) Xu, W., Mezencev, R., Kim, B., Wang, L., McDonald, J. and Sulchek, T. (2012) 'Cell Stiffness is a Biomarker of the Metastatic Potential of Ovarian Cancer Cells' *PLOS ONE*, 7(10): e46609.

14) Pachenari, M., Seyedpour, S. M., Janmaleki, M., Babazadeh Shayan, S., Taranejoom S. and Hooseinkhani, H. (2014) 'Mechanical Properties of Cancer Cytoskeleton Depend on Actin Filaments to Microtubules Content: Investigating Different Grades of Colon Cancer Cell Lines', *Journal of Biomechanics*, 47(2): 373-379.

15) Spilker, R. L., Suh, J.-K. and Mow, V. C. (1988) 'A Finite Element Formulation of the Non-Linear Biphasic Model for Articular Cartilage and Hydrated Soft Tissues Including Strain-Dependent Permeability', in Spilker, R. L. and Simon, B. R. (ed.) *Computational Methods in Bioengineering*, New York: American Society of Mechanical Engineers.

16) Riches, P. E. (2014) *BE900: Tissue Mechanics - Biphasic Theory Notes*, University of Strathclyde: Department of Biomedical Engineering.

17) Mow, V. C., Kuei, S. C., Lai, W. M. and Armstrong, C. G. (1980) 'Biphasic Creep and Stress Relaxation of Articular Cartilage in Compression: Theory and Experiments', *Journal of Biomechanics*, 102(1): 73-84.

18) Prendergast, P. J., van Driel, W. D. and Kuiper, J.-H. (1996) 'A Comparison of Finite Element Codes for the Solution of Biphasic Poroelastic Problems', *Proceedings of the Institution of Mechanical Engineers, Part H: Journal of Engineering in Medicine*, 210(2): 131-136.

19) Maas, S., Rawlins, D., Weiss, J. and Ateshian, G. (2013) *FEBio: Finite Elements for Biomechanics (Version 1.8) – User's Manual* [online]
Available at: http://mrl.sci.utah.edu/software/febio/ [Accessed: July 2014].

20) Ateshian, G. A., Warden, W. H., Kim, J. J., Grelsamer, R. P. and Mow, V. C. (1997) 'Finite Deformation Biphasic Material Properties of Bovine Articular Cartilage from Confined Compression Experiments', *Journal of Biomechanics*, 30(11-12): 1157-1164.

21) Périé, D., Korde, D. and Iatridis, J. C. (2005) 'Confined Compression Experiments on Bovine Nucleus Pulposus and Annulus Fibrosus: Sensitivity of the Experiment in the Determination of Compressive Modulus and Hydraulic Permeability', *Journal of Biomechanics*, 38(11): 2164-2171.

22) Mass, S. A., Ellis, B. J., Ateshian, G.A. and Weiss, J. A. (2012) 'FEBio: Finite Elements for Biomechanics' *Journal of Biomechanical Engineering*, 134(1): 011005.

23) Matthews, F. L. and West, J. B. (1972) 'Finite Element Displacement Analysis of a Lung', *Journal of Biomechanics*, 5(6): 591-600.

24) Belytschko, T., Kulak, R. F. and Schultz, A. B. (1974) 'Finite Element Stress Analysis of an Intervertebral Disc', *Journal of Biomechanics*, 7(3): 277-285.

25) Ateshian, G. A., Maas, S. A. and Weiss, J. A. (2010) 'Finite Element Algorithm for Frictionless Contact of Porous Permeable Media under Finite Deformation and Sliding', *Journal of Biomechanical Engineering*, 136(6): 061006.

26) Schmid-Schönbein, G. W. and Diller, K. R. (2005) 'Transport Processes in Biomedical Systems: A Roadmap for Future Research Directions', *Annals of Biomedical Engineering*, 33(9): 1136-1141.

27) Portnoy, S., Yamitzky, G., Yizhar, Z., Kristal, A., Oppenheim, U., Siev-Ner, I. and Gefen, A. (2007) 'Real-Time Patient-Specific Finite Element Analysis of Internal Stresses in the Soft Tissues of a Residual Limb: A New Tool for Prosthetic Fitting', *Annals of Biomedical Engineering*, 35(1): 120-135.

28) Ateshian, G. A., Albro, M. B, Maas, S. and Weiss, J. A. (2011) 'Finite Element Implementation of Mechano-Chemical Phenomena in Neutral Deformable Porous Media under Finite Deformation', *Journal of Biomechanical Engineering*, 133(8): 081005.

29) Guo, H. and Spilker, R. L. (2011) 'Biphasic Finite Element Modelling of Hydrated Soft Tissue Contact using an Augmented Lagrangian Method', *Journal of Biomechanical Engineering*, 133(11): 111001.

30) Bonet, J., and Wood, R. D., (1997) *Nonlinear Continuum Mechanics for Finite Element Analysis*, 2nd Edition, USA: Cambridge University Press.

31) Farrell, M. D. and Riches, P. E. (2012) 'Poisson's Ratio of Nucleus Pulposus Tissue: Comparison of Experimental Results with a Biphasic Poroviscoelastic Finite Element Model', in *Euromech 534 Colloquium: Advanced Experimental Approaches and Inverse Problems in Tissue Biomechanics*, 2012-05-29 - 2012-05-31, St Etienne.

32) Meng, Q., Zhingmin, J., Fisher, J. and Wilcox, R. (2013) 'Comparison between FEBio and ABAQUS for Biphasic Contact Problems', *Journal of Engineering in Medicine*, 227(9): 1009-1019.

33) Biddiss, E. A., Bogoch, E. R. and Meguid, S. A. (2004) 'Three-Dimensional Finite Element Analysis of Prosthetic Finger Joint Implants', *International Journal of Mechanics and Materials in Design*, 1(4): 317-328.

9. Appendices

Appendix 1: Young's modulus Calculation

Re-arranging Equation 3, and using $\nu = 0.125$[31] gives:

$$E = \frac{H_A(1+\nu)(1-2\nu)}{(1-\nu)}$$

$$E = \frac{1x10^3 Pa \times (1+0.125) \times \big(1-(2\times 0.125)\big)}{(1-0.125)}$$

$$E = \frac{1x10^3 Pa \times 1.125 \times 0.75}{0.875}$$

$$E = \frac{843.75}{0.875} Pa$$

$$\underline{E = 964.29 Pa}$$

Therefore, converting into the input units of *PreView* ($MPa \equiv \frac{N}{mm^2}$) gives:

$$E = 964.29x10^{-6} MPa$$

$$E = 0.00096429 MPa$$

$$\underline{E \cong 0.001 MPa}$$

Appendix 2: Addition of log output to *FEBio* file

Within the *<Output>* section of the *.feb* file (see Appendix 9), the following script should be added – with data = *Fz* for a force output, and data = *z* for a displacement output in the *rigid_body_data data = …* part.

```
<logfile>
    <rigid_body_data data="..." file = "....txt" delim=",">
    </rigid_body_data>
</logfile>
```

Appendix 3: MATLAB code for extraction of Output Force data

```
clear all
close all

[filenames,pathname] = uigetfile('*.txt','MultiSelect','on');

cd(pathname);

numfiles = size(filenames,2);

col = {'k' 'b' 'r' 'g' 'k.' 'b.' 'r.' 'g.'};

qq1=figure;
qq2=figure;
qq3=figure;

for ii = 1:numfiles
    i = 0; % time
    j = 1; % nodes

    filename = filenames{ii};

    t1 = strfind(filename,'_p');
    t2 = strfind(filename,'E');
    t3 = strfind(filename,'.txt');
    t4 = strfind(filename,'bp');

    perm(ii) = str2num(filename(t1+2:t2-1))
    E(ii) = str2num(filename(t2+1:t3-1))
    level(ii) = str2num(filename(t4+2))

    if level(ii) == 4
        lvl_ind = 1;
    else
        lvl_ind = 2;
    end;

    if perm(ii) == 0
        if E(ii) == 0
            control = ii;
        end;
    end;

    fid=fopen(filename);

    lines = 0;
    count = 0;

    while 1
        tline = fgetl(fid);
        if ~ischar(tline), break, end
        lines = lines + 1;
    end;

    frewind(fid);

    h = waitbar(0,'Reading file...');
```

```
    while 1
        tline = fgetl(fid);
        count = count+1;
        if ~ischar(tline), break, end

        if strcmp(tline(1:5),'*Time')
            i = i+1;
            time(ii,i,1) = str2num(tline(10:size(tline,2)));
        end;

        if strcmp(tline(1:5),'*Data')
            tline = fgetl(fid);
            count = count+1;
            while strcmp(tline(1),'*') == 0
                [node_txt,rem] = strtok(tline,',');
                rigid_body(ii,i,j) = str2num(node_txt);
                [data_txt,rem] = strtok(rem,',');
                rigid_body_data(ii,i,j) = str2num(data_txt);
                j = j+1;
                tline = fgetl(fid);
                count = count+1;
                if ~ischar(tline), break, end
            end;
            j = 1;
        end;

        waitbar(count/lines);
    end

    % gradient calcs

    for kk = 2:i-1
        grad_rgb(ii,kk)     =     (rigid_body_data(ii,kk+1,lvl_ind)-
rigid_body_data(ii,kk-1,lvl_ind))./(time(ii,kk+1,1)-time(ii,kk-
1,1));
    end;
    grad_rgb(ii,1) = 0;
    grad_rgb(ii,i) = 0;

    close(h);
    fclose(fid);
    figure(qq1);

plot(squeeze(time(ii,:,1)),squeeze(rigid_body_data(ii,:,lvl_ind)));
    hold on;
    figure(qq2);

semilogx(squeeze(time(ii,:,1)),squeeze(rigid_body_data(ii,:,lvl_ind)
));
    hold on;
    figure(qq3);
    semilogx(squeeze(time(ii,:,1)),squeeze(grad_rgb(ii,:)));
    hold on;
    minii(ii) = min(rigid_body_data(ii,:,lvl_ind))
    endii(ii)                                                    =
rigid_body_data(ii,find(rigid_body_data(ii,:,lvl_ind),1,'last'),lvl_
ind);
end;
```

```
dminii = minii - minii(control)
dendii = endii - endii(control)

figure
plot(minii)
title('peak stress');
figure
plot(endii)
title('Eq stress');

figure
plot(dminii)
title('dpeak stress');
figure
plot(dendii)
title('dEq stress');

xlswrite('new_outputfile.xls',[level' perm' E' minii' endii' dminii'
dendii']);
```

Appendix 4: Calculation of Tissue Parameters for *PreView* Input

Dimensions of the testing dish (Figure 10) were measured to be:

$$Diameter = 15mm$$

$$Depth = 16mm$$

However, as can be seen, the testing dish is cylindrical. Therefore the rectangle tissue modelled in *PreView* should be the same volume as the equivalent cylindrical tissue sample that would be used experimentally.

Presuming the tissue only takes up half of the depth of the testing dish, i.e. $Depth = 8mm$, the volume of the tissue would be (where $r = \frac{diameter}{2}$ and $h = depth$):

$$V = \pi r^2 h$$

$$V = \pi \times 7.5mm \times 7.5mm \times 8mm$$

$$\underline{V = 1413.72mm^3}$$

Assuming the same volume for a rectangle, also of depth $8mm$, the dimension (in mm)would be:

x	13.3
y	13.3
z	8

Appendix 5: MATLAB Code for Extraction of Output Displacement Data

```
clear all
close all

[filenames,pathname] = uigetfile('*.txt','MultiSelect','on');

cd(pathname);

hh = waitbar(0);

numfiles = size(filenames,2);

col = {'k' 'b' 'r' 'g' 'k.' 'b.' 'r.' 'g.'};

qq1=figure;
qq2=figure;
qq3=figure;

for ii = 1:numfiles

    i = 0; % time
    j = 1; % nodes

    filename = filenames{ii};

    t1 = strfind(filename,'_p');
    t2 = strfind(filename,'E');
    t3 = strfind(filename,'.txt');
    t4 = strfind(filename,'bp');

    perm(ii) = str2num(filename(t1+2:t2-1));
    E(ii) = str2num(filename(t2+1:t3-1));
    level = str2num(filename(t4+2));

    if perm(ii) == 0
        if E(ii) == 0
            control = ii;
        end;
    end;

    fid=fopen(filename);

    lines = 0;
    count = 0;

    while 1
        tline = fgetl(fid);
        if ~ischar(tline), break, end
        lines = lines + 1;
    end;

    frewind(fid);
```

```
    while 1
        tline = fgetl(fid);
        count = count+1;
        if ~ischar(tline), break, end

        if strcmp(tline(1:5),'*Time')
            i = i+1;
            time(ii,i,1) = str2num(tline(10:size(tline,2)));
            if time(ii,i,1) >= 100
                if time(ii,i-1,1) < 100
                    t100 = i;
                end;
            end;
        end;

        if strcmp(tline(1:5),'*Data')
            tline = fgetl(fid);
            count = count+1;
            while strcmp(tline(1),'*') == 0
                [node_txt,rem] = strtok(tline,',');
                rigid_body(ii,i,j) = str2num(node_txt);
                [data_txt,rem] = strtok(rem,',');
                rigid_body_data(ii,i,j) = str2num(data_txt);
                j = j+1;
                tline = fgetl(fid);
                count = count+1;
                if ~ischar(tline), break, end
            end;
            j = 1;
        end;
    end

    for kk = 2:i-1
        grad_rgb(ii,kk)        =        (rigid_body_data(ii,kk+1,1)-
rigid_body_data(ii,kk-1,1))./(time(ii,kk+1,1)-time(ii,kk-1,1));
    end;
    grad_rgb(ii,1) = 0;
    grad_rgb(ii,i) = 0;

    fclose(fid);

    minii(ii) = min(rigid_body_data(ii,:,1));
    endii(ii)                                                    =
rigid_body_data(ii,find(rigid_body_data(ii,:,1),1,'last'),1);
    t100data(ii) = rigid_body_data(ii,t100,1);

    waitbar(ii/numfiles);

 end;

close(hh);
dminii = minii - minii(control);
dendii = endii - endii(control);
dt100data = t100data - t100data(control);

xlswrite('new_outputfile.xls',[perm'  E'  minii'  endii'  t100data'
dminii' dendii' dt100data']);
```

Appendix 6: Data Points of Peak and Equilibrium Positions for Force Control Test (all models)

Bp	Data Point	p	E	Equilibrium Position (mm)	Position at t=100s (mm)	Change in Eq Position (mm)	Change in Position at t=100s (mm)
0	**0**	0	0	8.2	8.1998	0	0
1	1	-100	0	8.7909	8.8187	0.5909	0.6189
1	2	-100	250	8.8379	8.878	0.6379	0.6782
1	3	-100	500	8.838	8.8782	0.638	0.6784
1	4	-100	750	8.8381	8.8782	0.6381	0.6784
1	5	-100	1000	8.8381	8.8783	0.6381	0.6785
1	6	-10	0	8.3305	8.6361	0.1305	0.4363
1	7	-10	250	8.4274	8.7381	0.2274	0.5383
1	8	-10	500	8.4276	8.7383	0.2276	0.5385
1	9	-10	750	8.4277	8.7384	0.2277	0.5386
1	10	-10	1000	8.4277	8.7384	0.2277	0.5386
1	11	0	0	8.2	8.1998	0	0
1	12	0	250	8.2997	8.3641	0.0997	0.1643
1	13	0	500	8.3	8.3645	0.1	0.1647
1	14	0	750	8.3	8.3646	0.1	0.1648
1	15	0	1000	8.3001	8.3647	0.1001	0.1649
1	16	10	0	8.1995	8.0494	-0.0005	-0.1504
1	17	10	250	8.299	8.221	0.099	0.0212
1	18	10	500	8.2993	8.2214	0.0993	0.0216
1	19	10	750	8.2993	8.2216	0.0993	0.0218
1	20	10	1000	8.2994	8.2216	0.0994	0.0218
1	21	100	0	8.1995	8.0317	-0.0005	-0.1681
1	22	100	250	8.2991	8.2034	0.0991	0.0036
1	23	100	500	8.2993	8.2038	0.0993	0.004
1	24	100	750	8.2994	8.2039	0.0994	0.0041
1	25	100	1000	8.2994	8.204	0.0994	0.0042
2	1	-100	0	8.6949	8.6205	0.4949	0.4207
2	2	-100	250	8.7416	8.6648	0.5416	0.465
2	3	-100	500	8.7417	8.6649	0.5417	0.4651
2	4	-100	750	8.7417	8.665	0.5417	0.4652
2	5	-100	1000	8.7417	8.665	0.5417	0.4652
2	6	-10	0	8.296	8.4818	0.096	0.282
2	7	-10	250	8.3881	8.5657	0.1881	0.3659
2	8	-10	500	8.3883	8.5659	0.1883	0.3661
2	9	-10	750	8.3884	8.566	0.1884	0.3662
2	10	-10	1000	8.3884	8.566	0.1884	0.3662
2	11	0	0	8.2	8.1999	0	1E-04
2	12	0	250	8.2995	8.3047	0.0995	0.1049
2	13	0	500	8.2997	8.305	0.0997	0.1052
2	14	0	750	8.2998	8.3051	0.0998	0.1053
2	15	0	1000	8.2998	8.3051	0.0998	0.1053
2	16	10	0	8.1994	8.1073	-0.0006	-0.0925
2	17	10	250	8.299	8.2142	0.099	0.0144
2	18	10	500	8.2993	8.2144	0.0993	0.0146
2	19	10	750	8.2993	8.2145	0.0993	0.0147
2	20	10	1000	8.2994	8.2146	0.0994	0.0148

2	21	100	0	8.1994	8.0961	-0.0006	-0.1037
2	22	100	250	8.2991	8.203	0.0991	0.0032
2	23	100	500	8.2993	8.2033	0.0993	0.0035
2	24	100	750	8.2994	8.2034	0.0994	0.0036
2	25	100	1000	8.2994	8.2034	0.0994	0.0036
3	1	-100	0	8.6006	8.4341	0.4006	0.2343
3	2	-100	250	8.6469	8.477	0.4469	0.2772
3	3	-100	500	8.6471	8.4821	0.4471	0.2823
3	4	-100	750	8.6471	8.4827	0.4471	0.2829
3	5	-100	1000	8.6471	8.4828	0.4471	0.283
3	6	-10	0	8.2658	8.3534	0.0658	0.1536
3	7	-10	250	8.355	8.4107	0.155	0.2109
3	8	-10	500	8.3552	8.4108	0.1552	0.211
3	9	-10	750	8.3553	8.4109	0.1553	0.2111
3	10	-10	1000	8.3553	8.4109	0.1553	0.2111
3	11	0	0	8.2	8.1999	0	1E-04
3	12	0	250	8.2993	8.2577	0.0993	0.0579
3	13	0	500	8.2995	8.2579	0.0995	0.0581
3	14	0	750	8.2996	8.2579	0.0996	0.0581
3	15	0	1000	8.2996	8.2579	0.0996	0.0581
3	16	10	0	8.1994	8.1519	-0.0006	-0.0479
3	17	10	250	8.299	8.2086	0.099	0.0088
3	18	10	500	8.2993	8.2087	0.0993	0.0089
3	19	10	750	8.2993	8.2088	0.0993	0.009
3	20	10	1000	8.2994	8.2088	0.0994	0.009
3	21	100	0	8.1994	8.1462	-0.0006	-0.0536
3	22	100	250	8.2991	8.2027	0.0991	0.0029
3	23	100	500	8.2993	8.2028	0.0993	0.003
3	24	100	750	8.2994	8.2028	0.0994	0.003
3	25	100	1000	8.2994	8.2029	0.0994	0.0031
4	1	-100	0	8.50804	8.3121	0.30804	0.1123
4	2	-100	250	8.55431	8.33205	0.35431	0.13225
4	3	-100	500	8.55441	8.33214	0.35441	0.13234
4	4	-100	750	8.55445	8.33217	0.35445	0.13237
4	5	-100	1000	8.55447	8.33219	0.35447	0.13239
4	6	-10	0	8.23991	8.26925	0.03991	0.06945
4	7	-10	250	8.32846	8.29927	0.12846	0.09947
4	8	-10	500	8.32865	8.29935	0.12865	0.09955
4	9	-10	750	8.32872	8.29938	0.12872	0.09958
4	10	-10	1000	8.32875	8.2994	0.12875	0.0996
4	11	0	0	8.2	8.19985	0	5E-05
4	12	0	250	8.29913	8.22769	0.09913	0.02789
4	13	0	500	8.29935	8.22777	0.09935	0.02797
4	14	0	750	8.29943	8.22779	0.09943	0.02799
4	15	0	1000	8.29947	8.22781	0.09947	0.02801
4	16	10	0	8.19947	8.17809	-0.00053	-0.02171
4	17	10	250	8.29905	8.20514	0.09905	0.00534
4	18	10	500	8.29927	8.20521	0.09927	0.00541
4	19	10	750	8.29935	8.20524	0.09935	0.00544
4	20	10	1000	8.29939	8.20525	0.09939	0.00545

4	21	100	0	8.19944	8.17547	-0.00056	-0.02433
4	22	100	250	8.29906	8.20243	0.09906	0.00263
4	23	100	500	8.29928	8.2025	0.09928	0.0027
4	24	100	750	8.29935	8.20253	0.09935	0.00273
4	25	100	1000	8.29939	8.20254	0.09939	0.00274
5	1	-100	0	8.4173	8.244	0.2173	0.0442
5	2	-100	250	8.4642	8.2524	0.2642	0.0526
5	3	-100	500	8.4644	8.2524	0.2644	0.0526
5	4	-100	750	8.4644	8.2524	0.2644	0.0526
5	5	-100	1000	8.4644	8.2525	0.2644	0.0527
5	6	-10	0	8.2201	8.2265	0.0201	0.0267
5	7	-10	250	8.31	8.2392	0.11	0.0394
5	8	-10	500	8.3102	8.2392	0.1102	0.0394
5	9	-10	750	8.3103	8.2392	0.1103	0.0394
5	10	-10	1000	8.3103	8.2392	0.1103	0.0394
5	11	0	0	8.2	8.1998	0	0
5	12	0	250	8.2991	8.212	0.0991	0.0122
5	13	0	500	8.2993	8.212	0.0993	0.0122
5	14	0	750	8.2994	8.212	0.0994	0.0122
5	15	0	1000	8.2994	8.212	0.0994	0.0122
5	16	10	0	8.1996	8.1913	-0.0004	-0.0085
5	17	10	250	8.2991	8.2034	0.0991	0.0036
5	18	10	500	8.2993	8.2034	0.0993	0.0036
5	19	10	750	8.2994	8.2034	0.0994	0.0036
5	20	10	1000	8.2994	8.2034	0.0994	0.0036
5	21	100	0	8.1996	8.1902	-0.0004	-0.0096
5	22	100	250	8.2991	8.2023	0.0991	0.0025
5	23	100	500	8.2993	8.2024	0.0993	0.0026
5	24	100	750	8.2994	8.2024	0.0994	0.0026
5	25	100	1000	8.2994	8.2024	0.0994	0.0026
6	1	-100	0	8.3289	8.2146	0.1289	0.0148
6	2	-100	250	8.3786	8.2176	0.1786	0.0178
6	3	-100	500	8.3787	8.2176	0.1787	0.0178
6	4	-100	750	8.3788	8.2176	0.1788	0.0178
6	5	-100	1000	8.3788	8.2176	0.1788	0.0178
6	6	-10	0	8.2069	8.2086	0.0069	0.0088
6	7	-10	250	8.3008	8.2133	0.1008	0.0135
6	8	-10	500	8.301	8.2133	0.101	0.0135
6	9	-10	750	8.3011	8.2133	0.1011	0.0135
6	10	-10	1000	8.3011	8.2133	0.1011	0.0135
6	11	0	0	8.2	8.1998	0	0
6	12	0	250	8.299	8.205	0.099	0.0052
6	13	0	500	8.2993	8.2051	0.0993	0.0053
6	14	0	750	8.2993	8.2051	0.0993	0.0053
6	15	0	1000	8.2994	8.2051	0.0994	0.0053
6	16	10	0	8.1998	8.1971	-0.0002	-0.0027
6	17	10	250	8.2991	8.2026	0.0991	0.0028
6	18	10	500	8.2993	8.2026	0.0993	0.0028
6	19	10	750	8.2994	8.2026	0.0994	0.0028
6	20	10	1000	8.2994	8.2026	0.0994	0.0028

6	21	100	0	8.1998	8.1968	-0.0002	-0.003
6	22	100	250	8.2991	8.2023	0.0991	0.0025
6	23	100	500	8.2993	8.2023	0.0993	0.0025
6	24	100	750	8.2994	8.2023	0.0994	0.0025
6	25	100	1000	8.2994	8.2023	0.0994	0.0025
7	1	-100	0	8.2456	8.2039	0.0456	0.0041
7	2	-100	250	8.3083	8.2048	0.1083	0.005
7	3	-100	500	8.3085	8.2048	0.1085	0.005
7	4	-100	750	8.3085	8.2049	0.1085	0.0051
7	5	-100	1000	8.3085	8.2049	0.1085	0.0051
7	6	-10	0	8.2011	8.202	0.0011	0.0022
7	7	-10	250	8.2991	8.2038	0.0991	0.004
7	8	-10	500	8.2993	8.2038	0.0993	0.004
7	9	-10	750	8.2994	8.2038	0.0994	0.004
7	10	-10	1000	8.2994	8.2038	0.0994	0.004
7	11	0	0	8.2	8.1998	0	0
7	12	0	250	8.2991	8.2025	0.0991	0.0027
7	13	0	500	8.2993	8.2025	0.0993	0.0027
7	14	0	750	8.2994	8.2026	0.0994	0.0028
7	15	0	1000	8.2994	8.2026	0.0994	0.0028
7	16	10	0	8.1999	8.1993	-1E-04	-0.0005
7	17	10	250	8.2991	8.2023	0.0991	0.0025
7	18	10	500	8.2993	8.2023	0.0993	0.0025
7	19	10	750	8.2994	8.2023	0.0994	0.0025
7	20	10	1000	8.2994	8.2023	0.0994	0.0025
7	21	100	0	8.1999	8.1992	-1E-04	-0.0006
7	22	100	250	8.2991	8.2022	0.0991	0.0024
7	23	100	500	8.2993	8.2023	0.0993	0.0025
7	24	100	750	8.2994	8.2023	0.0994	0.0025
7	25	100	1000	8.2994	8.2023	0.0994	0.0025

Appendix 7: Data Points of Peak and Equilibrium Forces for Displacement Control Test (all models)

Bp	Data Point	Perm	E	Peak Force	Eq Force (N)	dPeak Force (N)	dEq Force (N)
0	**0**	0	0	-0.14289	-0.00962256	0	0
1	1	-100	0	-0.346331	-0.0561149	-0.194359	-0.04649568
1	2	-100	250	-0.559799	-0.074063	-0.407827	-0.06444378
1	3	-100	500	-0.568541	-0.0739702	-0.416569	-0.06435098
1	4	-100	750	-0.572024	-0.0739344	-0.420052	-0.06431518
1	5	-100	1000	-0.573942	-0.0739187	-0.42197	-0.06429948
1	6	-10	0	-0.227266	-0.0116231	-0.075294	-0.00200388
1	7	-10	250	-0.462471	-0.0115758	-0.310499	-0.00195658
1	8	-10	500	-0.469472	-0.0115746	-0.3175	-0.00195538
1	9	-10	750	-0.47196	-0.0115733	-0.319988	-0.00195408
1	10	-10	1000	-0.473233	-0.0115704	-0.321261	-0.00195118
1	11	0	0	-0.151972	-0.00961922	0	0
1	12	0	250	-0.245677	-0.0109279	-0.093705	-0.00130868
1	13	0	500	-0.246678	-0.0109313	-0.094706	-0.00131208
1	14	0	750	-0.247028	-0.0109324	-0.095056	-0.00131318
1	15	0	1000	-0.247189	-0.0109327	-0.095217	-0.00131348
1	16	10	0	-0.121453	-0.00958162	0.030519	3.76E-05
1	17	10	250	-0.162612	-0.0109193	-0.01064	-0.00130008
1	18	10	500	-0.162915	-0.0109227	-0.010943	-0.00130348
1	19	10	750	-0.162989	-0.0109236	-0.011017	-0.00130438
1	20	10	1000	-0.163036	-0.0109242	-0.011064	-0.00130498
1	21	100	0	-0.116752	-0.0095787	0.03522	4.05E-05
1	22	100	250	-0.15265	-0.0109185	-0.000678	-0.00129928
1	23	100	500	-0.152853	-0.0109219	-0.000881	-0.00130268
1	24	100	750	-0.152962	-0.010923	-0.00099	-0.00130378
1	25	100	1000	-0.152995	-0.0109235	-0.001023	-0.00130428
2	1	-100	0	-0.15204	-0.0366625	-5.7E-05	-0.02704234
2	2	-100	250	-0.152067	-0.0463263	-8.4E-05	-0.03670614
2	3	-100	500	-0.152066	-0.0463538	-8.3E-05	-0.03673364
2	4	-100	750	-0.15206	-0.0463628	-7.7E-05	-0.03674264
2	5	-100	1000	-0.15206	-0.0463674	-7.7E-05	-0.03674724
2	6	-10	0	-0.152022	-0.0138192	-3.9E-05	-0.00419904
2	7	-10	250	-0.15207	-0.0156197	-8.7E-05	-0.00599954
2	8	-10	500	-0.152066	-0.0156239	-8.3E-05	-0.00600374
2	9	-10	750	-0.152056	-0.0156254	-7.3E-05	-0.00600524
2	10	-10	1000	-0.152057	-0.015626	-7.4E-05	-0.00600584
2	11	0	0	-0.151983	-0.00962016	0	0
2	12	0	250	-0.152048	-0.0109749	-6.5E-05	-0.00135474
2	13	0	500	-0.152049	-0.0109782	-6.6E-05	-0.00135804
2	14	0	750	-0.152056	-0.0109791	-7.3E-05	-0.00135894
2	15	0	1000	-0.152031	-0.0109796	-4.8E-05	-0.00135944
2	16	10	0	-0.151927	-0.00954746	5.6E-05	7.27E-05
2	17	10	250	-0.151995	-0.010922	-1.2E-05	-0.00130184
2	18	10	500	-0.151986	-0.0109254	-3E-06	-0.00130524
2	19	10	750	-0.151978	-0.0109266	5E-06	-0.00130644
2	20	10	1000	-0.151988	-0.0109271	-5E-06	-0.00130694

2	21	100	0	-0.151901	-0.009543	8.2E-05	7.742E-05
2	22	100	250	-0.151962	-0.010919	2.1E-05	-0.001299
2	23	100	500	-0.151962	-0.010922	2.1E-05	-0.001302
2	24	100	750	-0.151994	-0.010923	-1.1E-05	-0.001303
2	25	100	1000	-0.151964	-0.010924	1.9E-05	-0.001304
3	1	-100	0	-0.151987	-0.025155	-2.6E-05	-0.015534
3	2	-100	250	-0.151985	-0.028937	-2.4E-05	-0.019316
3	3	-100	500	-0.151971	-0.028947	-1E-05	-0.019325
3	4	-100	750	-0.151985	-0.02895	-2.4E-05	-0.019329
3	5	-100	1000	-0.151984	-0.028952	-2.3E-05	-0.019331
3	6	-10	0	-0.151987	-0.013537	-2.6E-05	-0.003916
3	7	-10	250	-0.151986	-0.015434	-2.5E-05	-0.005813
3	8	-10	500	-0.151984	-0.015438	-2.3E-05	-0.005817
3	9	-10	750	-0.151985	-0.01544	-2.4E-05	-0.005819
3	10	-10	1000	-0.151991	-0.015441	-3E-05	-0.00582
3	11	0	0	-0.151961	-0.009621	0	0
3	12	0	250	-0.151985	-0.01102	-2.4E-05	-0.001399
3	13	0	500	-0.151984	-0.011024	-2.3E-05	-0.001403
3	14	0	750	-0.151971	-0.011025	-1E-05	-0.001404
3	15	0	1000	-0.15199	-0.011026	-2.9E-05	-0.001404
3	16	10	0	-0.151987	-0.009528	-2.6E-05	9.299E-05
3	17	10	250	-0.151991	-0.010925	-3E-05	-0.001303
3	18	10	500	-0.15199	-0.010928	-2.9E-05	-0.001307
3	19	10	750	-0.151992	-0.010929	-3.1E-05	-0.001308
3	20	10	1000	-0.15199	-0.01093	-2.9E-05	-0.001308
3	21	100	0	-0.151987	-0.009523	-2.6E-05	9.845E-05
3	22	100	250	-0.151991	-0.010919	-3E-05	-0.001298
3	23	100	500	-0.15199	-0.010923	-2.9E-05	-0.001301
3	24	100	750	-0.15199	-0.010924	-2.9E-05	-0.001303
3	25	100	1000	-0.15199	-0.010924	-2.9E-05	-0.001303
4	1	-100	0	-0.151985	-0.018991	-4E-06	-0.009369
4	2	-100	250	-0.151968	-0.020937	1.3E-05	-0.011316
4	3	-100	500	-0.151966	-0.020942	1.5E-05	-0.011321
4	4	-100	750	-0.15199	-0.020944	-9E-06	-0.011322
4	5	-100	1000	-0.151968	-0.020945	1.3E-05	-0.011323
4	6	-10	0	-0.151964	-0.012528	1.7E-05	-0.002906
4	7	-10	250	-0.151968	-0.014059	1.3E-05	-0.004438
4	8	-10	500	-0.151965	-0.014063	1.6E-05	-0.004441
4	9	-10	750	-0.151992	-0.014064	-1.1E-05	-0.004443
4	10	-10	1000	-0.151963	-0.014065	1.8E-05	-0.004443
4	11	0	0	-0.151981	-0.009622	0	0
4	12	0	250	-0.151956	-0.011022	2.5E-05	-0.0014
4	13	0	500	-0.151977	-0.011025	4E-06	-0.001404
4	14	0	750	-0.151991	-0.011027	-1E-05	-0.001405
4	15	0	1000	-0.151969	-0.011027	1.2E-05	-0.001406
4	16	10	0	-0.151981	-0.009526	0	9.56E-05
4	17	10	250	-0.151966	-0.010925	1.5E-05	-0.001303
4	18	10	500	-0.151967	-0.010928	1.4E-05	-0.001307
4	19	10	750	-0.151992	-0.01093	-1.1E-05	-0.001308
4	20	10	1000	-0.151969	-0.01093	1.2E-05	-0.001309

4	21	100	0	-0.151981	-0.00952	0	0.0001014
4	22	100	250	-0.151991	-0.010919	-1E-05	-0.001298
4	23	100	500	-0.15199	-0.010923	-9E-06	-0.001301
4	24	100	750	-0.15199	-0.010924	-9E-06	-0.001302
4	25	100	1000	-0.15199	-0.010925	-9E-06	-0.001303
5	1	-100	0	-0.151987	-0.015241	-2.20E-05	-0.005619
5	2	-100	250	-0.151947	-0.016405	1.80E-05	-0.006784
5	3	-100	500	-0.151945	-0.016408	2.00E-05	-0.006786
5	4	-100	750	-0.151972	-0.016409	-7.00E-06	-0.006787
5	5	-100	1000	-0.151973	-0.01641	-8.00E-06	-0.006788
5	6	-10	0	-0.151964	-0.011478	1.00E-06	-0.001856
5	7	-10	250	-0.151947	-0.012705	1.80E-05	-0.003083
5	8	-10	500	-0.15198	-0.012708	-1.50E-05	-0.003087
5	9	-10	750	-0.15197	-0.012709	-5.00E-06	-0.003088
5	10	-10	1000	-0.15197	-0.01271	-5.00E-06	-0.003088
5	11	0	0	-0.151965	-0.009622	0	0
5	12	0	250	-0.151956	-0.010988	9.00E-06	-0.001366
5	13	0	500	-0.15195	-0.010991	1.50E-05	-0.001369
5	14	0	750	-0.15197	-0.010992	-5.00E-06	-0.00137
5	15	0	1000	-0.151973	-0.010993	-8.00E-06	-0.001371
5	16	10	0	-0.151968	-0.009542	-3.00E-06	7.94E-05
5	17	10	250	-0.151952	-0.010923	1.30E-05	-0.001302
5	18	10	500	-0.151951	-0.010927	1.40E-05	-0.001305
5	19	10	750	-0.151949	-0.010928	1.60E-05	-0.001306
5	20	10	1000	-0.151972	-0.010929	-7.00E-06	-0.001307
5	21	100	0	-0.151969	-0.009537	-4.00E-06	8.49E-05
5	22	100	250	-0.151952	-0.010919	1.30E-05	-0.001298
5	23	100	500	-0.15195	-0.010923	1.50E-05	-0.001301
5	24	100	750	-0.151949	-0.010924	1.60E-05	-0.001302
5	25	100	1000	-0.151971	-0.010925	-6.00E-06	-0.001303
6	1	-100	0	-0.151953	-0.01274	0	-0.003118
6	2	-100	250	-0.151969	-0.013501	-1.6E-05	-0.003878
6	3	-100	500	-0.15196	-0.013503	-7E-06	-0.00388
6	4	-100	750	-0.151944	-0.013503	9E-06	-0.003881
6	5	-100	1000	-0.151957	-0.013504	-4E-06	-0.003882
6	6	-10	0	-0.151986	-0.010574	-3.3E-05	-0.000952
6	7	-10	250	-0.151969	-0.011627	-1.6E-05	-0.002005
6	8	-10	500	-0.151966	-0.01163	-1.3E-05	-0.002008
6	9	-10	750	-0.151948	-0.011631	5E-06	-0.002009
6	10	-10	1000	-0.151973	-0.011631	-2E-05	-0.002009
6	11	0	0	-0.151953	-0.009622	0	0
6	12	0	250	-0.151969	-0.010946	-1.6E-05	-0.001324
6	13	0	500	-0.151966	-0.010949	-1.3E-05	-0.001327
6	14	0	750	-0.151985	-0.01095	-3.2E-05	-0.001328
6	15	0	1000	-0.15197	-0.010951	-1.7E-05	-0.001329
6	16	10	0	-0.151953	-0.009574	0	4.797E-05
6	17	10	250	-0.151978	-0.010921	-2.5E-05	-0.001299
6	18	10	500	-0.151967	-0.010925	-1.4E-05	-0.001303
6	19	10	750	-0.151943	-0.010926	1E-05	-0.001304
6	20	10	1000	-0.151949	-0.010926	4E-06	-0.001304

6	21	100	0	-0.151969	-0.00957	-1.6E-05	5.182E-05
6	22	100	250	-0.151969	-0.010919	-1.6E-05	-0.001297
6	23	100	500	-0.151959	-0.010923	-6E-06	-0.001301
6	24	100	750	-0.151959	-0.010924	-6E-06	-0.001302
6	25	100	1000	-0.151977	-0.010924	-2.4E-05	-0.001302
7	1	-100	0	-0.145746	-0.010977	0	-0.001355
7	2	-100	250	-0.147495	-0.011509	-0.001749	-0.001887
7	3	-100	500	-0.147495	-0.011511	-0.001749	-0.001889
7	4	-100	750	-0.147495	-0.011511	-0.001749	-0.001889
7	5	-100	1000	-0.147495	-0.011512	-0.001749	-0.001889
7	6	-10	0	-0.145746	-0.009896	0	-0.000274
7	7	-10	250	-0.147495	-0.010981	-0.001749	-0.001359
7	8	-10	500	-0.147495	-0.010984	-0.001749	-0.001362
7	9	-10	750	-0.147495	-0.010985	-0.001749	-0.001363
7	10	-10	1000	-0.147495	-0.010986	-0.001749	-0.001363
7	11	0	0	-0.145746	-0.009622	0	0
7	12	0	250	-0.147495	-0.010922	-0.001749	-0.0013
7	13	0	500	-0.147495	-0.010925	-0.001749	-0.001303
7	14	0	750	-0.147495	-0.010927	-0.001749	-0.001304
7	15	0	1000	-0.147495	-0.010927	-0.001749	-0.001305
7	16	10	0	-0.145746	-0.009607	0	1.564E-05
7	17	10	250	-0.147495	-0.01092	-0.001749	-0.001297
7	18	10	500	-0.147495	-0.010923	-0.001749	-0.001301
7	19	10	750	-0.147495	-0.010924	-0.001749	-0.001302
7	20	10	1000	-0.147495	-0.010925	-0.001749	-0.001302
7	21	100	0	-0.145746	-0.009605	0	1.706E-05
7	22	100	250	-0.147495	-0.010919	-0.001749	-0.001297
7	23	100	500	-0.147495	-0.010923	-0.001749	-0.0013
7	24	100	750	-0.147495	-0.010924	-0.001749	-0.001301
7	25	100	1000	-0.147495	-0.010924	-0.001749	-0.001302

Appendix 8: Results from Busby *et al.* Investigation (2013[4])

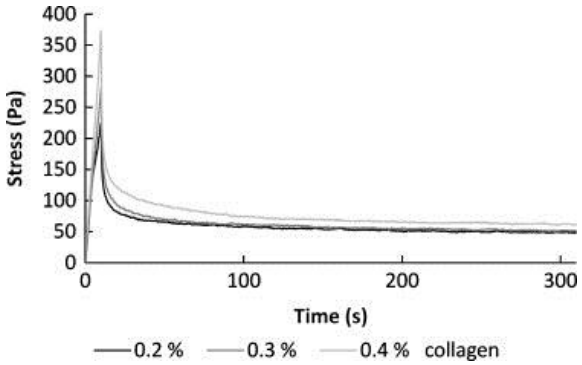

Figure 1, taken from Busby *et al.* (2013) – "Confined Compression of Collagen Hydrogels"

*"Average compressive stress (*n=*8) in response to ramp-hold compressive strain (0.5%/s) for collagen hydrogels of different concentrations."*

Appendix 9: Example *.feb* File

The following *.feb* file is for the two-layer biphasic model created in the model validation section (Section 3.1).

```
<?xml version="1.0" encoding="ISO-8859-1"?>
<febio_spec version="1.2">
	<Globals>
		<Constants>
			<T>0</T>
			<R>0</R>
			<Fc>0</Fc>
		</Constants>
	</Globals>
	<Material>
		<material id="1" name="Rigid Body - Plunger" type="rigid body">
			<density>1</density>
			<center_of_mass>0,0,22.5</center_of_mass>
		</material>
		<material id="2" name="Rigid Body - Handle" type="rigid body">
			<density>1</density>
			<center_of_mass>0,0,28.5</center_of_mass>
		</material>
		<material id="3" name="Material3" type="biphasic">
			<phi0>0</phi0>
			<solid type="neo-Hookean">
				<density>1</density>
				<E>1</E>
				<v>0.1</v>
			</solid>
			<permeability type="perm-const-iso">
				<perm>0.001</perm>
			</permeability>
		</material>
	</Material>
	<Geometry>
		<Nodes>
			<node id="1">-5.0000000e+000,-5.0000000e+000, 0.0000000e+000</node>
			...
			<node id="824">1.5000000e+000,1.5000000e+000, 3.2000000e+001</node>
		</Nodes>
		<Elements>
			<hex8 id="1" mat="3">   1,  203,  304,  102,   2,  204,  305,  103</hex8>
			<hex8 id="202" mat="2">   817,   821,   823,   819,   818,   822,   824,
820</hex8>
		</Elements>
	</Geometry>
	<Boundary>
		<fix>
			<node id="1" bc="xyz"/>
			<node id="102" bc="xyz"/>
			<node id="203" bc="xyz"/>
			<node id="304" bc="xyz"/>
		</fix>
```

```
		<fix>
			<node id="1" bc="xy"/>
			...
			<node id="808" bc="xy"/>
		</fix>
		<fix>
			<node id="505" bc="p"/>
			<node id="606" bc="p"/>
			<node id="707" bc="p"/>
			<node id="808" bc="p"/>
		</fix>
		<contact type="rigid">
			<node id="505" rb="1"></node>
			<node id="606" rb="1"></node>
			<node id="707" rb="1"></node>
			<node id="808" rb="1"></node>
		</contact>
		<contact type="rigid joint">
			<tolerance>0.1</tolerance>
			<penalty>1</penalty>
			<body_a>1</body_a>
			<body_b>2</body_b>
			<joint>0,0,25</joint>
		</contact>
		<contact type="tied-biphasic">
			<laugon>0</laugon>
			<tolerance>0.2</tolerance>
			<gaptol>0</gaptol>
			<ptol>0</ptol>
			<penalty>1000</penalty>
			<auto_penalty>0</auto_penalty>
			<two_pass>1</two_pass>
			<search_tol>0.01</search_tol>
			<pressure_penalty>1</pressure_penalty>
			<symmetric_stiffness>0</symmetric_stiffness>
			<search_radius>1</search_radius>
			<surface type="master">
				<quad4 id="1">  101,  303,  404,  202</quad4>
			</surface>
			<surface type="slave">
				<quad4 id="1">  405,  506,  708,  607</quad4>
			</surface>
		</contact>
</Boundary>
<Constraints>
		<rigid_body mat="1">
			<trans_x type="fixed"></trans_x>
			<trans_y type="fixed"></trans_y>
			<rot_x type="fixed"></rot_x>
			<rot_y type="fixed"></rot_y>
			<rot_z type="fixed"></rot_z>
		</rigid_body>
		<rigid_body mat="2">
			<trans_x type="fixed"></trans_x>
			<trans_y type="fixed"></trans_y>
```

```
                        <rot_x type="fixed"></rot_x>
                        <rot_y type="fixed"></rot_y>
                        <rot_z type="fixed"></rot_z>
                </rigid_body>
        </Constraints>
        <LoadData>
                <loadcurve id="1" type="smooth">
                        <loadpoint>0,0</loadpoint>
                        <loadpoint>100,-2</loadpoint>
                </loadcurve>
        </LoadData>
        <Output>
                <logfile>
                        <rigid_body_data data="Fz" file = "Fz_aim22.txt" delim=",">
                        </rigid_body_data>
                </logfile>
                <plotfile type="febio">
                        <var type="displacement"/>
                        <var type="effective fluid pressure"/>
                        <var type="fluid flux"/>
                        <var type="stress"/>
                </plotfile>
        </Output>
        <Step name="Biphasic">
                <Module type="poro"/>
                <Control>
                        <time_steps>2000000</time_steps>
                        <step_size>0.1</step_size>
                        <max_refs>15</max_refs>
                        <max_ups>10</max_ups>
                        <dtol>0.001</dtol>
                        <etol>0.01</etol>
                        <rtol>0</rtol>
                        <ptol>0.01</ptol>
                        <lstol>0.9</lstol>
                        <time_stepper>
                                <dtmin>0.001</dtmin>
                                <dtmax>100</dtmax>
                                <max_retries>5</max_retries>
                                <opt_iter>40</opt_iter>
                        </time_stepper>
                </Control>
                <Constraints>
                        <rigid_body mat="1">
                                <trans_z type="prescribed" lc="1">1</trans_z>
                        </rigid_body>
                </Constraints>
        </Step>
</febio_spec>
```